AN ABSTRACT OF THE THESIS OF

Stephanie A. Schmidt for the degree of Master of Science in Forest Ecosystems and Society presented on December 5, 2019

Title: Buzzing Bolbomyiidae and Air Temperature Monitoring Methods: Investigating Long-Term Ecological Data from the H.J. Andrews Experimental Forest

Abstract approved:

_____

Mark Schulze and Lisa M. Ganio

The short-term duration of most ecological studies can make it difficult to capture the long-term dynamics of ecosystems and populations. Infrequent or high-impact events can be missed, or erroneously documented as baselines. Long-term ecological research enables a deeper understanding of complex processes, provides a foundation for future insights, and can help improve research methods and management. In my research, I used long-term data collected at the H.J. Andrews Experimental Forest in Oregon's Western Cascades, established by the U.S. Forest Service in 1948. The H.J. Andrews Experimental Forest is one of 80 U.S. Forest Service Experimental Forests and one of 28 sites in the National Science Foundation-funded Long-Term Ecological Research Network.

Air temperature is a critical variable in ecology because it regulates biological processes, influencing growth, development, reproduction, thermoregulation, and the phenology of organisms, as well as biogeochemical rates. Air temperature data has been recorded globally for hundreds of years, and is one of the most highly leveraged research investments. However, air temperature time series can include substantial

random variation and systematic deviation (bias) from non-climatic artifacts, such as instrument configuration and instrument and method changes. The goal of my first study was to quantify measurement differences between the current air temperature instrument used at H.J. Andrews Experimental Forest's primary climate station and three other instruments that have been used there over the past twenty years. The current instrument is widely considered to be the most accurate, while the other instruments are prone to warm-biased measurements. The magnitude of bias depends on siting and environmental conditions (particularly incoming solar radiation, albedo, and wind speed), time of day, and the measurement's temporal and statistical aggregation. While other field studies have quantified differences between air temperature instruments, they were typically only a few weeks duration and did not explore how bias aggregates at different temporal and statistical resolutions. Using data collected continuously over a period of six years, we found that measurement differences for average temperatures in the daytime were as large as 7.7°C, median differences up to 0.9°C, and that as many as 68% of measurements had differences +/-0.4ºC. Daily maximum resolution was the most sensitive to differences, with median differences up to 1.2°C, and as many as 78% of measurements with differences +/-0.4ºC. H.J. Andrew's air temperature data are publically available on the web site, and often used by researchers in trend analyses, such as for climate change. Data from warm-biased instruments, especially when combined and treated as continuous with data from more accurate instruments, can complicate analyses and may lead to erroneous conclusions. One of the practical goals of the study was to explore if incoming solar radiation, reflected solar radiation, and wind speed observations recorded concurrently with air temperature data can be used to model measurement differences. We found that differences can be relatively well-estimated using models incorporating these variables. The results of this study will be used to supplement H.J. Andrews air temperature data and metadata, and can potentially be used by researchers to adjust measurements taken by warm-biased instruments at the H.J. Andrews climate station.

The goal of my second study was to evaluate how terrestrial flying insect abundance and thermal patterns vary across landscape gradients over a period of five

years, and if there is a relationship between abundance and thermal variation. Complex forest landscapes like H.J. Andrews can contain a variety of microclimates, which have the potential to act as refugia for insects and other wildlife in changing climate conditions. Even though insects are the most abundant and diverse organisms, they are underrepresented in the literature, with a bias towards species of medical and economic importance. This study contributes valuable information about the springtime abundance dynamics of a broad flying forest insect population, as well as three genera from the Diptera (true flies) and Coleoptera (beetles) orders, for which there is little information in the literature. We found that thermal patterns (represented as cumulative growing degree days) and insect abundance (broadly and for the three genera) were widely variable across sixteen sites within a year, and less variable within sites over five years. One year in particular (2011) had dramatically different abundance patterns than the other four years of the study. We also modeled the relationship between cumulative growing degree-days and insect abundance at each site, and found the relationship was widely variable in a sampling year among sites, as well as within sites among sampling years, suggesting that factors other than thermal accumulation may strongly influence abundance. These types of long-term studies are important to establish baselines and understand the environmental conditions under which terrestrial flying insect abundance within a forest can fluctuate, as well as the habitat characteristics that may be associated with abundance.

©Copyright by Stephanie A. Schmidt
December 5, 2019
All Rights Reserved

Buzzing Bolbomyiidae and Air Temperature Monitoring Methods: Investigating Long-Term Ecological Data from the H.J. Andrews Experimental Forest

by
Stephanie A. Schmidt

A THESIS

submitted to

Oregon State University

in partial fulfillment of
the requirements for the
degree of

Master of Science

Presented December 5, 2019
Commencement June 2020

Master of Science thesis of Stephanie A. Schmidt presented on December 5, 2019

APPROVED:

Co-Major Professor, representing Forest Ecosystems and Society

Co-Major Professor, representing Forest Ecosystems and Society

Head of the Department of Forest Ecosystems and Society

Dean of the Graduate School

I understand that my thesis will become part of the permanent collection of Oregon State University libraries. My signature below authorizes release of my thesis to any reader upon request.

Stephanie A. Schmidt, Author

ACKNOWLEDGEMENTS

I would like to thank my committee, Lisa Ganio, Mark Schulze, and Sherri Johnson for their support, time, and guidance throughout my program. I feel very lucky to have worked with such a caring, thoughtful group.

Much gratitude to the H.J. Andrews Experimental Forest organization for funding my assistantship and research. Research was conducted at H.J. Andrews Experimental Forest, which is funded by the U.S. Forest Service, Pacific Northwest Research Station. Data were provided by the H.J. Andrews Experimental Forest and Long Term Ecological Research program, administered cooperatively by the USDA Forest Service Pacific Northwest Research Station, Oregon State University, and the Willamette National Forest. This material is based upon work supported by the National Science Foundation.

A huge thank you to the Information Management team at H.J. Andrews for the moral support and kindness, and the constructive feedback that improved my analysis and presentations. I also appreciate all the time they took to impart the complexity of gathering and managing environmental data.

Special thanks also to Chris Daly for sharing so much climate analysis expertise and helping me to parse out my analysis to increase the practical impact. Many thanks also to Ariel Muldoon for teaching me the technical skills to analyze and visualize my data, and for her assistance with the insect abundance statistical modeling.

Thanks to all the friends and peers that have helped me and commiserated along the way. But most of all, thanks to my partner Tim Glidden. Your love of natural spaces and curiosity opened a whole new world to me. You've inspired me so much, and I wouldn't have made it here without your encouragement, support, and patience.

CONTRIBUTION OF AUTHORS

Mark Schulze designed and assembled the air temperature sensor comparison experiment (Chapter 2). Data was collected and processed by the H.J. Andrews Experimental Forest Information Management team.

Mark Schulze and Sherri Johnson designed and assembled the insect abundance experiment (Chapter 3) with the assistance of Judith Li. Data was collected by numerous field crew members, and processed by student lab members led by Bill Gerth.

Data analysis and interpretation for both experiments was conducted by Stephanie A. Schmidt with input and help from Lisa Ganio, Mark Schulze, Sherri Johnson, and Ariel Muldoon.

TABLE OF CONTENTS

Page

CHAPTER 1: GENERAL INTRODUCTION 1

CHAPTER 2: MEASUREMENT DIFFERENCES BETWEEN AIR TEMPERATURE INSTRUMENTS AND IMPLICATIONS FOR TREND ANALYSES 2

Introduction 2

Methods 5

Research site 5
Instrumentation 5
Data collection and processing 6
Data aggregation 7
Data analysis 8

Results 11

Study site climate conditions 11
Distribution of measurement differences 11
Explanatory variable relationships 13
Growing degree-day accumulation comparison 14
Estimation of measurement differences 14

Discussion 15

Literature cited 22

Figures 25

Tables 34

TABLE OF CONTENTS (Continued)

Page

CHAPTER 3: MICROCLIMATE AND ABUNDANCE OF FLYING INSECTS IN A CONIFER FOREST 42

Introduction 42

Methods 45

Research sites 45
Insect sampling and processing 45
Climate data collection and processing 46
Data and statistical analysis 48

Results 49

Thermal variation 49
Insect abundance 50
Relationship between sample abundance and air temperature and precipitation during the sampling period 50
Comparison of cumulative abundance per sampling and cumulative GDD relationships 51

Discussion 51

Literature cited 54

Figures 59

Tables 70

CHAPTER 4: GENERAL CONCLUSION 72

BIBLIOGRAPHY 73

APPENDICES 80

Appendices of Figures 81
Appendices of Tables 97

LIST OF FIGURES

Figure Page

2.1 Timeline of air temperature instrumentation at H.J. Andrews PRIMET station 25

2.2 Differences (ºC) between wind-ventilated and aspirated air temperature instruments by time of day 26

2.3 Density plot of differences in the daytime 15-minute average observations.....27

2.4. Ridgeline plots with monthly distribution of daytime 15-minute average ΔTs (°C).....28

2.5. Density plot of ΔTs (°C) for the daily average, daily maximum, monthly mean daily average and monthly mean daily maximum observations.....29

2.6. Plots of cumulative GDD using two different calculation methods 30

2.7. Daytime 15-minute average observation ΔTs (°C) against incoming solar radiation (W/m^2), albedo (W/m^2), and wind speed (m/s)..... 31

2.8. Plots of explanatory variable relationships 32

2.9. Estimated vs. observed ΔTs (°C) for each best estimation model 33

3.1 Relative location of study sites within the H.J. Andrews Experimental Forest 59

3.2 Cumulative GDD by day of year paneled by sampling year 60

3.3 Cumulative GDD by day of year paneled by site 61

3.4 Relationship between elevation and winter and spring GDD.....62

3.5 Last day of year with > 50% snow cover by site and sampling year 63

3.6 Cumulative abundance per sampling day vs. day of year, paneled by site and sampling year 64

3.7 *Scellus* cumulative abundance per sampling day vs. day of year, paneled by site and sampling year 65

3.8 *Bolbomyia* cumulative abundance per sampling day vs. day of year, paneled by site and sampling year 66

LIST OF FIGURES (Continued)

Figure Page

3.9 *Anaspis* cumulative abundance per sampling day vs. day of year, paneled by site and sampling year 67

3.10 Abundance per sampling day vs. average hourly temperature and proportion of days with measurable precipitation during the sampling period 68

3.11 Estimates and confidence intervals of the change in cumulative abundance per sampling day per cumulative GDD 69

LIST OF TABLES

Table Page

2.1 Instrumentation summary 34

2.2 Summary of data by instrument 35

2.3 Summary of ΔT (°C) for daytime, nighttime and all 15-minute average measurements 36

2.4 Summary of ΔTs (°C) for daily average, daily maximum, monthly mean daily average, and monthly mean daily maximum statistics 37

2.5 Comparison of two GDD accumulation methods 38

2.6 Estimation model explanatory variables for each instrument 39

2.7 Adjusted R^2 values for single variable models 40

2.8 Comparison of estimated vs. observed ΔTs (°C) for daytime 15-minute average measurements 41

3.1 Site characteristics 70

3.2 Number of samples and sampling days at each site 71

LIST OF APPENDIX FIGURES

Figure Page

A.1 Autocorrelation plots of time series of instrument ΔTs 81

A.2 Time series of the 15-minute average air temperature for each instrument.....82

A.3 Ridgeline plots of distribution of 15-minute average daytime incoming solar radiation and albedo & all wind speeds by season.....83

A.4 Density plot of ΔTs for all 15-minute average observations 84

A.5 Density plot of ΔTs for 15-minute average nighttime observations.....85

A.6 Density plot of ΔTs for daily minimum observations.....86

A.7 Density plot of ΔTs for all monthly mean daily minimum observations.....87

A.8 Conditioning plots of daytime 15-minute average observation ΔTs (°C) against incoming solar radiation (W/m^2), albedo (W/m^2), and wind speed (m/s) 88

A.9 Model residuals against observed incoming solar radiation (W/m^2), albedo (W/m^2), and wind speed (m/s)..... 89

A.10 Conditioning plots of model residuals against incoming solar radiation (W/m^2), albedo (W/m^2), and wind speed (m/s)..... 90

A.11 Plot of albedo (W/m^2) against ΔTs by season.....93

A.12 Cumulative abundance per sampling day on the last day of sampling 94

A.13 Cumulative abundance per sampling day by daylength.....95

A.14 Insect families identified in 2009 by site 96

LIST OF APPENDIX TABLES

Table Page

A.1 Summary statistics of observations for all resolutions and instruments 97

A.2 Summary statistics of ΔTs (°C) for daily minimum observations 102

A.3 Summary statistics of ΔTs (°C) for monthly mean daily minimum observations.....103

A.4 Summary statistics for binned daytime 15-minute average observations.....104

A.5 Regression results and optimism-corrected coefficient estimates for each best estimation model 105

A.6 Number of imputed hourly air temperature records by site and sampling year.....106

A.7 Regression equations for imputed air temperature values 107

A.8 Count of insects by family and study site from 2009 sampling year.....108

DEDICATION

This work is dedicated to my mom and dad. Mom, I wish that you were here to see me achieve this. Thank you for making college a non-negotiable, and for everything you sacrificed so your children could be successful. I miss you and think about you every single day. Dad, thank you for teaching me about persistence, and how sometimes we have to just get up and do the work, even when we're exhausted and things seem bleak. I love you, and thank you for everything that you did to help me to achieve this goal.

CHAPTER 1: GENERAL INTRODUCTION

The short-term duration of most ecological studies can make it difficult to capture the long-term dynamics of ecosystems and populations. Infrequent or high-impact events can be missed, or can be erroneously documented as baselines when they occur during small study windows. Long-term ecological research can enable a deeper understanding of complex processes, provide a foundation for future insights, and improve research methods and management.

In my research, I used data collected in two long-term studies at the H.J. Andrews Experimental Forest in Oregon's Western Cascades, established by the U.S. Forest Service in 1948 and one of 28 stations in the National Science Foundation-funded Long-Term Ecological Research Network. In my first chapter, I examine measurement differences between four types of instruments which have been used for various durations in the past 50 years to collect air temperature data of record at a benchmark meteorological station. I evaluate how much measurement differences among instruments can be explained by three environmental variables, and how differences may impact trend analyses. The broader purpose of this study was to improve air temperature collection methods, as well as inform researchers how method changes could potentially impact analyses and how to adjust their analysis methods to account for these changes.

In my second chapter, I examine insect abundance and air temperature data collected in the spring for five years at 16 sites representative of H.J. Andrews' diverse landscape gradients. I evaluate the variability of insect abundance and thermal patterns between and within sites over time, as well as how the relationship between insect abundance and growing degree-days differed between sites. This study provides foundational knowledge about thermal and insect abundance patterns at H.J. Andrews, which will be synthesized with similar studies of vegetation and birds in the forest, allowing researchers to better understand the complex dynamics of trophic linkages within the forest.

CHAPTER 2: MEASUREMENT DIFFERENCES BETWEEN AIR TEMPERATURE INSTRUMENTS AND IMPLICATIONS FOR TREND ANALYSES

INTRODUCTION

Climate change impacts are a key research focus across ecological domains. High-quality climate data are necessary to construct models to accurately estimate and predict trends and ecosystem changes. As sensor technology has improved and decreased in cost, environmental sensor networks have proliferated. Data publishing efforts have given researchers access to extensive global climate datasets at ever-increasing temporal resolution (Daly 2006, Hampton et al. 2013, Rundel et al. 2009). Affordable sensor technology has also enabled researchers to deploy exponentially more sensors and gather climate data at finer spatial resolutions (Potter et al. 2013). However, abundant data are not necessarily high-quality or consistent data.

Climate time series can include substantial random variation and systematic deviation (bias) from non-climatic artifacts, such as instrument configuration and instrument and method changes (Michener 2015, Peterson et al. 1998, Quayle et al. 1991, Thorne et al. 2016). These inconsistencies over space and time lead to additional variation that can complicate trend analyses, making it difficult to accurately identify climate change signals (Peterson et al. 1998, Thorne et al. 2005). Researchers who are unaware or underestimate the impact of this additional variation may draw incorrect conclusions due to unaccounted for effects (Peterson et al. 1998). For example, high-elevation warming in the western United States was overestimated by approximately 1°C per decade due to systematic measurement bias in the SNOTEL network from method and instrument changes which were unaccounted for in analyses (Oyler et al. 2015). Bias can also propagate in subsequent studies when climate datasets are reused. In the case of the SNOTEL network, propagated bias in climate data products were found to amplify minimum temperature warming estimates over three decades by 217-562% (Oyler et al. 2015).

A key challenge for climate data reuse is that much historic weather station data were collected using methods best suited for near-term weather forecasting, not continuous, long-term analyses (Thorne et al. 2005). Documentation and metadata related to siting, instrumentation, methods, and timing of changes are widely variable; and this issue is prevalent in most data repositories (Hampton et al. 2013, Thorne et al. 2005, Trewin 2010). Metadata on quality control procedures, including changes to raw data, are often incomplete (Michener 2015). Even when

quality metadata are available, it can be difficult for researchers to find and understand how best to incorporate this information (Peterson et al. 1998).

Bias arising from changes to air temperature instruments are mainly a function of differences in instrument performance. Air temperature instruments have two main components: a sensor and a radiation shield. The radiation shield protects the sensor from direct and indirect radiation and other elements (Thomas and Smoot 2013). Ideally, the sensor is at equilibrium with the ambient air temperature and delivers an accurate measurement. However, the shield can create a concentrated space for convection and conduction around the sensor, and these microclimate effects can cause systematic deviations from the true ambient temperature (Lin et al. 2001a, Lin et al. 2001b).

These systematic deviations are commonly referred to as "radiation bias," and are well-documented in the literature. Both field and lab experiments have linked deviations in wind ventilated instruments to incoming solar radiation and wind speed (Hubbard et al. 2001, Lin et al. 2001a, Lin et al. 2001b, Lin et al. 2001c, Mauder et al. 2008, Richardson et al. 1999). These deviations have been found to be up to 4ºC at low wind speeds (< 2 m/s) (Hubbard et al. 2004, Lin et al. 2001c, Richardson et al. 1999). The height at which instruments are located and site surface conditions can influence environmental interactions which impact instrument performance (Ashcroft 2018, Nakamura and Mahrt 2005). When wind-ventilated instruments are located over snow, 30-minute mean deviations can be up to 10ºC due to albedo effects (Huwald et al. 2009). Passive instruments with custom-fabricated shields were found to experience a deviation of 0.7ºC for every 10% of impervious site surface area (Terando et al. 2017). Custom-fabricated shield performance is particularly concerning as construction and materials aren't typically standardized or well-documented, and are often deployed without testing or calibrating with higher-quality instrumentation (Terando et al. 2017). Mechanically ventilated (aspirated) shields are considered the best option and the "gold standard" as they ensure adequate airflow across the sensor body, independent of site conditions (Thomas and Smoot 2013).

Biases can also propagate depending on data aggregation and the choice of summary statistics. Before digital sensors were widely available, daily average temperature was recorded by taking the average of the maximum and minimum temperatures recorded by a maximum-minimum thermometer (Wang 2014). Growing degree-days (GDD), used in agricultural and ecological phenology studies, have long been derived using this method to calculate daily

average temperature. Now that researchers have access to high-resolution data, a more accurate daily average temperature can be calculated. However, issues can arise when comparing GDD accumulation estimates derived from these different daily average temperature calculation methods (Weiss and Hays 2005). Daily average temperatures calculated from maximum and minimum temperatures are biased primarily because they're only based on two measurements, leaving most of the day unmonitored. There is also systematic bias due to differences in the drivers of daytime warming and nighttime cooling, which are dependent upon geography and other factors (Wang 2014). This bias is reduced when using high-resolution measurements to calculate the daily average temperature.

Here we examine the differences in air temperature measurements between an instrument with a fan-aspirated shield (the reference) and three with wind-ventilated shields, including the extent to which variation in these differences can be explained by environmental variables. Each of these instruments have been used historically at H.J. Andrews Experimental Forest and Long-Term Ecological Research Site, where climate monitoring has been conducted since the 1950s. Instrumentation at the site has been regularly upgraded as new technology and methods have developed (Figure 2.1). These changes in air temperature instrumentation changes at one of the site's primary meteorological stations are a good example of how frequently these types of discontinuities can occur in a long-term climate dataset.

Previous studies have assessed the measurement differences between air temperature instruments using various shields. However, long-term field studies conducted over a range of environmental conditions that compare a manufactured aspirated shield with both manufactured and custom-fabricated wind-ventilated shields are lacking, as is evaluation of how these differences may propagate in data at different temporal and statistical aggregations. We examined: 1) air temperature measurement differences between aspirated and wind-ventilated radiation shields, 2) how air temperature measurement differences may aggregate in common summary statistics (high-resolution average, daily average, maximum, and minimum; monthly mean daily average, maximum, and minimum; and growing degree-days), and 3) the degree to which measurement differences can be explained by incoming solar radiation, albedo, and wind speed using modeling techniques that can be relatively easily applied by researchers.

METHODS

Research site

The study was located at the Primary Meteorological Station (PRIMET) at H.J. Andrews Experimental Forest, located in Oregon's Western Cascades (44.21, -122.26, elevation 430m). The PRIMET site is approximately 29 x 23 m^2, exposed and relatively flat, with conifer forests outside the perimeter. It is located in the bottom of a valley with steep ridges to the southeast and northwest. Annual precipitation is 2200 mm, which occurs primarily November through May. Snow can accumulate at this site in winter, but it does not remain for long periods. Summers are generally dry and warm, with cool nights and occasional thunderstorms.

Instrumentation

General instrument descriptions

Instruments measuring air temperature, wind speed, incoming solar radiation and reflected solar radiation (see Table 2.1 for photos and specifications) were placed side-by-side at 1.5m above the ground. There were four air temperature instruments, all using an identical sensor (Campbell Scientific 107 thermistor) but different radiation shields: 1) fan-aspirated (ASP or aspirated), 2) cotton region shelter (CRS), 3) Gill multi-plate (Gill), and 4) a custom-fabricated shield developed by staff at the research site (HJA). One propeller anemometer was used to measure wind speed. One upward-facing pyranometer measured incoming solar radiation (ISR), and one down-facing pyranometer measured reflected solar radiation (for brevity, we use the term "albedo", though it is technically reflected solar radiation and not albedo). All sensors were connected to the same data logger (Campbell Scientific CR1000).

Air temperature instrument radiation shield descriptions

Fan-aspirated shields use a blower motor to draw air over the shield, providing ventilation independent of wind speed (Richardson et al. 1999) and are currently considered the best-performing shield option (Thomas and Smoot 2013). However, their power requirements limit use at remote sites without line power or solar arrays. They are also more expensive than other shield options.

The CRS (sometimes referred to as a Stevenson screen) has been used for many decades at meteorological stations (Hubbard et al. 2001). It is a wooden cabinet painted white to reflect

solar radiation, allowing passive airflow through slats. The structures are large, originally built to accommodate liquid-in-glass maximum and minimum thermometers (Hubbard et al. 2001). The development of small and accurate temperature sensors led to the development of smaller radiation shields. The CRS is still widely used, but smaller instruments have either replaced or supplemented the CRS at many stations (Hubbard et al. 2001).

The multi-plate Gill shield is commonly used at weather stations and in field experiments. The shield's parallel slats allow air flow across the sensor while shielding from direct solar radiation. However, some upwelling shortwave radiation can reach the sensor (Arck and Scherer 2001). For stations that consistently experience wind speeds greater than 1-2 m/s, this shield usually provides sufficient ventilation to mitigate radiation bias (Richardson et al. 1999).

The HJA is one of many custom-fabricated shields that researchers have developed as a cost-effective alternative to manufactured shields (Holden et al. 2013, Hubbart et al. 2005, Terando et al. 2017). The HJA consists of an 8-inch long, 3.5 inch diameter, schedule 40 PVC pipe split in half lengthwise and placed over ¾-inch diameter PVC tubing that houses the sensor (Smith 2002).

Data collection and processing

Air temperature, incoming solar radiation, albedo, and wind speed data were collected continuously between April 2011 and April 2017. Measurements were taken every 15 seconds, and the average for a 15-minute period (60 observations) was recorded (referred to hereafter as "15-minute average observations"). Additionally, from April 2015 to April 2017, measurements were taken every 15 seconds, and for each 5-minute period (20 observations), the maximum and minimum air temperature and maximum incoming solar radiation, albedo, and wind speed were recorded (referred to hereafter as "5-minute observations" with the relevant statistic specified). Table 2.2 outlines the data resolution, observation dates, and statistics collected for each instrument.

All data were reviewed for quality control using an automated process (GCE Data Toolbox Version 3.9.4b - https://gce-lter.marsci.uga.edu/public/im/tools/data_toolbox.htm). Rows with missing observations for aspirated air temperature, incoming solar radiation, albedo, or wind speed were removed, with a total of 6,097 rows (out of 210,504) removed from the 15-

minute data and 8,358 rows (out of 210,792) removed from the 5-minute data. Data logger issues from February 27-March 7, 2013 and August 2-31 in 2016 caused most missing values. Data flagged as questionable in the automated process were checked manually to determine if values were feasible. Additionally, a quality check was performed on the fan-aspirated air temperature observations, since the instrument can experience large daytime temperature spikes if power to the fan stops. The 15-minute average, 5-minute average, and 5-minute maximum observations were analyzed separately for these spikes. Fan-aspirated observations that deviated more than 0.4°C (double the range of sensor accuracy) warmer than the maximum simultaneous wind-ventilated instrument observation were examined using boxplots. Observations greater than twice the interquartile range above the median were checked manually to determine if they were feasible, and likely outliers were removed. Between these two quality checks (data flagged as questionable and the fan-aspirated observations), six values were removed from the 15-minute average data and none were removed from the 5-minute data (as values were determined to be feasible).

Data aggregation

The 5-minute observations were summarized with the following statistics: daily average (from 5-minute average), daily maximum (from 5-minute maximum), and daily minimum (from 5-minute minimum – air temperature only as incoming solar radiation, albedo, and wind speed were assumed to be zero). Only days missing less than one hour's worth of measurements were included. From the daily statistics, we calculated the monthly mean daily average (average of all daily average values for a month) monthly mean daily maximum (average of all daily maximum values for a month), and monthly mean daily minimum (average of all daily minimum values for a month). Observations from August 2016 were removed due to missing aspirated observations described above.

Cumulative growing degree-days were also calculated. A degree-day is typically calculated by taking a daily average air temperature statistic and subtracting a minimum threshold temperature specific to an organism of interest. Growing degree-days (GDD) are the cumulative sum of degree-days > 0 in a specified date range. As mentioned in the introduction, historic GDD calculation methods use the average of the daily maximum and minimum as the daily average temperature statistic. However, with recent availability of high-resolution data, a

potentially more accurate daily average can be calculated. Issues may arise in analysis when GDD accumulations are compared or synthesized when different methods for calculating the daily average temperature are used. To quantify the magnitude of difference between methods, we calculated GDD for the period November 2015 through July 2016 using two methods: one using the daily average air temperature calculated from 5-minute resolution measurements (T_{avg}), and the other using the average of the daily maximum and daily minimum air temperature (calculated as described in the previous paragraph) (T_{mma}). A minimum threshold temperature of 5°C (T_{base}), commonly used in insect studies (Hodgson et al. 2011), was applied in the degree-days calculation.

Data analysis

Air temperature measurement differences (referred to hereafter as "ΔT") were calculated for each of the three wind-ventilated instruments (CRS, Gill, and HJA) as the wind-ventilated instrument temperature measurement minus the fan-aspirated instrument temperature measurement (ºC). Positive ΔT indicates the wind-ventilated instrument measured warmer than the fan-aspirated, and negative ΔT indicates that the wind-ventilated instrument measured cooler. We define a "substantial" ΔT as $|\Delta T| > 0.4$°C. This threshold is double the range of sensor accuracy specified by the manufacturer in conditions that are most typical for the study site (see Table 2.1). The threshold is intended to distinguish ΔT due to inherent sensor error from error due to other variables.

Distribution of air temperature measurement differences

Histograms and summary statistics were used to examine ΔT distributions for the following statistics: 15-minute average (all and daytime-only observations), daily average, daily maximum, daily minimum, monthly mean daily average, monthly mean daily maximum, and monthly mean daily minimum. GDD derived using the two different calculation methods were compared both within and among shield types using summary statistics and graphically using line plots.

"Daytime" is defined as one hour after sunrise and one hour before sunset. This definition was necessary due to the topography of the mountainous research site (located in the bottom of a valley with steep ridges to the southeast and northwest), which impacts daylight

timing and reduces the amount of daylight that the site receives. Sunrise and sunset times are calculated using the StreamMetabolism package for R (R Core Team 2016, Sefick 2016), which uses National Oceanic and Atmospheric Administration (NOAA) solar calculation methodology for apparent sunrise and sunset (NOAA 2018). Seasons were defined based on equinox and solstice dates and times from NOAA (NOAA 2018).

Estimating measurement differences from incoming solar radiation, albedo, and wind speed

A key study objective was to examine if ΔT can be estimated by incoming solar radiation, albedo, and wind speed using regression methods relatively easily applied by researchers. Unless otherwise specified, explanatory variables are incoming solar radiation (W/m^2), albedo (W/m^2), and wind speed (m/s). For each wind-ventilated instrument (CRS, Gill, HJA) the relationship between daytime 15-minute average ΔT and incoming solar radiation, albedo, and wind speed were examined using scatterplots, conditioning plots, and with multiple regression. We excluded nighttime observations since our method of measuring incoming solar radiation and albedo would not properly capture the relationship with nighttime ΔT, and an appropriate measure (like net radiation) was not available. Additionally, the majority of substantial ΔTs ($|\Delta T| > 0.4°C$) occur during the daytime (Figure 2.2).

We chose not to use a time series analysis for these data. Rather, we patterned our regression analysis after a similar study analyzing ΔTs that used a method involving binning data to reduce the correlation among observations for analysis (Nakamura and Mahrt 2005). The range of daytime 15-minute average values for incoming solar radiation, albedo, and wind speed were each evenly split into 20 bin, resulting in 8,000 possible combinations of explanatory variables (20*20*20 = 8,000). The median observed value for each explanatory variable and the median observed ΔT for each unique combination of the three explanatory variable bins were used to create a new dataset for the statistical analysis. For example: in one bin, the incoming solar radiation range was 556-612 W/m^2 (median = 586.2 W/m^2), the albedo range was 101-126 W/m^2 (median = 114.0 W/m^2), and the wind speed range was 0.6-0.7 m/s (median = 0.6 m/s). The median observed CRS ΔT for those explanatory variable ranges was 1.1°C. The four median values then became one row in the new dataset used for analysis (CRS ΔT = 1.1°C, incoming solar radiation = 586.2 W/m^2, albedo = 114.0 W/m^2, wind speed = 0.6 m/s).

We carried out the regression analysis and model selection on the binned median values for the response and explanatory variables (referred to hereafter as "binned data"). Some bins represented explanatory variable ranges in which no response variable was observed, and these were treated as missing values. Weighting of the binned response values by the number of observations in each bin was not used.

Model selection

For each wind-ventilated instrument, conditioning plots of the daytime 15-minute average observations showed a non-linear ΔT response to incoming solar radiation, albedo, and wind speed, as well as potential interactions between these explanatory variables (Figure A.8). The full model for best subsets model selection included linear and quadratic terms for each of the explanatory variables, as well as interactions. We developed our set of candidate models as follows: 1) incoming solar radiation and wind speed were included as explanatory variables in all models because their relationship with ΔTs have been well-established in the literature, 2) albedo was allowed in models but not required, 3) any explanatory variable was allowed to present as either only linear, or linear plus quadratic terms, 4) all components of interactions were required to be main effects in the model. For example, for an interaction of wind speed and albedo^2, then wind speed, albedo, and albedo^2 were included as main effects in the model.

There were 24 candidate models evaluated in the selection process. Model selection was performed separately for each wind-ventilated instrument on the binned data (see Table A.4 for binned data summary statistics). Candidate models were evaluated for adherence to linear regression assumptions, including graphical examination of residuals for each model. Graphical examination of residuals from regression models suggested that the assumptions of multiple regression were met. A best "simple" model (no interaction terms) and a best "complex" model (interaction terms included) for each wind-ventilated air temperature instrument were selected based on: 1) high value of adjusted R^2, 2) low value of mean squared error (MSE), and 3) low value of AIC.

After models were selected, the R rms package was used to fit models using the ols() function. An optimism-corrected bootstrap procedure with 2,000 resamples was performed to adjust the precision of the regression coefficient estimates for overfitting bias using the bootcov() function (Harrell 2018, Harrell et al. 1996, Harrell et al. 2015, R Core Team 2016). Model

performance was evaluated using adjusted R^2 and MSE values and observed (binned data) vs. predicted data plots. Additionally, the regression coefficient estimates from each wind-ventilated instruments' respective best models were used to estimate ΔTs on the unbinned daytime 15-minute average observations, and the observed vs. estimated summary statistics were compared.

Data cleaning and statistical aggregation were performed using R (v. 3.6.1) (R Core Team 2016) and the tidyverse (v. 1.2.1) packages (Wickham 2017). All data exploration and analysis were performed using R (R Core Team 2016) and rms (v. 5.1-2) (Harrell 2018). Most visualizations were created using the ggplot2 (v. 3.2.1) package (Wickham 2016). Summary statistic tables were created using the stargazer (v. 5.2.2) package (Hlavac 2018). The forecast (v. 8.9) package (Hyndman et al. 2018) was used to generate ACF plots.

RESULTS

Study site climate conditions

Between April 2011 and April 2017, air temperatures measured by the fan-aspirated instrument ranged from -16.1°C to 40.4°C, median 8.2°C and mean 9.2°C (SD = 7.8°C) (*n* = 204,399). For observed incoming solar radiation, the maximum was 1112.0 W/m^2, minimum 0.00 W/m^2, and daytime median 121.0 W/m^2. For observed albedo, the maximum was 546.0 W/m^2, minimum 0.00 W/m^2, and daytime median 21.8 W/m^2. For observed wind speed, the maximum was 2.0 m/s, minimum 0.00 m/s, and median 0.00 m/s (Table A.1).

Climate conditions at the study site were seasonally variable (Figures A.3 & A.4). Winter and spring are typically cloudy, and incoming solar radiation and albedo were low in this period compared to the summer and fall. In the summer and early fall, median daytime incoming solar radiation was typical of clear, sunny days. Mean wind speed was slightly higher during the daytime than nighttime, and slightly higher during the summer and fall than compared to spring and winter. The site experienced periodic snow cover from November-March during the sampling period (with the amount of snow cover varying by year).

Distribution of air temperature measurement differences

The values for the 15-minute average ΔT values (the wind-ventilated instrument temperature measurement minus the fan-aspirated instrument temperature measurement) were considerably larger and more widely distributed in the daytime than at nighttime. Median daytime ΔT values were between 0.5-0.7ºC, while median nighttime ΔT values were between -

0.1- 0.04ºC (Table 2.3, daytime: Figure 2.3; nighttime: Figure A.5). The largest daytime ΔT values were between 3.3-6.5ºC larger than at nighttime, with the largest HJA daytime ΔTs up to 7.7°C, Gill up to 7.0°C, and CRS up to 4.0°C. Compared to nighttime, the daytime percentage of substantial ΔT values (|ΔT| > 0.4ºC) were nearly 10 times greater for the CRS and Gill and five times greater for the HJA.

The daytime 15-minute average ΔT values were most variable between April and September. This is the period at the study site when sunny days are most frequent. All instruments had greater median daytime ΔT values in the spring and summer than in the fall and winter. The median HJA daytime ΔT was substantial (|ΔT| > 0.4ºC) from April – September (Figure 2.4). October – March is peak rainy season, with infrequent clear days. Low solar angles, combined with steep terrain around the study site, limit the daily incoming solar radiation window in October – March, but substantial daytime ΔT values were still observed during this period, particularly for the HJA and Gill. For all daytime and nighttime 15-minute average observations combined, the median ΔT was close to zero for each instrument at 0.1°C for CRS and HJA and 0.03°C for Gill (Table 2.3). The percentage of substantial ΔT values for HJA was 35.3%, Gill 21.1%, and CRS 29.5%.

The median daily average and median daily maximum ΔT was 0.3ºC for the CRS (Table 2.4, Figure 2.5). The median Gill daily maximum ΔT was 0.5ºC, compared to a median daily average of 0.1ºC. The HJA median daily maximum ΔT was 1.2ºC, compared to a median daily average of 0.3ºC. The percent of substantial ΔT values were greater for the daily maximum than daily average for all instruments: CRS 13.9 percentage points greater, Gill 55.1 percentage points greater, and HJA 48.5 percentage points greater. The median daily minimum ΔT for all instruments was within 0.1ºC of zero, with between 2.7-11.3% of ΔT values considered substantial (|ΔT| > 0.4ºC) (Figure A.6 and Table A.2).

Each instruments' median monthly mean daily average ΔT was approximately equal to its median daily average ΔT (Table 2.4, Figure 2.5). The percentage of substantial ΔTs for the CRS monthly mean daily average increased to 43.5% from the daily average percentage of 30.8%, the percentage for the HJA decreased to 39.1% from 39.7%, and the percentage for the Gill decreased to 0.0% from 3.3%.

Each instruments' median monthly mean daily maximum ΔT was within 0.1ºC of its median daily maximum ΔT. The largest monthly mean daily maximum ΔTs were between 2.0-

3.8ºC smaller than the largest daily maximum ΔTs. However, for each instrument, the percentage of substantial ΔTs for the monthly mean daily maximum was at least 16 percentage points greater than its daily maximum percentage (Table 2.4, Figure 2.5), with the percentage for the HJA increasing to nearly 100%. Each instruments' median monthly mean daily minimum ΔT was equal to its median daily minimum ΔT, with all median values within 0.1ºC of zero, indicating that minimum temperature summary statistics are not as differentially sensitive to measurement differences as the maximum temperature. No substantial monthly mean daily minimum ΔTs were observed for any instrument (Figure A.7 and Table A.3).

Explanatory variable relationships

Scatterplots showed that the relationship between daytime 15-minute average ΔTs and incoming solar radiation, albedo, and wind were similar for each instrument (Figure 2.7). The ΔT values for each instrument became less variable and closer to zero with increasing wind speed. The ΔT values tended to increase with incoming solar radiation until ~ 600 W/m^2, then decreased at levels > ~ 600 W/m^2. Nearly all ΔT values were substantial (|ΔT| > 0.4ºC) when albedo was > 200 W/m^2. We were interested in knowing how snow cover was associated with albedo, so snow cover estimates from the study site from 2010-2012 were compared with albedo measurements from the same time period. Values of albedo > 200 W/m^2 were associated with values of snow cover > 40%. Values of snow cover > 40% were also associated with ΔTs > 4.0ºC for the HJA, and ΔTs > 2.5ºC for the CRS and Gill.

Conditioning plots showed a non-linear ΔT response to incoming solar radiation, albedo, and wind speed, as well as potential interactions between these explanatory variables (Figure A.8). When levels of incoming solar radiation were > 600 W/m^2 and albedo was > 200 W/m^2 simultaneously, 97% of ΔT values were substantial (|ΔT| > 0.4ºC). When wind speed was > 0.5 m/s, substantial ΔT values were less frequent, even when incoming solar radiation was > 600 W/m^2 and albedo was > 200 W/m^2.

We also evaluated the relationships between explanatory variables in the daytime 15-minute average data, and found that, as expected, there was a strong positive relationship between incoming solar radiation and albedo (Figure 2.8). Most (69%) incoming solar radiation observations > 600 W/m^2 occurred at wind speeds > 0.5 m/s (which may be adequate to mitigate

radiation bias according to some manufacturer specifications). Only 3 albedo observations > 200 W/m^2 were observed concurrent with wind speeds > 0.5 m/s.

Growing degree-day (GDD) accumulation method differences

Total GDD accumulation (November 2015-July 2016) was greater for all instruments when the daily average temperature was calculated using the daily maximum and minimum averaging method compared to averaging the high-resolution (5-minute average) observations (Figure 2.6). The largest within-instrument difference between the two methods was the HJA (243 GDD), and the smallest was the CRS (187 GDD) (Figure 2.6). The largest among-instrument differences when using the same method was between the fan-aspirated and the HJA, with a difference of 72 GDD using the high-resolution averaging method, and 115 GDD using the daily maximum and minimum averaging method (Table 2.5). Between instruments using two different methods, differences were 130-316 GDD.

Estimation of air temperature measurement differences

The candidate model rankings, based on evaluation of adherence to linear regression assumptions, high adjusted R^2, low MSE and AIC, and model complexity, were similar for all instruments. The best simple (no interaction terms) and complex (included interaction terms) models for each instrument included all linear terms (incoming solar radiation, albedo, and wind speed) (Table 2.6). In addition to the linear terms, in their respective simple models, the CRS included the incoming solar radiation quadratic term, the Gill included the albedo quadratic term, and the HJA included both the incoming solar radiation and albedo quadratic terms. All instruments had the same best complex model, which included all linear terms, quadratic terms for incoming solar radiation and albedo, and interactions between all terms (except between two quadratic terms, which was not allowed in models) (Table 2.6). None of the best models included a quadratic term for wind speed.

Table A.5 outlines the optimism-corrected estimates and regression statistics from the bootstrap resampling procedures performed on each best model. The complex models for each instrument had higher adjusted R^2 and lower MSE values than the simple models, however, for the CRS and HJA instruments, the differences between these metrics for the simple and complex models was small (adjusted R^2 difference 0.03 and 0.04 and MSE difference 0.01 and 0.05 for CRS and HJA, respectively) suggesting that the additional terms in complex models do not

account for additional substantive variation over the simpler models. Based on observed (binned data) vs. estimated plots (Figure 2.9), the simple models seemed to perform slightly better for the CRS and Gill, and the complex model better for the HJA.

Additionally, we tested model performance by using the best models' regression coefficients to estimate ΔTs in the unbinned daytime 15-minute average data. A comparison of the observed vs. estimated ΔT summary statistics (Table 2.8) showed that for the CRS, the summary statistics for the simple model's estimated ΔTs were closer to observed than the complex model, with estimated median and mean ΔT the same as observed. For the Gill and HJA, the summary statistics for the complex model's estimated ΔTs were closer to observed than the simple model, with estimated median and mean ΔT within 0.1ºC of observed. None of the models did well in estimating minimum ΔTs, with estimates between 1.1-2.2ºC off from the observed values.

DISCUSSION

This long-term field study assesses how air temperature measurements differ between an air temperature instrument with a fan-aspirated shield and three instruments with wind-ventilated shields in a range of weather conditions, allowing us to differentiate between instrument error and systematic deviations related to weather conditions. Our comparison shows that shield type influences the air temperature measurement, which has implications for calculations of long-term trends that use measurements from multiple instruments over time. We show that our custom-fabricated radiation shields are prone to producing systematic deviations, and maximum temperature statistics are particularly sensitive to these deviations. We also show that ΔTs can be partially explained by incoming solar radiation, albedo (technically reflected solar radiation based on our methods), and wind speed. However, the estimated relationships between ΔTs and these environmental variables differ by shield type. Statistical inference is limited to our study site.

Predictors of air temperature measurement differences

As expected, substantial ΔTs ($|\Delta T| > 0.4°C$) for all instruments were most common in the daytime, and were larger and more variable from April – September, when clear and sunny days are more frequent than in October – March. At wind speeds > 0.5 m/s, ΔTs were smaller and less

variable than at lower wind speeds, even at relatively high levels of incoming solar radiation and albedo. Contrary to expectation, ΔTs were less variable and decreased toward zero when incoming solar radiation was > 600 W/m^2 , in contrast to ΔTs when incoming solar radiation is < 600 W/m^2. However, ~70% of the incoming solar radiation observations that were > 600 W/m^2 occurred at wind speeds considered adequate to ventilate the shield and mitigate radiation bias (> 0.5 m/s). Albedo > 200 W/m^2 was associated with snow cover and particularly large ΔTs in all instruments (> 2.5°C). Local site conditions exerted strong influence on these patterns and interactions among environmental variables: wind speed and incoming solar radiation are highest and most predictable during summer afternoons when up valley flows dominate, and winter periods with snow cover and high reflected solar radiation are consistently calm. In models with a single predictor, reflected solar radiation (referred to in our study as "albedo", though it is not technically albedo) explained the most variation in ΔT for all instruments. These results suggests that researchers should consider the radiation bias effects on measurements due to albedo in air temperature instrument selection, siting, and data quality control. This is especially true for exposed study sites with ground surfaces vulnerable to upward heat flux, such as sites with impervious cover or those that experience snow accumulation.

In modeling the relationship between ΔTs and incoming solar radiation, albedo, and wind speed, we binned our time series data to reduce correlation between observations before performing multiple regression. We acknowledge that a time series analysis would likely produce more precise estimates, but our method still produced a model-estimated mean and median ΔT within 0.1ºC of the observed mean and median ΔT when applied the full, unbinned daytime 15-minute average data. So, regression modeling that includes incoming solar radiation, albedo, and wind speed may be a useful tool for researchers to estimate ΔTs between instruments using different shields. However, we acknowledge that the availability of concurrent data from co-located instruments measuring each of the variables used in our analysis may be a barrier to this approach.

Shield performance and statistic choices

There were considerable differences in the estimation of the air temperature maximum by the tested shields at daily and monthly mean daily temporal resolutions. The custom-fabricated HJA shield instrument had median daytime 15-minute average ΔTs up to 0.7ºC larger than the

manufactured CRS and Gill shield instruments. For all instruments, the median ΔTs for the maximum temperatures were larger than the median ΔTs for the average or minimum temperature of equivalent temporal resolution. These results align with other studies that have shown maximum temperatures are particularly prone to systematic deviations due to radiation bias. Extreme temperatures have become a focus in climate change research, and researchers should be aware of the potential for measurement bias in estimated maximum temperatures, even when using high-resolution measurements.

The CRS had the smallest median ΔT value for the maximum temperature statistic at all temporal resolutions, while the Gill had the smallest median ΔT value for the average temperature statistic at all temporal resolutions. The median ΔT for the minimum temperature statistic were smaller than the median ΔTs for the average and maximum temperature statistics, and no instrument had a median ΔT greater than 0.1ºC. This was expected, as minimum temperatures usually occur at nighttime, when radiation bias is least likely to cause measurement differences.

Our GDD accumulation comparison shows how shield-related measurement bias may carry into aggregated statistics. GDD is derived using a measure of daily average temperature. We compared GDD accumulations using two methods to calculate daily average temperature: the average of the daily maximum and daily minimum temperature vs. the average of all 5-minute temperature measurements for a day (288). We expect that GDD accumulation will differ between methods - independent of the air temperature instrument - due to different sources of bias in the daily average temperature calculation (Wang 2014). The magnitude of difference in GDD accumulation between methods in the fan-aspirated instrument is what might be expected due to difference in methods alone (with a key assumption that the instrument isn't vulnerable to shield-related bias). The GDD accumulation differences between the two methods were smaller for the CRS than for the fan-aspirated instrument. A potential explanation is that the CRS shield is a large cabinet, and heat takes longer to both build up and dissipate around the sensor than in compact shields (like the fan-aspirated). Thus, it is less sensitive to rapid ambient air temperature changes, as well as radiation bias. We see evidence of this in our analysis of the maximum temperature ΔTs , as the median and maximum ΔT for the CRS maximum temperature statistic were the smallest among all instruments at all temporal resolutions. So, the smaller difference in

GDD accumulation between the two methods within the CRS, compared to the other instruments, may partially be an artifact of the shield.

Shield-related measurement bias is most apparent when comparing GDD accumulation among instruments using the same daily average temperature calculation method. The Gill's compact design is more sensitive to rapid heating inside the shield than the CRS, especially in low-wind conditions. However, the compact design enables a more rapid response to ambient air temperature changes than the CRS, and thus more precise (and potentially more accurate) measurements. The Gill GDD accumulation for the high-resolution averaging method was closest to the fan-aspirated, which is expected based on our results (the Gill had the smallest median ΔT value for the average statistic at all temporal resolutions). While the HJA design is also compact, it apparently heats up quickly and stays warm (evidenced by our maximum statistics results), so it is not surprising it had the largest GDD accumulation when using the daily maximum and minimum averaging method.

Implications for data synthesis and analysis

Researchers should consider our study results when evaluating which air temperature data and instruments will best answer their specific research questions. Radiation bias can influence air temperature measurements, and our results demonstrate that deviations in measured air temperatures do not "average out" in a time series, even in coarse temporal resolutions like the monthly mean, so there is a risk in assuming that all air temperature data is accurate. Using biased data may lead to erroneous conclusions. A scenario where measurement bias could lead to incorrect conclusions is in phenology studies when, for example, historical GDD accumulations derived using the maximum-minimum averaging method for calculating daily average temperature are synthesized with accumulations derived using the high-resolution averaging method. In our results, the GDD accumulation on May 15, 2016 was 553 GDD for the HJA instrument using the maximum-minimum averaging method, compared to 384 GDD for the fan-aspirated instrument using the high-resolution averaging method – a difference of 169 GDD. According to a model sourced from Oregon State University's Integrated Plant Protection Center, adult emergence of the Asian Longhorned Beetle (*Anoplophora glabripennis (Motschulsky)*), a significant hardwood pest species, is estimated to begin at 442 GDD, with 25% adult emergence by 652 GDD (IPPC 2019). So, the difference in GDD accumulation between

two instruments using different methods is close to the difference between 1-25% adult emergence of an important pest species.

Instrument changes can introduce additional variation that can affect trend analysis. For example, if a time series starts with air temperature measurements collected using an instrument with a shield vulnerable to warm-biased measurements due to radiation bias, and the data record transitions to measurements collected by an instrument with a fan-aspirated shield, then relatively small warming trends - such as the IPCC's estimated 0.2ºC anthropogenic warming per decade - may not be detected since the measurement bias may be as large as the warming trend (Masson-Delmotte et al. 2018). As evidenced in this and other studies, custom-fabricated shields are particularly prone to measurement bias at a magnitude that could mask relatively small trend signals (Terando et al. 2017). However, if used consistently over time, the measurements from instruments with shields prone to radiation bias can still be effective in detecting patterns, such as ranking years or sites from cool to warm, depending on the precision of the evaluation and the statistic chosen.

Best practices for data collection and reuse

Researchers must consider bias in air temperature measurements, and the impact it may have on the answers to their research questions. If the "true" ambient air temperature is important for a research question, and measurement bias in instruments with lower-quality shields cannot be assessed, researchers should use an instrument with a high-quality shield or use published air temperature data that was collected using a high-quality shield. If the research budget doesn't accommodate the cost of a high-quality shield, consider whether data from a nearby weather station would be better than potentially biased data collected on-site. However, we acknowledge this can be a difficult decision, especially for research focused on microclimate. Despite their variable and sometimes marginal performance, custom-fabricated shields remain popular because high-quality shields are cost-prohibitive, especially for multi-site studies. The Gill shield used in this study cost $117, and the fan-aspirated shield cost $667, though less-expensive models are available. The CRS was almost $1,000, compared to approximately $10 for the PVC pipe used to create the HJA shield. Additionally, fan-aspirated shields require power, which may not be feasible at study sites. In choosing a design for (or developing) a custom-fabricated shield, researchers should consider: 1) Materials: some materials heat up and/or retain heat more than

others, 2) Airflow: openings for air must be balanced with the need to shield the sensor from direct and reflected solar radiation, and 3) Reflection: white surfaces are better to reflect solar radiation. However, to reiterate a key message of this study – even if you custom-fabricate a shield according to best practices, it is important to assess whether it can produce accurate and precise measurements.

Measurement bias can also be influenced by environmental factors at the study site, and there are some practical ways that researchers can mitigate this when using less-accurate shields. In considering study design and site selection, there is evidence that radiation bias occurs less frequently in areas with canopy cover and shade (Lundquist and Huggett 2008, Terando et al. 2017). Areas with average wind speeds greater than 1.0 m/s may also have fewer issues. Co-locating lower-quality instruments with a high-quality instrument for a period of time can also help researchers document the conditions when performance may be poor, and the magnitude of measurement bias that may occur. No matter what type of shield is used, if there is a mid-study instrument change, old and new instruments should be co-located for a period to calibrate measurements. Also, as part of data quality control before analysis, researchers should closely evaluate air temperatures for spikes when collected under conditions associated with bias. For example, at the H.J. Andrews study site, this would include clear, sunny days in warmer months, periods of low wind, and sunny days with snow cover.

Good metadata practices can also help to address measurement bias issues. When documenting and archiving their own climate data, researchers should include instrument configurations and specifications for any custom-fabricated instruments, as well as the details of any instrument or method changes occurring during the study. When using published data, researchers should scrutinize metadata for sensor or shield changes that have the potential to impact data before doing analysis.

Assumptions, inference, and limitations

A key assumption in our study is that the fan-aspirated air temperature instrument measures most closely to the actual ambient air temperature, and is not prone to bias. It is important to note that the statistical inference of this study is limited to our study site, and that its specific results should not be assumed to apply in other locations, as site conditions strongly influence air temperature instrument measurements (Milewska and Vincent 2016, Yamamoto et

al. 2017). For example, our study site had minimal wind speed variability and higher wind speeds in warm months than cool months, and experiences prolonged topographic and vegetation shading in winter months. Elements including ground surface reflectivity, surrounding vegetation mass and height, and humidity, as well as the vertical height in which instruments are placed, can also influence interactions that are known to cause radiation bias (Huwald et al. 2009, Nakamura and Marht 2005). Unexplained variance in our models suggest that non-shield-related factors may influence deviations from the true ambient air temperature at our study site, such as azimuth and cold-air drainage. It is also likely that there is a lag effect in the temperature and measurement difference response to the explanatory variables, and this lag is unaddressed in our models.

Conclusion

The open data movement has resulted in frequent calls for researchers to share, reuse, and synthesize published research data. Ecologists are encouraged to join their multiple (often small) dissociated studies into unified, strong foundations of knowledge. To achieve these goals, data standardization is crucial. Climate data is one of the most highly leveraged research investments, and perhaps the most used type of published data (Wallis 2010). Yet, even data from "official" meteorological stations following expert-recommended guidelines can have standardization issues. We encourage researchers to be vigilant in thoroughly documenting the climate data that they collect and share, as well as to be educated about the methods, instrumentation, and limitations of the climate data they reuse and synthesize. Making metadata and provenance more user-friendly and accessible to researchers is a worthy focus of future research and innovation. We also hope that more data sharing, reuse, and synthesis appeals are accompanied by educational resources and practical guidelines on domain-specific data quality concerns. Without education and awareness, ecology will have a foundation of flawed analyses, instead of the knowledge required to address challenges like climate change.

ACKNOWLEDGEMENTS

This work was funded by the Andrews LTER (National Science Foundation grant DEB 1440409) and USDA Forest Service, Pacific Northwest Research Station. Data and facilities were provided by the HJ Andrews Experimental Forest and Long Term Ecological Research

program, administered cooperatively by the USDA Forest Service Pacific Northwest Research Station, Oregon State University, and the Willamette National Forest.

LITERATURE CITED

Arck, M. and Scherer, D. 2001. A physically based method for correcting temperature data measured by naturally ventilated sensors over snow. Journal of Glaciology 47(159):665-670.

Ashcroft, M.B. 2018. Which is more biased: Standardized weather stations or microclimatic sensors? Ecology and Evolution 8(11):5231-5232.

Daly, C. 2006. Guidelines for assessing the suitability of spatial climate data sets. International Journal of Climatology: A Journal of the Royal Meteorological Society 26(6):707-721.

Hampton, S.E., Strasser, C.A., Tewksbury, J.J., Gram, W.K., Budden, A.E., Batcheller, A.L., Duke, C.S. and Porter, J.H. 2013. Big data and the future of ecology. Frontiers in Ecology and the Environment 11(3):156-162.

Harrell, F.E. 2018. rms: Regression Modeling Strategies. 5.1-2.

Harrell, F.E., Lee, K.L. and Mark, D.B. 1996. Multivariable prognostic models: issues in developing models, evaluating assumptions and adequacy, and measuring and reducing errors. Statistics in medicine 15(4):361-387.

Harrell, J.F.E., Bickel, P., Diggle, P., Fienberg, S.E., Gather, U., Olkin, I. and Zeger, S. 2015. Regression Modeling Strategies: With Applications to Linear Models, Logistic and Ordinal Regression, and Survival Analysis, Cham: Springer International Publishing, Cham.

Hlavac, M. 2018. stargazer: Well-Formatted Regression and Summary Statistics Tables. 5.2.2. https://CRAN.R-project.org/package=stargazer

Hodgson, J.A., Thomas, C.D., Oliver, T.H., Anderson, B.J., Brereton, T.M. and Crone, E.E. 2011. Predicting insect phenology across space and time. Global Change Biology 17(3):1289-1300.

Holden, Z.A., Klene, A.E., F. Keefe, R. and G. Moisen, G. 2013. Design and evaluation of an inexpensive radiation shield for monitoring surface air temperatures. Agricultural and Forest Meteorology 180:281-286.

Hubbard, K., Lin, X. and Walter-Shea, E. 2001. The effectiveness of the ASOS, MMTS, Gill, and CRS air temperature radiation shields. Journal of Atmospheric and Oceanic Technology 18(6):851-864.

Hubbard, K.G., Lin, X., Baker, C.B. and Sun, B. 2004. Air temperature comparison between the MMTS and the USCRN temperature systems. Journal of Atmospheric and Oceanic Technology 21(10):1590-1597.

Hubbart, J., Link, T., Campbell, C. and Cobos, D. 2005. Evaluation of a low-cost temperature measurement system for environmental applications. Hydrological Processes 19(7):1517-1523.

Huwald, H., Higgins, C.W., Boldi, M.-O., Bou-Zeid, E., Lehning, M. and Parlange, M.B. 2009. Albedo effect on radiative errors in air temperature measurements. Water Resources Research 45(8):1-13.

Hyndman, R., Athanasopoulos, G., Bergmeir, C., Caceres, G., Chhay, L., O'Hara-Wild, M., Petropoulos, F., Razbash, S., Wang, E. and Yasmeen, F. 2018. forecast: Forecasting functions for time series and linear models. 8.4. http://pkg.robjhyndman.com/forecast

Lin, X., Hubbard, K., Walter-Shea, E., Brandle, J. and Meyer, G. 2001a. Some perspectives on recent in situ air temperature observations: Modeling the microclimate inside the radiation shields. Journal of Atmospheric and Oceanic Technology 18(9):1470-1484.

Lin, X., Hubbard, K.G. and Meyer, G.E. 2001b. Airflow characteristics of commonly used temperature radiation shields. Journal of Atmospheric and Oceanic Technology 18(3):329-339.

Lin, X., Hubbard, K.G. and Walter-Shea, E.A. 2001c. Radiation loading model for evaluating air temperature errors with a non-aspirated radiation shield. Transactions of the ASAE 44(5):1299-1306.

Lundquist, J.D. and Huggett, B. 2008. Evergreen trees as inexpensive radiation shields for temperature sensors. Water Resources Research 44:5.

Mauder, M., Desjardins, R.L., Gao, Z. and van Haarlem, R. 2008. Errors of Naturally Ventilated Air Temperature Measurements in a Spatial Observation Network. Journal of Atmospheric and Oceanic Technology 25(11):2145-2151.

Michener, W.K. 2015. Ecological data sharing. Ecological Informatics 29:33-44.

Milewska, E.J. and Vincent, L.A. 2016. Preserving continuity of long-term daily maximum and minimum temperature observations with automation of reference climate stations using overlapping data and meteorological conditions. Atmosphere-Ocean 54(1):32-47.

Nakamura, R. and Mahrt, L. 2005. Air temperature measurement errors in naturally ventilated radiation shields. Journal of Atmospheric and Oceanic Technology 22(7):1046-1058.

NOAA. 2018. Solar Calculation Details. Accessed on 6/12/2018. https://www.esrl.noaa.gov/gmd/grad/solcalc/calcdetails.html

Oyler, J.W., Dobrowski, S.Z., Ballantyne, A.P., Klene, A.E. and Running, S.W. 2015. Artificial amplification of warming trends across the mountains of the western United States. Geophysical Research Letters 42(1):153-161.

Peterson, T.C., Easterling, D.R., Karl, T.R., Groisman, P., Nicholls, N., Plummer, N., Torok, S., Auer, I., Boehm, R. and Gullett, D. 1998. Homogeneity adjustments of in situ atmospheric climate data: a review. International Journal of Climatology 18(13):1493-1517.

Potter, K.A., Arthur Woods, H. and Pincebourde, S. 2013. Microclimatic challenges in global change biology. Global Change Biology 19(10):2932-2939.

Quayle, R.G., Easterling, D., Karl, T. and Hughes, P. 1991. Effects of recent thermometer changes in the cooperative station network. Bulletin Of The American Meteorological Society 72(11):1718-1723.

R Core Team. 2016. R: A language and environment for statistical computing. 3.4.3. R Foundation for Statistical Computing. https://www.R-project.org/

Richardson, S.J., Brock, F.V., Semmer, S.R. and Jirak, C. 1999. Minimizing errors associated with multiplate radiation shields. Journal of Atmospheric and Oceanic Technology 16(11):1862-1872.

RStudio Team. 2016. RStudio: Integrated Development for R. 1.1.383. RStudio, Inc. http://www.rstudio.com/

Rundel, P.W., Graham, E.A., Allen, M.F., Fisher, J.C. and Harmon, T.C. 2009. Environmental sensor networks in ecological research. New Phytologist 182(3):589-607.

Sefick, S.J. 2016. Stream Metabolism: A package for calculating single station metabolism from diurnal oxygen curves. 1.1.2.

Smith, J.W. (2002) Mapping the thermal climate of the H.J. Andrews Experimental Forest, Oregon. Retrieved from https://andrewsforest.oregonstate.edu/publications/3117

Terando, A.J., Youngsteadt, E., Meineke, E.K. and Prado, S.G. 2017. Ad hoc instrumentation methods in ecological studies produce highly biased temperature measurements. Ecology and Evolution 7(23):9890-9904.

Thomas, C. and Smoot, A. 2013. An Effective, Economic, Aspirated Radiation Shield for Air Temperature Observations and Its Spatial Gradients. Journal of Atmospheric and Oceanic Technology 30(3):526-537.

Thorne, P.W., Menne, M.J., Williams, C.N., Rennie, J.J., Lawrimore, J.H., Vose, R.S., Peterson, T.C., Durre, I., Davy, R., Esau, I., Klein-Tank, A.M.G. and Merlone, A. 2016. Reassessing changes in diurnal temperature range: A new data set and characterization of data biases. Journal of Geophysical Research: Atmospheres 121(10):5115-5137.

Thorne, P.W., Parker, D.E., Christy, J.R. and Mears, C.A. 2005. UNCERTAINTIES IN CLIMATE TRENDS: Lessons from Upper-Air Temperature Records. Bulletin Of The American Meteorological Society 86(10):1437-1442.

Trewin, B. 2010. Exposure, instrumentation, and observing practice effects on land temperature measurements. Wiley Interdisciplinary Reviews: Climate Change 1(4):490-506.

Wang, K. 2014. Sampling biases in datasets of historical mean air temperature over land. Scientific Reports 4:4637.

Weiss, A. and Hays, C.J. 2005. Calculating daily mean air temperatures by different methods: implications from a non-linear algorithm. Agricultural and Forest Meteorology 128(1):57-65.

Wickham, H. 2016. ggplot2: Elegant Graphics for Data Analysis. 3.0.0.9. Springer-Verlag. https://www.R-project.org/

Wickham, H. 2017. tidyverse: Easily Install and Load the 'Tidyverse'. 1.2.1. https://CRAN.R-project.org/package=tidyverse

Yamamoto, K., Togami, T., Yamaguchi, N. and Ninomiya, S. 2017. Machine Learning-Based Calibration of Low-Cost Air Temperature Sensors Using Environmental Data. Sensors 17(6):1290.

FIGURES

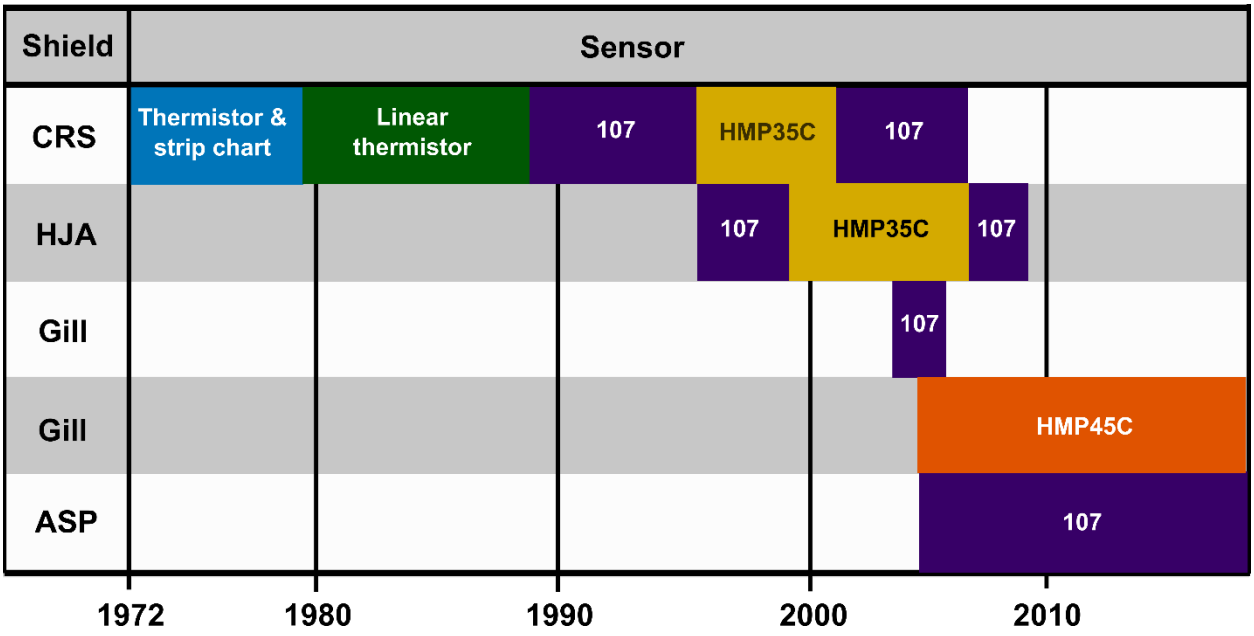

Figure 2.1 Timeline shows various radiation shield and sensor combinations that have been used to record air temperature historically at PRIMET. The 107 thermistor sensor was used with all instruments in this study (details in Table 1). The Campbell Scientific HMP35C and HMP45C sensors require a larger shield than the 107 thermistor.

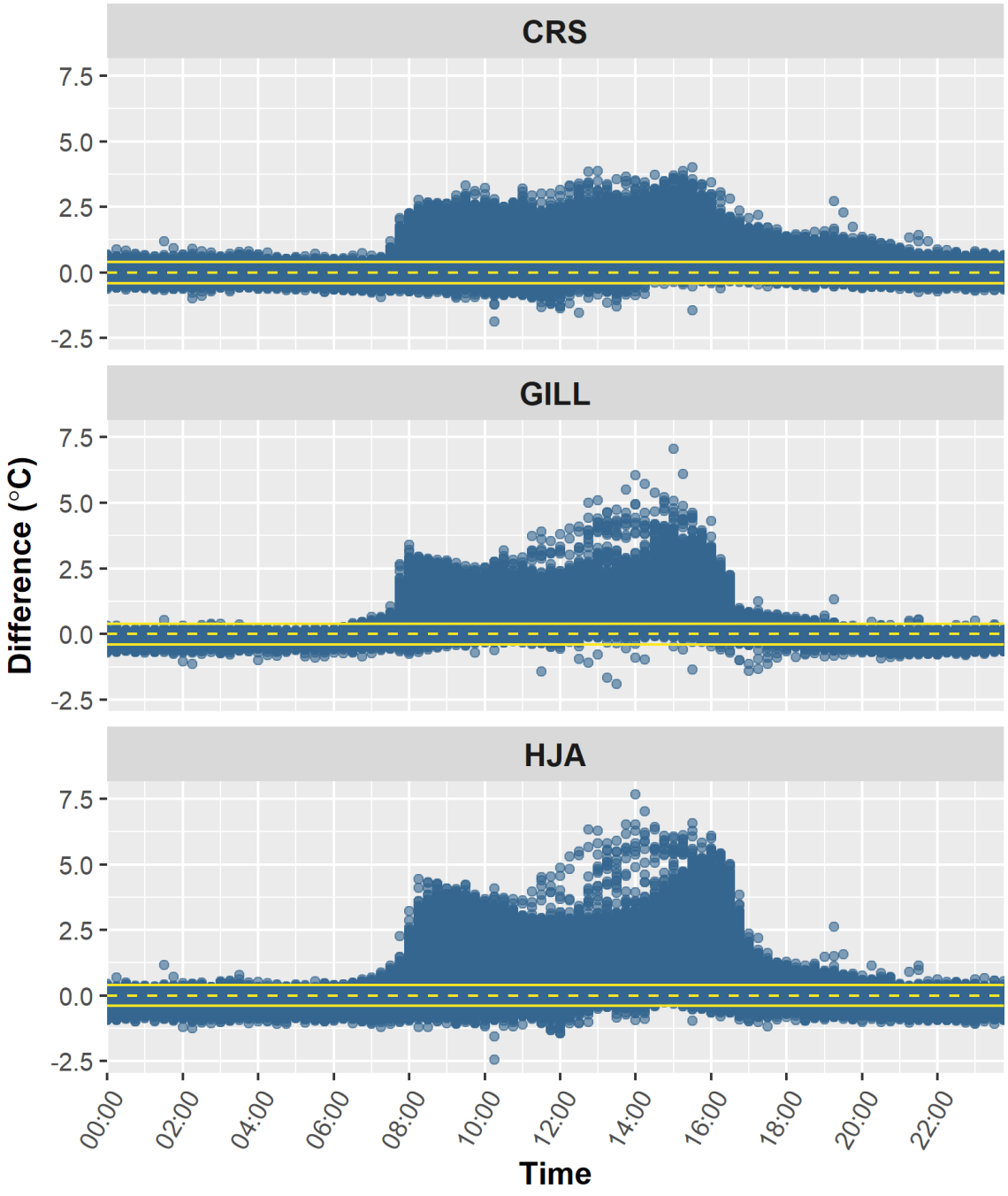

Figure 2.2 Figure shows the ΔTs between three wind-ventilated air temperature instruments and a fan-aspirated instrument by time of day (15-minute average observations, n = 204,399). Darker areas have more observations. Solid yellow lines encompass ΔTs not considered substantial (|ΔT| < 0.4°C). Dashed yellow line indicates ΔT = 0. Most substantial differences occur during the daytime.

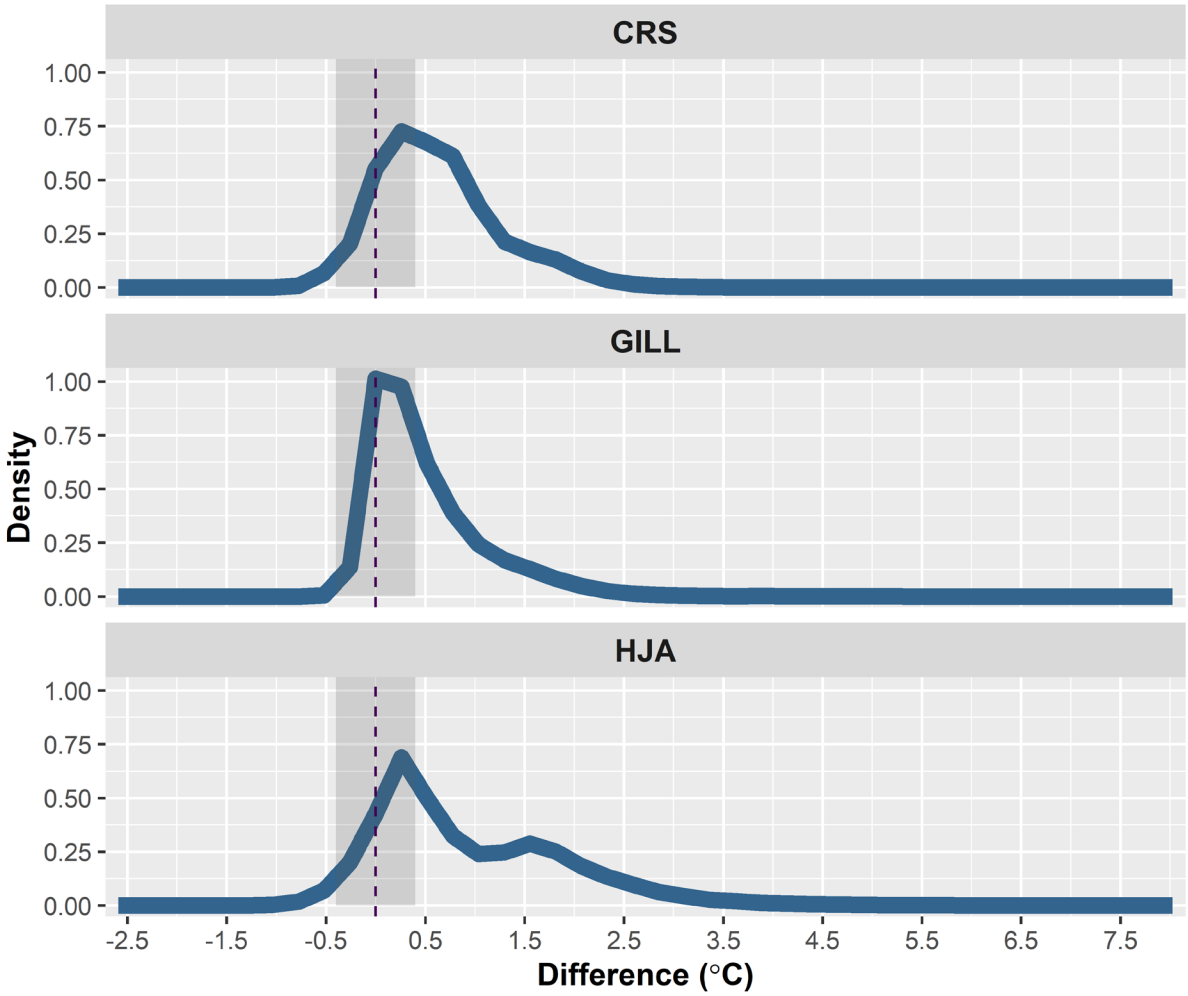

Figure 2.3 Density plot of ΔTs for the daytime 15-minute average observations. Differences are calculated as the wind-ventilated instrument measurement minus the fan-aspirated instrument measurement. Vertical dashed line indicates ΔT = 0. The ΔTs outside the shaded region are considered substantial (|ΔT| > 0.4°C).

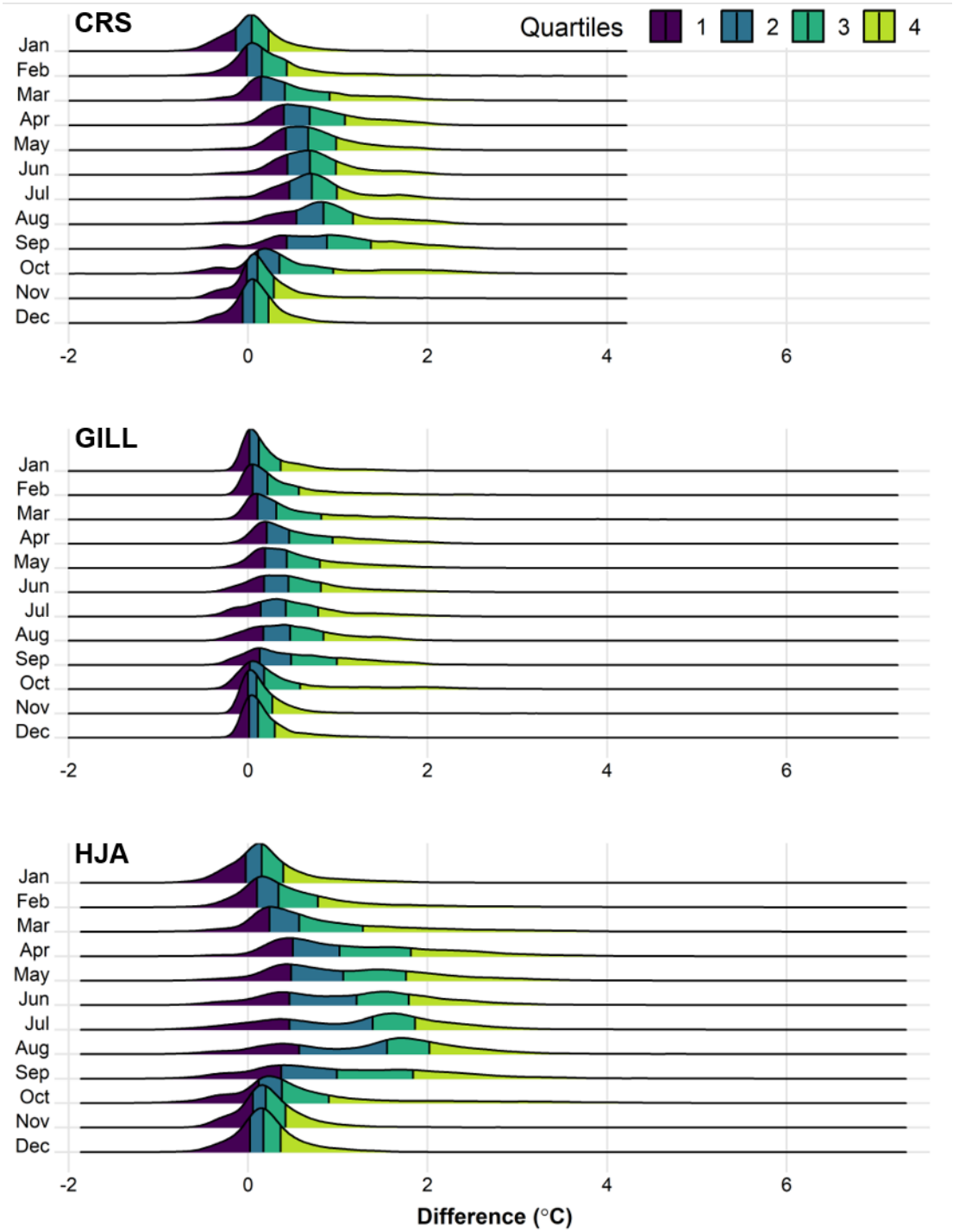

Figure 2.4 Ridgeline plots show the monthly distribution of differences in the daytime 15-minute average observations. Colors denote quartiles: first – purple, second – blue, third – green, fourth - yellow.

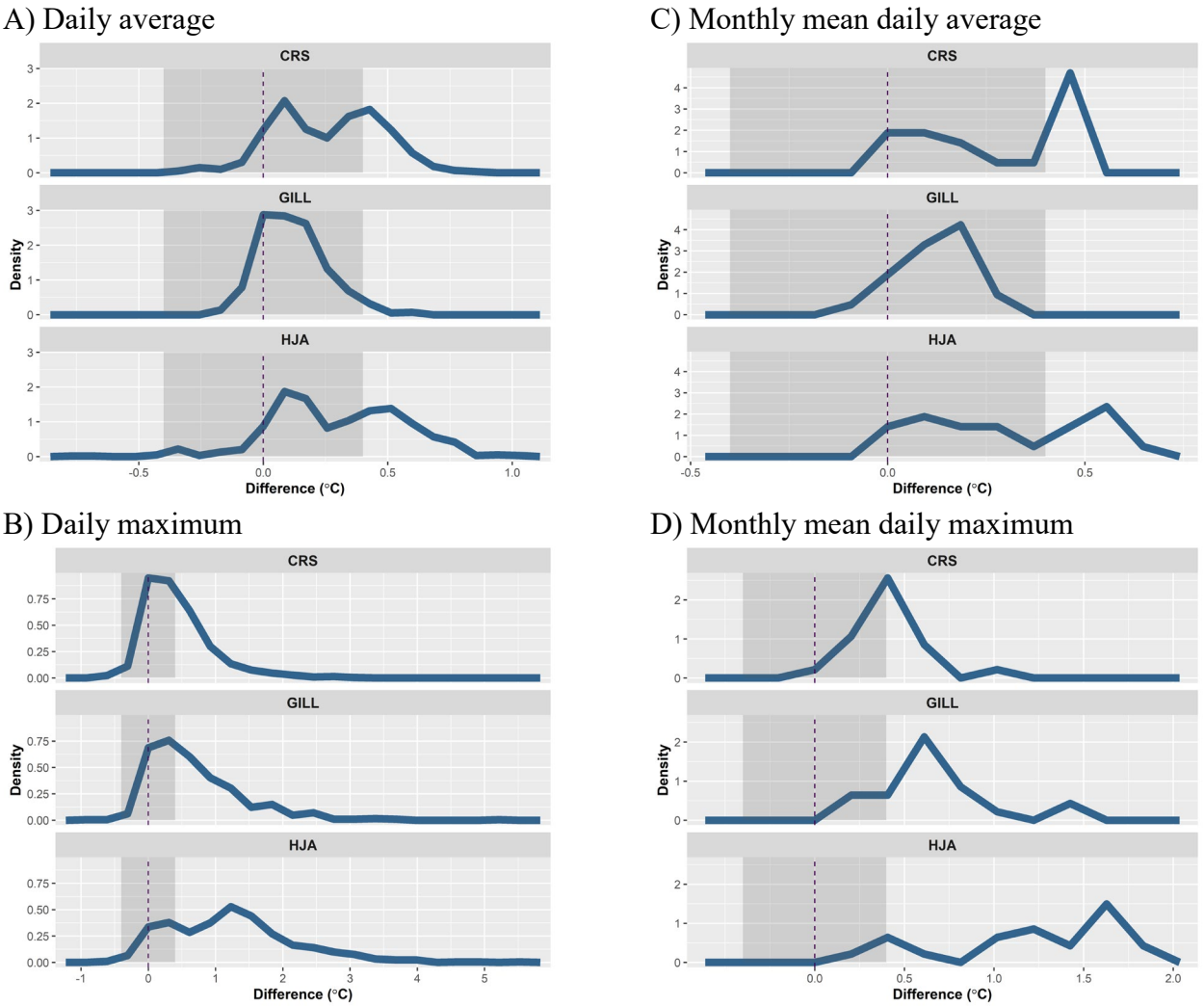

Figure 2.5 Density plot of ΔTs (°C) for the A) daily average, B) daily maximum, C) monthly mean daily average and D) monthly mean daily maximum observations. The ΔTs are calculated as the wind-ventilated instrument measurement – aspirated instrument measurement. Vertical dashed line indicates ΔT = 0. The ΔTs outside the shaded region are considered substantial (|ΔT| > 0.4°C).

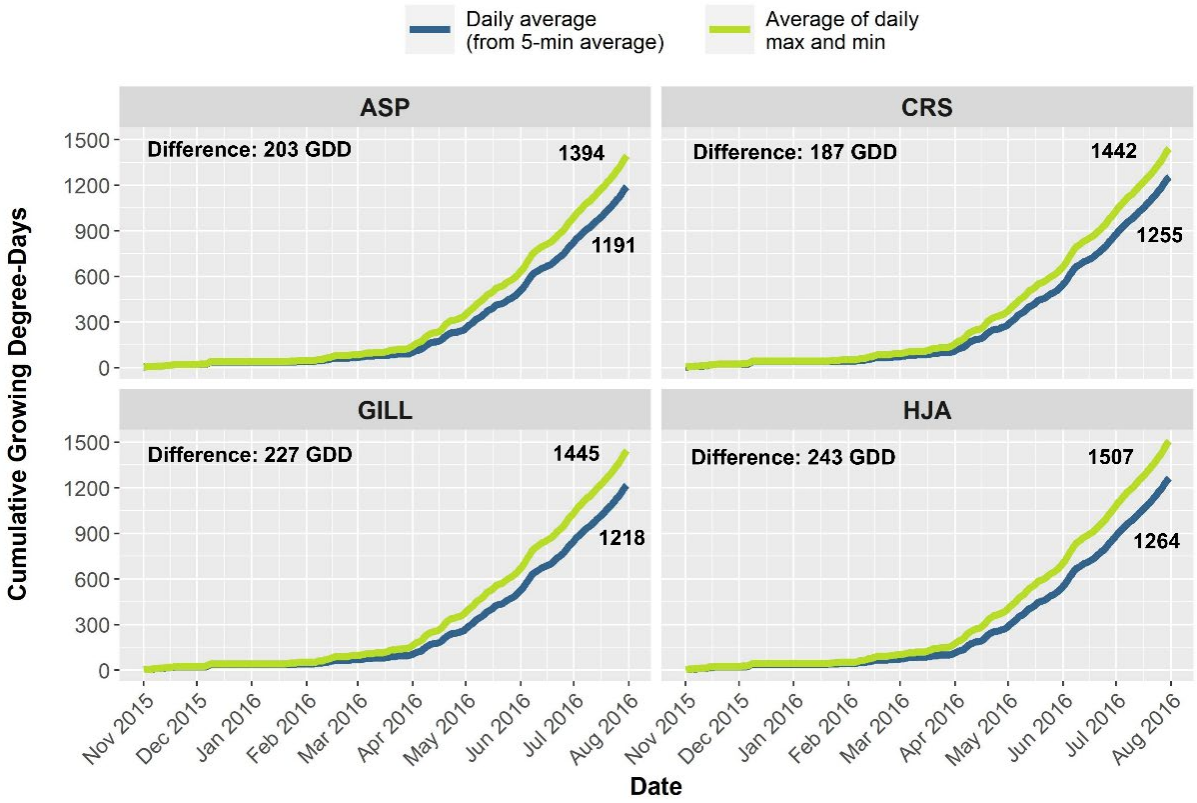

Figure 2.6 Plots comparing cumulative growing degree-days (GDD) for each instrument using two methods: one using the daily average temperature (blue line) and the other using the average of the daily maximum and minimum temperature (green line). Using the average of the daily maximum and minimum temperature results in greater cumulative GDD for each instrument.

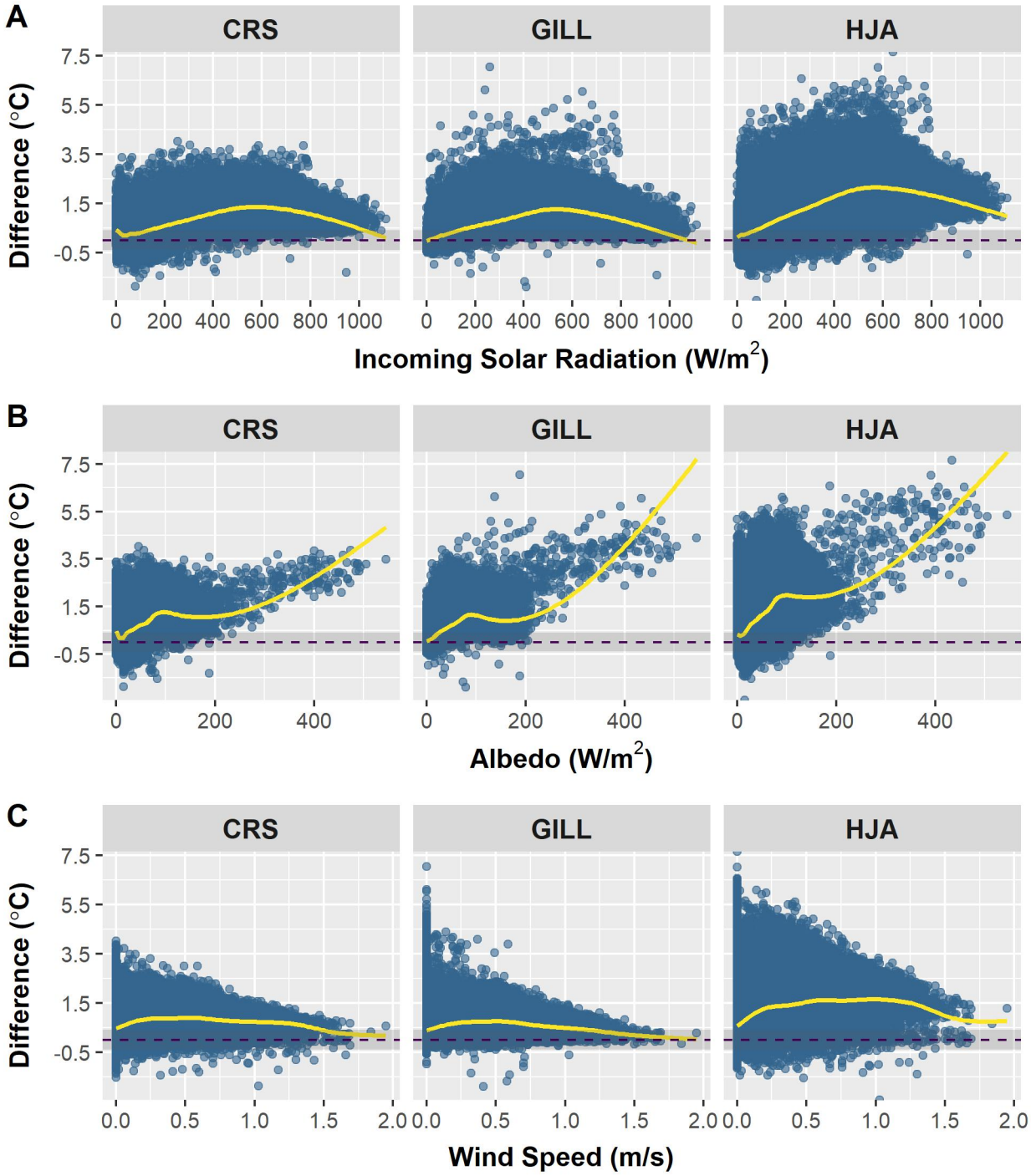

Figure 2.7 Plots showing daytime 15-minute average observation ΔTs (°C) against: (A) incoming solar radiation (W/m^2), (B) albedo (W/m^2), and (C) wind speed (m/s). The ΔTs outside the shaded region are considered substantial (|ΔT| > 0.4°C). The dashed line indicates ΔT = 0. The yellow line is the GAM smoothing curve (cubic regression spline).

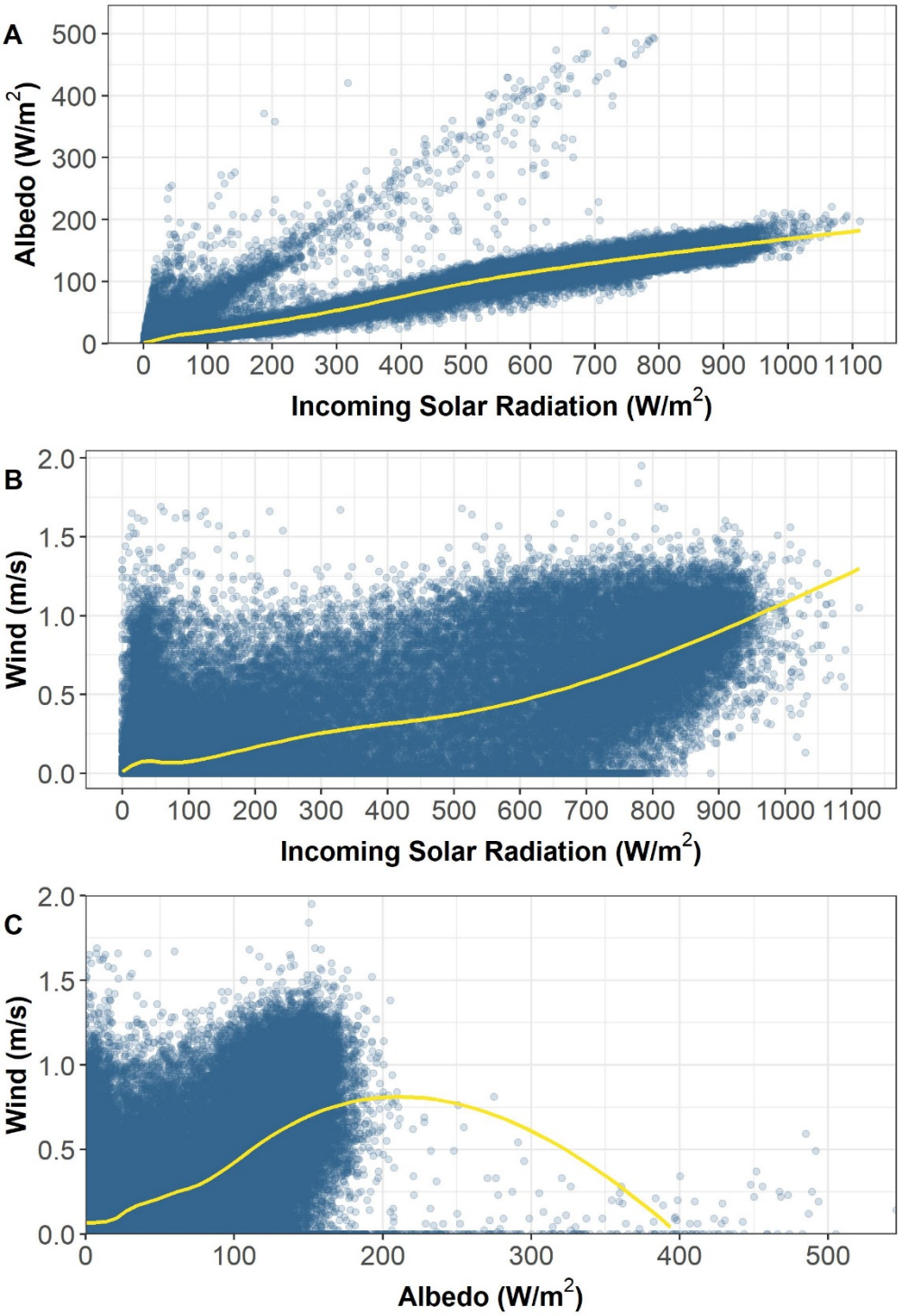

Figure 2.8 Plots show daytime 15-minute average observations of explanatory variable relationships: (A) incoming solar radiation (W/m^2) vs. albedo (W/m^2), (B) incoming solar radiation (W/m^2) vs. wind speed (m/s) and (C) albedo (W/m^2) vs. wind speed (m/s). The yellow line is the GAM smoothing curve (cubic regression spline).

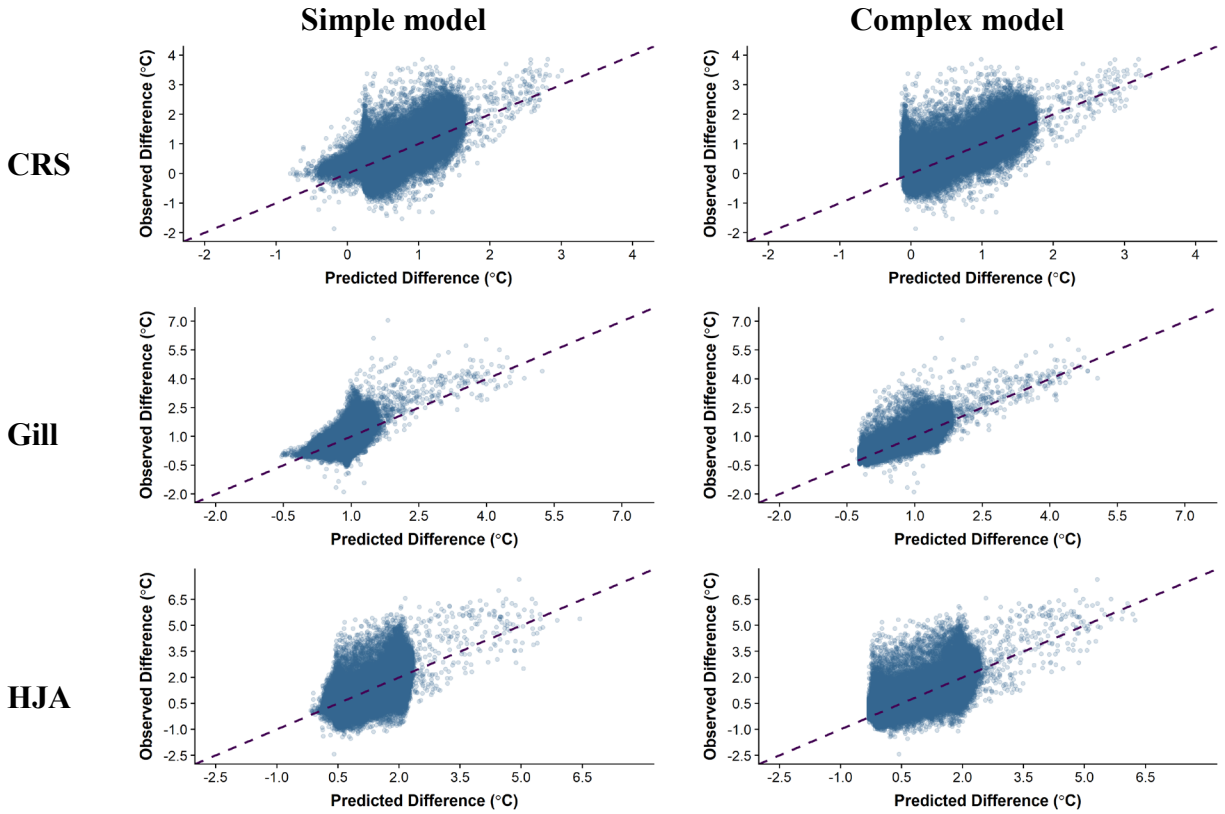

Figure 2.9 Plots show the estimated vs. observed differences (°C) for each best model. Dark dashed line indicates where the estimated difference equals the observed difference. Note that x-axis and y-axis scales are different for each instrument.

TABLES

Table 2.1 Summary of instrumentation used in the study. All air temperature sensors manufactured by Campbell Scientific. Photos sources: ASP, Gill, Wind from R.M. Young; ISR, ALB from Campbell Scientific; CRS from NovaLynx; HJA author photo.

	Instrumentation	Code	Description	Specifications
	Fan-aspirated (reference): air temperature	**ASP**	107 thermistor sensor; R.M. Young 43502-L compact aspirated shield	Sensor accuracy: ±0.2°C between 0 and 60 ±0.4°C below 0 to -35; shield radiation error <0.2°C @ 1000 W/m^2
	Cotton region shelter: air temperature	**CRS**	107 thermistor sensor; NovaLynx 380-605 large instrument shelter	Sensor accuracy: ±0.2°C between 0 and 60 ±0.4°C below 0 to -35; shield information not available
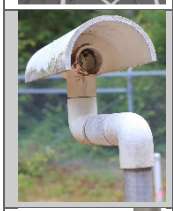	HJA/PVC shield: air temperature	**HJA**	107 thermistor sensor; shield: 8-inch long, 3.5 inch diameter, schedule 40 PVC pipe split in half lengthwise over PVC tubing containing sensor	
	Gill shield: air temperature	**Gill**	107 thermistor sensor; R.M. Young 41303-5A 6-plate solar radiation shield	
	Pyranometer (facing upward): incoming solar radiation	**ISR**	CM3 Kipp & Zonen	Response time: 18s; spectral range 305-2800 nm; sensitivity: 10-35 µV/W/m^2; error: ±25 W/m^2
	Pyranometer (facing downward): albedo	**ALB**	CM3 Kipp & Zonen	Response time: 18s; spectral range 305-2800 nm; sensitivity: 10-35 µV/W/m^2; error: ±25 W/m^2
	Anemometer: wind speed	**WIND**	R.M. Young 05103	Resolution: 1.0 m/s ; accuracy: ±0.3 m/s or 1% of reading

Table 2.2 Data for the study were recorded at two temporal resolutions and in three statistical formats (average, maximum, minimum). The table outlines the dates for which observations were logged, the resolution at which they were recorded, and the statistics recorded.

Resolution	Instruments	Dates	Statistics
15-minute	ASP, CRS, Gill, HJA, ISR, ALB, WIND	4/2011 – 4/2017	Average for a 15-minute period (60 observations per period)
5-minute	ASP, CRS, Gill, HJA	4/2015 – 4/2017	Average, maximum, and minimum for a 5-minute period (20 observations per period)
5-minute	ISR, ALB, WIND	4/2015 – 4/2017	Average and maximum for a 5-minute period (20 observations per period)

Table 2.3 Summary of daytime, nighttime, and all (daytime and nighttime combined) 15-minute average ΔTs (°C). The ΔTs were calculated as the wind-ventilated instrument measurement minus the aspirated instrument measurement. A "substantial ΔT" is defined as |ΔT| > 0.4°C. The percentage in the last column of the table is the percentage of the *n* ΔT values considered substantial. The maximum and median ΔTs were larger and more variable in the daytime than at nighttime.

CRS	***n***	**Min**	**Max**	**Median**	**Mean**	**St Dev**	**Substantial ΔT**
Daytime	87,129	-1.9	4.0	0.5	0.6	0.6	60.6%
Nighttime	117,270	-1.0	1.7	0.04	0.04	0.2	6.5%
All	204,399	-1.9	4.0	0.1	0.3	0.5	29.5%
Gill	***n***	**Min**	**Max**	**Median**	**Mean**	**St Dev**	**Substantial ΔT**
Daytime	87,129	-1.9	7.0	0.3	0.5	0.6	43.9%
Nighttime	117,270	-1.4	0.7	-0.1	-0.1	0.1	4.1%
All	204,399	-1.9	7.0	-0.03	0.1	0.5	21.1%
HJA	***n***	**Min**	**Max**	**Median**	**Mean**	**St Dev**	**Substantial ΔT**
Daytime	87,129	-2.4	7.7	0.7	0.9	1.0	65.0%
Nighttime	117,270	-1.3	1.2	-0.1	-0.1	0.2	13.1%
All	204,399	-2.4	7.7	0.1	0.3	0.8	35.3%

Table 2.4 Summary of ΔTs (°C) for: **A)** daily average, **B)** daily maximum, **C)** monthly mean daily average, and **D)** monthly mean daily maximum statistics. The ΔTs were calculated as the wind-ventilated instrument measurement minus the aspirated instrument measurement. A "substantial ΔT" is defined as |ΔT| > 0.4°C. The percentage in the last column of the table is the percentage of the *n* ΔT values that were considered substantial.

A) Daily average

Instrument	*n*	Min	Max	Median	Mean	St Dev	Substantial ΔTs
CRS	700	-0.3	0.9	0.3	0.3	0.2	30.8%
Gill	700	-0.2	0.6	0.1	0.1	0.1	3.3%
HJA	700	-0.7	1.1	0.3	0.3	0.3	39.7%

B) Daily maximum

Instrument	*n*	Min	Max	Median	Mean	St Dev	Substantial ΔTs
CRS	697	-0.7	3.0	0.3	0.4	0.5	44.7%
Gill	697	-0.8	5.2	0.5	0.7	0.7	58.4%
HJA	697	-0.8	5.6	1.2	1.2	0.9	78.2%

C) Monthly mean daily average

Instrument	*n*	Min	Max	Median	Mean	St Dev	Substantial ΔTs
CRS	23	-0.03	0.5	0.3	0.3	0.2	43.5%
Gill	23	-0.05	0.3	0.1	0.1	0.1	0.0%
HJA	23	-0.03	0.6	0.3	0.3	0.2	39.1%

D) Monthly mean daily maximum

Instrument	*n*	Min	Max	Median	Mean	St Dev	Substantial ΔTs
CRS	23	0.1	1.0	0.4	0.4	0.2	60.9%
Gill	23	0.3	1.4	0.6	0.7	0.3	82.6%
HJA	23	0.3	1.8	1.3	1.2	0.5	95.7%

Table 2.5 Comparison of total GDD accumulation (November 2015-July 2016) between two methods for calculating the daily average temperature: A) average of the daily maximum and minimum temperature; B) average of all five 5-minute average observations in a day. Accumulation differences were variable among instruments using the same method (3-113 GDD difference), and between instruments using different methods (130-316 GDD difference). For individual instruments, the difference in GDD accumulation between methods was 187-243 GDD.

	Total GDD Accumulation: November 2015-July 2016			
Method	**ASP**	**CRS**	**Gill**	**HJA**
Daily maximum & minimum average	1394	1442	1445	1507
Daily average of all 5-minute observations	1191	1255	1218	1264

Table 2.6 The explanatory variables included in the best models for each wind-ventilated instrument. ISR = incoming solar radiation (W/m^2), ALB = albedo (W/m^2), WIND = wind speed (m/s). A dot in the box indicates that the variable is included in the model. The best complex model was the same for all instruments. All candidate models were forced to include ISR and WIND.

Term	CRS Simple	Gill Simple	HJA Simple	Complex (All)
ISR	•	•	•	•
ALB	•	•	•	•
WIND	•	•	•	•
ISR^2	•		•	•
ALB^2		•	•	
ISR*ALB				•
ISR*WIND				•
ISR^2* ALB				•
ISR^2*WIND				•
ALB*WIND				•

Table 2.7 Table shows the adjusted R^2 value for models that included only the explanatory variable term listed in the column. Models were fit on the binned data. Albedo alone explained more variation in ΔT for each instrument than incoming solar radiation or wind speed.

Instrument	**Incoming solar radiation (W/m^2)**	**Albedo (W/m^2)**	**Wind speed (m/s)**
CRS	0.14	0.53	0.29
Gill	0.02	0.61	0.37
HJA	0.11	0.49	0.10

Table 2.8 A comparison of the summary statistics for the observed vs. estimated ΔTs in the daytime 15-min average data. For the CRS, the summary statistics for the simple model's estimated ΔTs were closer to observed than the complex model, with estimated median and mean ΔT the same as observed. For the Gill and HJA, the summary statistics for the complex model's estimated ΔTs were closer to observed than the simple model, with estimated median and mean ΔT within 0.1ºC of observed.

Statistic	Observed ΔT (ºC)	Simple Model Estimated ΔT (ºC)	Complex Model Estimated ΔT (ºC)
CRS			
Min	-1.9	-0.8	-0.1
Max	4.0	3.0	3.4
Median	0.5	0.5	0.4
Mean	0.6	0.6	0.5
SD	0.6	0.4	0.5
Substantial ΔTs	60.6%	63.6%	47.7%
GILL			
Min	-1.9	-0.5	-0.4
Max	7.0	5.2	5.0
Median	0.3	0.9	0.3
Mean	0.5	0.9	0.4
SD	0.6	0.3	0.5
Substantial ΔTs	43.9%	96.2%	45.6%
HJA			
Min	-2.4	-0.2	-0.3
Max	7.7	6.4	6.3
Median	0.7	1.0	0.6
Mean	0.9	1.1	0.8
SD	1.0	0.6	0.9
Substantial ΔTs	65.0%	95.9%	56.4%

CHAPTER 3: MICROCLIMATE AND ABUNDANCE OF FLYING INSECTS IN A CONIFER FOREST

INTRODUCTION

Recent increases in global surface temperatures have been found to impact insect phenology and abundance (Bale et al. 2002, Deutsch et al. 2008, Menzel et al. 2006, Parmesan 2006, Parmesan and Yohe 2003, Woods et al. 2015). Many insects are poikilotherms with limited thermoregulation ability, so climate has a strong direct influence on their development, reproduction, and behavior. Most projections of future climate change are at coarse spatial scales, but climate conditions at a fine spatial scale (often referred to as microclimate) are most relevant to insects (Kingsolver et al. 2011, Woods et al. 2015).

Complex montane forest environments can have heterogeneous microclimates, with wide spatiotemporal variation in air temperature, forms of precipitation, moisture, wind, and incoming solar radiation intensity (Chen et al. 1999, Frey et al. 2016). Microclimate is influenced by landscape characteristics such as latitude, elevation, slope, aspect, vegetation, and canopy cover (Dobrowski 2011). In the northern hemisphere at latitudes between 30°-55°, aspect strongly influences the amount of heat that slopes receive from the sun. South-facing slopes receive more direct sunlight, and are typically warmer and drier than north-facing slopes, effecting vegetation composition. Air temperature tends to decrease with increasing elevation, but in montane environments with steep slopes and narrow valleys, cold air drainage and pooling result in temperature inversions where exposed slopes and ridges can be warmer than the valley below (Daly et al. 2010). Vegetation composition and structure also influence microclimate. In a study at an old-growth Douglas-fir forest in southern Washington, the mean daily average air temperature at the forest interior was 0.95°C lower than at the edges during a 35-day period in the summer. Forest vegetation can also reduce variation in temperature. The difference between the daily average maximum and minimum temperature at the forest interior was 4.7°C lower than at an exposed clearcut site. Mean wind velocity and incoming solar radiation were also found to be lower, and relative humidity higher, at the forest interior compared to clearcut (Chen et al. 1993).

Understanding and quantifying microclimatic variation is integral to predicting organism response to climate change, and has been a key ecological research focus (Chen et al. 1999, De

Frenne et al. 2013, Hodkinson 2005, Potter et al. 2013, Storlie et al. 2014, Woods et al. 2015). Insect life cycle event timing is often driven by environmental cues such as thermal accumulation, chilling, photoperiod, and precipitation (Forrest 2016, Hodkinson 2005, Kingsolver et al. 2011, Wolda 1988). Due to their diverse life history and adaptation strategies, predicting insect response to climate change is complex (Forrest 2016, Kingsolver et al. 2011). For a multivoltine species, early spring warming and snowmelt may result in early emergence and multiple broods, and consequently, increased abundance (Forrest 2016, Saunders 2002). However, for a species that requires a certain period of winter chilling to signal that it's safe to terminate diapause, early spring warming and snowmelt can significantly lengthen pupae development time and result in decreased abundance (Forrest 2016, Stålhandske et al. 2015). Studies have shown that heterogeneous microclimates within forests may act as "microrefugia" - areas of favorable climate within regions of unfavorable climate - for insects and other organisms adapting to climate change (Buckley et al. 2013, Dobrowski 2011, Frey et al. 2016, Kearney et al. 2009, Maclean et al. 2015). However, life history characteristics, such as dispersal ability and range, will impact whether insects can take advantage of microrefugia.

Insect response to environmental conditions is also mediated by trophic and community interactions (Gilman et al. 2010, Ovaskainen et al. 2013, Pureswaran et al. 2018). There has been significant research on potential phenological "mismatch" in trophic interactions related to climate change (Gilman et al. 2010, Parmesan 2006, Parmesan and Yohe 2003, Thackeray et al. 2016, Thackeray et al. 2010, Visser and Both 2005). As earlier spring warming can advance plant phenology, the phenology of herbivorous insects, pollinators, and parasitoids must also advance to acquire sufficient resources for reproduction and development (Parmesan 2006). Photoperiod is not impacted by climate warming, and there is concern that some insect and bird species which rely on photoperiod cues may miss optimal resource windows advanced by warming, such as plant leafout, which could have rippling trophic effects (Gwinner 1990, Hodgson et al. 2011).

Recent studies have shown evidence of steep insect abundance and biomass declines which may be linked to climate change and phenological mismatch, raising public alarm about an "insect apocalypse" (Hallmann et al. 2017, Jarvis 2018, Lister and Garcia 2018, Sánchez-Bayo and Wyckhuys 2019). Researchers warn that these insect declines could have calamitous impacts to ecosystem structure and function, since insects are the sole or primary food source for

a number animal species, and an integral part of food webs, in addition to providing ecosystem services like pollination and decomposition (Noriega et al. 2018, Ovaskainen et al. 2013). However, there are significant knowledge gaps about the life history, species interactions, and population dynamics of many insect taxa, making generalized conclusions about global trends unreliable (Cardoso et al. 2019, Cardoso et al. 2011, Fisher 2019, Saunders et al. 2019, Visser and Both 2005). Insects are the most abundant and diverse group of organisms, but are underrepresented in the scientific literature, with limited geographic representation and taxonomic bias towards species of medical and economic importance (Noriega et al. 2018, Saunders et al. 2019, Titley et al. 2017, Wolda 1988).

Knowledge gaps about insect life history and population dynamics, changing climate conditions, and trophic synchrony have resulted in a high degree of uncertainty about future insect populations and potential impacts to community structure and function. Our observational study contributes to the field by examining thermal variation and its relationship to the spring activity of terrestrial flying insects over five years at the H.J. Andrews Experimental Forest and Long-Term Ecological Research Station in Oregon. We examine the general abundance of terrestrial flying insects at H.J. Andrews, as well as the abundance of three select genera: 1) Diptera: Dolichopodidae: Scellus (long-legged flies), 2) Diptera: Bolbomyiidae: Bolbomyia (tiny black flies), and 3) Coleoptera: Scraptiidae: Anaspis (small beetles). Our research questions are:

1. How do cumulative growing degree-days (GDD) vary in a sampling year among sixteen study sites and within a site among sampling years?
2. How does cumulative abundance per sampling day vary in a sampling year among sixteen study sites and within a site among sampling years?
3. What is the relationship within a site between abundance per sampling day and: 1) air temperature during the sampling period and 2) the proportion of days with measurable precipitation during the sampling period?
4. How much does the slope of the relationship between cumulative abundance per sampling day and cumulative GDD differ among sixteen study sites in a sampling year?

METHODS

Research sites

Insect sampling took place between the months of March and July in 2009-2014 at sixteen sites within the H.J. Andrews Experimental Forest and Long-Term Ecological Research site (44.21, -122.26). Due to challenges with study start-up and consistent data collection in 2009, data from this sampling year is excluded unless otherwise noted. H.J. Andrews is a conifer-dominated forest occupying 6,400 hectares of the Lookout Creek Watershed, located in the western slopes of the Cascade Range, approximately 80.5 km east of Eugene, Oregon. H.J. Andrews' complex terrain experiences a range of interesting climate phenomena, including temperature inversions and cold-air drainage. Thus, it provides an ideal location to evaluate the ways that spatial variation in microclimate can impact forest insect abundance. The sixteen study sites were selected based on representation of landscape gradients at H.J. Andrews, varying in elevation (460m to 1300m), slope (10.8% to 79.2%), aspect (30° to 347°), and relative forest age (with "young" defined as 40-60 years since last harvest "old" defined as unlogged stands with dominant canopy trees 150-500 years old). All sites were located at the forest interior, away from road edges. Sites were also selected based on proximity to existing long-term climate monitoring stations and forest plots. Proximity to these stations allowed for data quality checks and validation using similar temperature data, as well as to associate microclimate conditions to long-term climate station records. Site characteristics are outlined in Table 3.1, and a map with study site locations is shown in Figure 3.1.

Insect sampling and processing

At each site, flying insects were collected using a single malaise trap suspended from a central line suspended between two trees with the bottom of the trap 0.3-0.5m above ground. For logistics and consistency among sites, malaise traps were hung at locations within a 25m radius of an air temperature instrument at plot center, in an area that was at least 2x2m and free of shrubs. Traps were set and collected at each site approximately weekly from March to July in 2010-2014. Due to early season access and the risk of trap damage in snowstorms, trapping start dates at higher elevation sites typically lagged behind those of low elevations sites. Other logistical constraints precluded a strict seven-day sampling window for every site/trapping bout.

Hence, the total number of samples collected and total number of sampling days at each site was variable in each sampling year (Table 3.2).

Weekly samples were preserved with 95% ethanol and delivered to a lab at Oregon State University. Samples were examined using a binocular dissecting microscope. In 2009, samples were fully processed, and then partially processed in 2010-2014. In fully processed samples, all winged insects were counted and identified to varying taxonomic levels, from order to genus, depending on key availability and ease of use (Table A.8) (McAlpine et al. 1981, Covell 1984, Arnett 2000, Arnett and Thomas 2001, Arnett et al. 2002, Triplehorn and Johnson 2005, Merritt and Cummins 2008) (*note that these citations are listed separately in Literature Cited under the "Insect identification" header*). For partially processed samples, total counts of all flying insects and counts of three genera were recorded: Diptera: Dolichopodidae: Scellus (long-legged flies), Diptera: Bolbomyiidae: Bolbomyia (tiny black flies), and Coleoptera: Scraptiidae: Anaspis (small beetles) (Johnson and Li 2016). These taxa were selected as they are common and abundant at H.J. Andrews, and would allow for cross-site comparisons. Taxonomic data from the 2009 pilot year were used as an indicator of the types and diversity of insects captured with the sampling method, but per-sample abundance data from this year were omitted from analyses due to the degree of inconsistency in trapping periods.

Climate data collection and processing

Air temperature data were recorded year-round at each site using Onset Hobo U22-001 (accuracy 0.2°C) temperature sensors with a custom-fabricated shield. Shields were 8 inches long and made from a 3.5-inch diameter schedule 40 PVC pipe split in half lengthwise (Johnson and Frey 2009). The air temperature instrument was located on a fiberglass pole 1.5 m above ground in a shaded understory location, and instantaneous air temperature was recorded at 15-minute intervals. An automated quality assurance program developed in Python was used to identify and flag impossible and missing values in the data, and to detect when sensors were buried by snow (Johnson and Frey 2009). Data were also checked manually, and values were compared to those from nearby temperature stations to identify erroneous snow flags (i.e., data flagged as "sensor buried by snow" when no snow was at that site), temperature spikes, and other questionable values not identified by the Python program. For missing data and periods when the sensor was buried by snow, data were filled using regression relationships with other sensors

(Table A.6 and Table A.7). Regressions were calculated using the best fit with other sensors during periods of time when the full data were available. The hourly average air temperature was calculated after quality control and assurance processes.

Cumulative growing degree-days (GDD) was selected as a thermal measure. It has long been used in plant and insect phenology studies, since physiological development begins at a temperature threshold unique to the organism, and is then mediated by immediate conditions (Crimmins and Crimmins 2019, Hodgson et al. 2011, Snyder et al. 1999, Zalom and Goodell 1983). We calculated cumulative GDD for each site based on a method established for a concurrent vegetation phenology study at H.J. Andrews (Ward et al. 2018). We established a minimum threshold temperature of 5°C (T_{base}), commonly used for insect development and reproduction (Hodgson et al. 2011). The average daily degree-day was calculated by summing the hourly average temperature degrees (°C) > T_{base} for a day, then dividing by 24. For each site and sampling year of the study, the cumulative sum of average daily degree-days (referred to hereafter as "cumulative GDD") was calculated for the period beginning December 1 of the year prior to sampling through the date of the last sample collection (variable by site and year).

Daily total precipitation (mm) was recorded at the H.J. Andrews Primary Meteorological Station (PRIMET) site (44.21, -122.26, elevation 430m). The PRIMET site is approximately 29 x 23 m^2, exposed and relatively flat, with conifer forests outside the perimeter. Precipitation was measured using a heated tipping bucket gage at a height of 100 cm. All precipitation data were evaluated using automated (GCE Data Toolbox Version 3.9.4b - https://gce-lter.marsci.uga.edu/public/im/tools/data_toolbox.htm) and manual quality control processes, which included checks for questionable and missing values (Daly and McKee 2019).

We estimated the last day of significant snow cover - defined as snow cover > 50% and deep enough to bury herbaceous plants - at each plot in each sampling year. Observations of snow cover and depth were made on all site visits. For sites at which snow melt occurred prior to the first visit of the year, we used supplemental data from snowstakes located in forest understory at comparable elevation and aspect (Levno and Schulze 2017) and on snowfall and melt from meteorological stations spanning the elevation gradient (Daly and McKee 2019) to infer last day of snow cover.

Finally, daylength data for each site, based on latitude and day of year, was generated using the R geosphere (v. 1.5-10) package (Hijmans 2019).

Data and statistical analysis

Due to variation in the number of days insects were sampled at each site, two insect count response variables were used: 1) "abundance per sampling day" is the total number of insects collected in a sample divided by the number of sampling days, and 2) "cumulative abundance per sampling day" is the cumulative sum of abundance per sampling day, as of the sample collection date (both response variables have $n = 935$; for sample size per site in each sampling year, see "Total samples collected" columns in Table 3.2).

Scatterplots were used to evaluate how both cumulative GDD and cumulative abundance per sampling day varied within the spring sampling season among the 16 sites and within sites among the five sampling years. Scatterplots were also used to evaluate the relationship between abundance per sampling day and the average hourly air temperature and proportion of days with measurable precipitation during each sampling period (defined as the date a malaise trap was set through the day before the trap was collected). Average hourly air temperature during the sampling period was calculated by taking the average of all hourly air temperature measurements in the sampling period. Proportion of days with measurable precipitation was calculated by summing the number of days in the sampling period with a precipitation measurement > 0.0 mm and dividing by the total number of days in the sampling period.

To evaluate how much the relationship between cumulative abundance per sampling day and cumulative GDD differed between the 16 sampling sites in each sampling year, we estimated the slope of the regression of cumulative GDD on cumulative abundance per sampling day for each site. To perform the analysis, we first separated data by sampling year, and then fit a generalized least squares (GLS) model to the data for each sampling year using the R nlme package (Pinheiro et al. 2017). The interaction between site (as a categorical variable) and cumulative GDD, allowed the slope of cumulative GDD to vary by site. A check of model assumptions showed autocorrelation of observations within sites, and non-constant residual variance in each sampling year. A Gaussian spatial correlation structure was added to the original models to address autocorrelation within sites by day of year, and the assumption of constant residual variance among sites was relaxed. A graphical evaluation of semivariograms and residual vs. fitted plots showed that model assumptions were now adequately met. We then used the emtrends function in the R emmeans package to generate the cumulative GDD slope estimate and confidence intervals for each site, and to make pairwise comparisons (Lenth 2019). The p-values of pairwise

comparisons include a Tukey method adjustment for comparing the 16 site estimates. Estimates and confidence intervals, as well as comparisons, were visually evaluated using scatterplots.

RESULTS

Thermal variation

Among sites within a sampling year, there was wide variation in cumulative GDD by day of year 90 (beginning of April, "winter GDD") and by day of year 180 (end of June, "spring GDD") (Figure 3.2, Figure 3.4). In 2011-2013, winter GDD for all sites were typically < 100 GDD, and in 2011 and 2012, low- and high-elevation sites had similar accumulation. The smallest range of winter GDD values among sites was in 2011. Winter GDD in 2010 and 2014 were greater than average, with some lower-elevation sites accumulating > 100 GDD, and with a larger range of values among sites than in other years. Average winter GDD for the sites was smallest in 2011 and largest in 2014. During the sampling season, in 2010, 2011, and 2013, and beginning in May, (~ day of year 120-150) GDD accumulation rates at sites below 650m elevation start to increase more than at higher-elevation sites. In contrast, GDD accumulation rates in 2012 and 2014 were more similar among sites through the spring than in 2010, 2011 and 2013. In all years, spring GDD was generally ordered from warmest to coolest by low to high elevation, with some exceptions (Figure 3.4). Site rankings from coolest to warmest were the same for both winter and spring GDD in 2011 (the coolest year based on average spring GDD) and in 2014 (the warmest year based on average spring GDD). In 2010, average winter GDD was the second warmest of all years, but average spring GDD was the second coldest of all years. So, winter GDD is not necessarily an indicator of spring GDD. Within a site, among sampling years, the winter GDD values differed by as little as 25 GDD (PC9) to as much as 93 GDD (PC12) (median 57 degree-days) (Figure 3.3). Spring GDD values differed by as little as 237 GDD (PC9) to as much as 318 GDD (PC5) (median difference 263 GDD).

Some snow was present at sites < 650m in 2010 and 2012 to approximately day of year 85 (Figure 3.5), and GDD accumulation rates at sites < 650m in 2010 and 2012 were nearly identical to each other (Figure 3.3). At sites between 650m-1100m in elevation, snow presence was variable among years, until as late as day of year 146 (PC9) in 2012. PC7 had the most variability in snow presence, with no snow detected in some years and presence up to day of year 105 in 2011. At sites > 1175m, snow presence was relatively consistent inter-annually, with

snow present on median to approximately day of year 125. In 2011, snow persisted up to day of year 158, and in 2014, only persisted to day of year 94 at one site (PC13).

Insect abundance

Among sites in each sampling year, cumulative abundance per sampling day by day of year was variable (Figure 3.6). Generally, cumulative abundance per sampling day either increased steadily across the sampling period (sites PC1, PC2, PC4 and PC14) or increased starting around day of year 120, such as at PC7. In 2011, there were anomalously large abundance values (relative to other years) at all but lower-elevation sites PC4 and PC5 and higher-elevation sites PC17 and PC18. Mid-elevation sites generally had greater cumulative abundance per sampling day. There were no clear patterns of cumulative abundance per sampling day by slope, aspect, or forest age. Within sites among sampling years, abundance accumulation patterns were generally consistent, with the exception of most sites in 2011 (the coldest year) and at some sites in 2014 (the warmest year). The difference between the most and least cumulative abundance per sampling day on the last day of sampling among years was the smallest at PC4 (difference of 6) and the largest at PC9 (difference of 153) (Figure A.12).

The *Scellus* was most abundant at sites > 900m in elevation (Figure 3.7). The lowest cumulative abundance per sampling day was in 2011 and highest in 2014. The *Bolbomyia* was most abundant at sites > 900m in elevation and of old forest age, with lowest overall cumulative abundance per sampling day in 2014 and highest in 2011 (the opposite of the *Scellus*) (Figure 3.8). *Anaspis* cumulative abundance per sampling day was not clearly associated with elevation or forest stage. *Anaspis* had the lowest overall cumulative abundance per sampling day in 2012 and highest in 2014 (Figure 3.9). Where present, each genera's cumulative abundance per sampling day rate tended to increase markedly around day of year 135, when daylength reaches about 14 hours (Figure A.13). *Scellus* and *Bolbomyia* abundance appeared to be associated with snowmelt at sites with elevation > 965m, as they did not begin to substantially accumulate until after snowmelt, which was similar to general insect abundance.

Relationship between sample abundance and air temperature and precipitation during the sampling period

Temperature and precipitation during the sampling period can impact insect activity, and thereby the number of insects collected in a sample, so we examined this relationship.

Abundance per sampling day (the total insects collected in a sample divided by the number of sampling days) had a positive relationship with the average hourly temperature during the sampling period, and a negative relationship with the proportion of days with measurable precipitation (Figure 3.10). However, these relationships were not particularly strong at most sites. Based on R^2 values, there was a stronger relationship at sites > 1100m elevation with average hourly temperature and proportion of days with measurable precipitation than at lower elevation sites.

Comparison of cumulative abundance per sampling day and cumulative GDD relationships

There was strong statistical evidence that the estimates of the change in cumulative abundance per sampling day for each cumulative GDD (slopes from the regression models) varied among sites and that this persisted in all years (2010: $F_{15,153} = 35.0$, 2011: $F_{15,140} = 28.5$, 2012: $F_{15,154} = 141.2$, 2013: $F_{15,161} = 62.5$, 2014: $F_{15,167} = 102.4$, $p < .0001$ all years, $\alpha = 0.05$) (Figure 3.11). Year 2011 had the largest estimates of change in cumulative abundance per sampling day for each cumulative GDD, as well as the largest confidence intervals, for most sites. In other years, at sites < 650m elevation (PC1, PC2, PC4, PC5), estimates of the change in cumulative abundance per sampling day for each cumulative GDD were fairly similar within sites among years, and were generally smaller and less variable than at higher-elevation sites. Pairwise comparisons of slope estimates by site showed that the coldest year, 2011, had the lowest proportion of sites with statistically significant slope differences (0.23). The largest proportion of sites with statistically significant slope differences (0.56) occurred in 2010, a year with high winter GDD (cumulative GDD on day of year 90), relatively late snow at all sites, and relatively low spring GDD (cumulative GDD on day of year 180).

DISCUSSION

We found that GDD accumulation and insect abundance were widely variable at sites with differing topography within H.J. Andrews. GDD accumulation was not consistently correlated with site-level cumulative abundance per sampling day, perhaps due to the large number and diversity of taxa at each site. The presence of many different microclimates across the landscape interacting with diverse insect taxa, the composition of which varies by site, may make it difficult to predict site-level abundance based on simple temperature metrics.

Elevation was more reliably associated with spring GDD (cumulative degree days on day of year 90) than winter GDD (cumulative growing degree days on day of year 180) in each year. The range of winter and spring GDD within a site among sampling years was also not consistently associated with elevation. Topography and other climate factors, such as cold-air drainage and pooling, may explain why elevation and thermal accumulation were not reliably associated with GDD. For example, site PC5 was consistently warmer than three nearby sites (PC1, PC2, PC4) that were between 160-180m lower in elevation (Figure 3.4). These sites are in an area where cold-air drainage and pooling can occur in calm and clear conditions during the winter. Additionally, PC5 has a south-facing aspect and is the most exposed site, while the lower-elevation sites are north-facing and more shaded. Site PC12, located on a ridge, was consistently ~50 GDD warmer than site PC11, despite having a similar aspect, a slightly lower elevation, and an older forest age. Site PC9, which is shaded and frequently experiences cold-air pooling, had a lower median winter GDD than site PC17, which is located on a ridge at an elevation 300m higher. However, the median spring GDD at PC9 was higher than at PC17. The frequency of persistent cold-air pooling decreases in the spring, so air temperatures, and thus thermal accumulation, become more consistently associated with elevation through the season (Crimmins and Crimmins 2019).

GDD accumulation has been shown to be a consistent predictor of emergence for specific insect species, but our results show differential relationships between cumulative GDD and cumulative abundance per sampling day among and within sites, indicating it may not be a reliable predictor of general flying insect abundance within H.J. Andrews. Some sites had similar GDD accumulation but much different cumulative abundance per sampling day. For example, winter and spring GDD, as well as GDD accumulation rates, were nearly identical at PC1 and PC4 in each year, as was snow persistence. However, abundance patterns were noticeably different in every year except 2010 (which had the least variation in abundance among all sites), with final cumulative abundance differing by as much as 230 in 2013. Within most sites, the cumulative GDD slope estimates were substantially larger in 2011 relative to other sampling years, suggesting that other climate variables can strongly influence abundance.

The differential abundance response to GDD at each site is likely partially explained by variance in the response of diverse insect taxa at each site. Each insect species responds in a different way to environmental conditions - including thermal accumulation and chilling over the

winter and local conditions during the spring - based on their life history and functional characteristics. To continue the comparison of PC1 and PC4, approximately 20 more insect families were identified at PC1 than PC4 in a 2009 family-level identification by site (Figure A.14, Table A.8). It's possible that the more diverse composition of insect taxa at PC1 is related to the increased abundance at that site. Adding to the complexity of understanding insect response, in the analysis of the *Scellus*, *Bolbomyia*, and *Anaspis* genera, we saw that insects that are more closely related don't necessarily have the most similar abundance response. *Scellus* and *Bolbomyia*, both from order *Diptera*, had less similar site association and abundance relationships with GDD accumulation than *Scellus* did with *Anaspis*, a member of order *Coleoptera.* However, both *Scellus* and *Bolbomyia* tend to accumulate abundance at sites > 965m after snowmelt, while *Anaspis* abundance did not appear to be associated with snowmelt. Information on the life history characteristics of these particular genera are sparse, making explanations of some of the seemingly contradictory associations difficult. For example, McAlpine et al (1981) was one of the few sources with life history information documented for the *Scellus*, and stated the genus is very sensitive to cold temperatures (McAlpine et al. 1981). We found that *Scellus* at H.J. Andrews were associated with cooler mid- and high-elevation sites, though their abundance was greater at those sites in warmer years (2013 and 2014), and abundance generally increased after snowmelt.

We acknowledge that our study has some limitations. Our sampling method did not include sites at elevations between 650-900m, which limits our study inference. Some low- and high-elevation sites were relatively close in distance compared to intermediate-elevation sites, so it's possible spatial proximity influenced similarities observed among those sites. Road access and potential (and actual) trap damage from heavy snowfall, limited early-season sampling at some higher elevation sites and resulted in uneven sampling effort in some years. Due to the vast diversity of terrestrial flying insects, a single (and often multiple) trapping method cannot capture the full range of taxa at a site. Malaise traps are commonly used in flying insect studies, but can be biased towards day-active species. Future studies could include multiple trapping methods to potentially capture a broader range of taxa. Finally, due to the extremely labor-intensive nature of insect processing and identification and budget constraints, there was a tradeoff between a long-term study of general abundance with identification of a few common taxa, or a short-term study with more granular insect identification. Consequently, information

on the broader insect taxa composition by site for the full sampling period was not available, which may limit our ability to explain some of the observed abundance patterns, since insect life history information can't be linked to the observed thermal and abundance patterns.

Even with these limitations, this study provides an important contribution to understanding some of the patterns and variability of flying insects in a conifer forest and how they might be influenced by air temperature and topography. The importance of multi-year sampling was well-demonstrated with our study as well – if our sampling window had not included 2011, or only included 2011, our conclusions may have been very different and potentially flawed.. With the specter of climate change, there is a need to establish baselines of insect abundance and variability for groups that are not traditionally a research focus, especially in light of potential impacts on forest food webs, which could have cascading effects on ecosystem function and biodiversity. Long-term studies like this can provide key foundational knowledge to enable better management and resource allocation, such as partitioning future study efforts based on functional groupings or key species in trophic linkages.

LITERATURE CITED

Bale, J.S., Masters, G.J., Hodkinson, I.D., Awmack, C., Bezemer, T.M., Brown, V.K., Butterfield, J., Buse, A., Coulson, J.C. and Farrar, J. 2002. Herbivory in global climate change research: direct effects of rising temperature on insect herbivores. Global Change Biology 8(1):1-16.

Buckley, L.B., Tewksbury, J.J. and Deutsch, C.A. 2013. Can terrestrial ectotherms escape the heat of climate change by moving? Proceedings of the Royal Society B: Biological Sciences 280(1765):20131149.

Cardoso, P., Branco, V.V., Chichorro, F., Fukushima, C.S. and Macías-Hernández, N. 2019. Can we really predict a catastrophic worldwide decline of entomofauna and its drivers? Global Ecology and Conservation 20:e00621.

Cardoso, P., Erwin, T.L., Borges, P.A.V. and New, T.R. 2011. The seven impediments in invertebrate conservation and how to overcome them. Biological Conservation 144(11):2647-2655.

Chen, J., Franklin, J.F. and Spies, T.A. 1993. Contrasting microclimates among clearcut, edge, and interior of old-growth Douglas-fir forest. Agricultural and Forest Meteorology 63(3-4):219-237.

Chen, J., Saunders, S.C., Crow, T.R., Naiman, R.J., Brosofske, K.D., Mroz, G.D., Brookshire, B.L. and Franklin, J.F. 1999. Microclimate in forest ecosystem and landscape ecology: variations in local climate can be used to monitor and compare the effects of different management regimes. Bioscience 49(4):288-297.

Crimmins, M.A. and Crimmins, T.M. 2019. Does an Early Spring Indicate an Early Summer? Relationships Between Intraseasonal Growing Degree Day Thresholds. Journal of Geophysical Research: Biogeosciences 124(8):2628-2641.

Daly, C., Conklin, D.R. and Unsworth, M.H. 2010. Local atmospheric decoupling in complex topography alters climate change impacts. International Journal of Climatology 30(12):1857-1864.

Daly, C. and McKee, W.A. 2019. Meteorological data from benchmark stations at the Andrews Experimental Forest, 1957 to present (MS00103). Forest Science Data Bank. https://doi.org/10.6073/pasta/c96875918bb9c86d330a457bf4295cd9

De Frenne, P., Rodríguez-Sánchez, F., Coomes, D.A., Baeten, L., Verstraeten, G., Vellend, M., Bernhardt-Römermann, M., Brown, C.D., Brunet, J. and Cornelis, J. 2013. Microclimate moderates plant responses to macroclimate warming. Proceedings of the National Academy of Sciences 110(46):18561-18565.

Deutsch, C.A., Tewksbury, J.J., Huey, R.B., Sheldon, K.S., Ghalambor, C.K., Haak, D.C. and Martin, P.R. 2008. Impacts of climate warming on terrestrial ectotherms across latitude. Proceedings of the National Academy of Sciences 105(18):6668-6672.

Dobrowski, S.Z. 2011. A climatic basis for microrefugia: the influence of terrain on climate. Global Change Biology 17(2):1022-1035.

Fisher, M. 2019. The small, the hidden, the less-loved: conserving other species. Oryx 53(2):199-200.

Forrest, J.R.K. 2016. Complex responses of insect phenology to climate change. Current Opinion in Insect Science 17(Supplement C):49-54.

Frey, S.J.K., Hadley, A.S., Johnson, S.L., Schulze, M., Jones, J.A. and Betts, M.G. 2016. Spatial models reveal the microclimatic buffering capacity of old-growth forests. Science advances 2(4).

Gilman, S.E., Urban, M.C., Tewksbury, J., Gilchrist, G.W. and Holt, R.D. 2010. A framework for community interactions under climate change. Trends in Ecology & Evolution 25(6):325-331.

Gwinner, E. 1990. Circannual rhythms in bird migration: control of temporal patterns and interactions with photoperiod. In Bird migration. pp. 257-268, Springer.

Hallmann, C.A., Sorg, M., Jongejans, E., Siepel, H., Hofland, N., Schwan, H., Stenmans, W., Müller, A., Sumser, H. and Hörren, T. 2017. More than 75 percent decline over 27 years in total flying insect biomass in protected areas. Plos One 12(10):e0185809.

Hijmans, R.J. 2019. geosphere: Spherical Trigonometry. 1.5-10. https://CRAN.R-project.org/package=geosphere

Hodgson, J.A., Thomas, C.D., Oliver, T.H., Anderson, B.J., Brereton, T.M. and Crone, E.E. 2011. Predicting insect phenology across space and time. Global Change Biology 17(3):1289-1300.

Hodkinson, I.D. 2005. Terrestrial insects along elevation gradients: species and community responses to altitude. Biological Reviews 80(3):489-513.

Jarvis, B. 2018. The Insect Apocalypse Is Here: What does it mean for the rest of life on Earth? The New York Times. Accessed on 12/17/2019. https://www.nytimes.com/2018/11/27/magazine/insect-apocalypse.html

Johnson, S. and Frey, S.J.K. 2009. Air temperature at core phenology sites and additional bird monitoring sites in the Andrews Experimental Forest, 2009-Present. Forest Science Data Bank, Corvallis, Oregon. Retrieved from:

http://andlter.forestry.oregonstate.edu/data/abstract.aspx?dbcode=MS045 doi:http://dx.doi.org/10.6073/pasta/f64dc0ba1f0e2015a6b4da92939efe37

Johnson, S. and Li, J. 2016. Aquatic and terrestrial insect activity phenology with trap collections at the Andrews Experimental Forest, 2009-2014. Forest Science Data Bank, Corvallis, OR. Retrieved from: http://andlter.forestry.oregonstate.edu/data/abstract.aspx?dbcode=SA025 doi: http://dx.doi.org/10.6073/pasta/89707e1fc94c1d4fa96f48fc5f273c59

Kearney, M., Shine, R. and Porter, W.P. 2009. The potential for behavioral thermoregulation to buffer "cold-blooded" animals against climate warming. Proceedings of the National Academy of Sciences 106(10):3835-3840.

Kingsolver, J.G., Arthur Woods, H., Buckley, L.B., Potter, K.A., MacLean, H.J. and Higgins, J.K. 2011. Complex life cycles and the responses of insects to climate change. Integrative and Comparative Biology 51(5):719-732.

Lenth, R. 2019. emmeans: Estimated Marginal Means, aka Least-Squares Means. R package. 1.4.2. https://CRAN.R-project.org/package=emmeans

Levno, A. and Schulze, M. 2017. Snow depth and snow water equivalent measurements along a road course and historic snow course in the Andrews Experimental Forest, 1978 to present. Forest Science Data Bank, Corvallis, Oregon. Retrieved from: http://andlter.forestry.oregonstate.edu/data/abstract.aspx?dbcode=MS045 doi:http://dx.doi.org/10.6073/pasta/ff5465b74f592e3114138a79d5cfe290

Lister, B.C. and Garcia, A. 2018. Climate-driven declines in arthropod abundance restructure a rainforest food web. Proceedings of the National Academy of Sciences 115(44):E10397-E10406.

Maclean, I., Hopkins, J.J., Bennie, J., Lawson, C.R. and Wilson, R.J. 2015. Microclimates buffer the responses of plant communities to climate change. Global Ecology and Biogeography 24(11):1340-1350.

McAlpine, J., Peterson, B., Shewell, G., Teskey, H., Vockeroth, J. and Wood, D. 1981. Manual of Nearctic Diptera, Volume 1, Research Branch Agriculture Canada.

Menzel, A., Sparks, T.H., Estrella, N., Koch, E., Aasa, A., Ahas, R., Alm-Kubler, K., Bissolli, P., Braslavska, O., Briede, A., Chmielewski, F.M., Crepinsek, Z., Curnel, Y., Dahl, A., Defila, C., Donnelly, A., Filella, Y., Jatcza, K., Mage, F., Mestre, A., Nordli, O., Penuelas, J., Pirinen, P., Remisova, V., Scheifinger, H., Striz, M., Susnik, A., Van Vliet, A.J.H., Wielgolaski, F.E., Zach, S. and Zust, A. 2006. European phenological response to climate change matches the warming pattern. Global Change Biology 12(10):1969-1976.

Noriega, J.A., Hortal, J., Azcárate, F.M., Berg, M.P., Bonada, N., Briones, M.J.I., Del Toro, I., Goulson, D., Ibanez, S., Landis, D.A., Moretti, M., Potts, S.G., Slade, E.M., Stout, J.C., Ulyshen, M.D., Wackers, F.L., Woodcock, B.A. and Santos, A.M.C. 2018. Research trends in ecosystem services provided by insects. Basic and Applied Ecology 26:8-23.

Ovaskainen, O., Skorokhodova, S., Yakovleva, M., Sukhov, A., Kutenkov, A., Kutenkova, N., Shcherbakov, A., Meyke, E. and Delgado, M.D.M. 2013. Community-level phenological response to climate change. Proceedings of the National Academy of Sciences of the United States of America 110(33):13434.

Parmesan, C. 2006. Ecological and evolutionary responses to recent climate change. Annual Review of Ecology, Evolution, and Systematics 37:637-669.

Parmesan, C. and Yohe, G. 2003. A globally coherent fingerprint of climate change impacts across natural systems. Nature 421:37.

Pinheiro, J., Bates, D., DebRoy, S., Sarkar, D., Heisterkamp, S. and Van Willigen, B. 2017. Package 'nlme'. 3.1-141.

Potter, K.A., Arthur Woods, H. and Pincebourde, S. 2013. Microclimatic challenges in global change biology. Global Change Biology 19(10):2932-2939.

Pureswaran, D.S., Roques, A. and Battisti, A. 2018. Forest Insects and Climate Change. Current Forestry Reports.

Sánchez-Bayo, F. and Wyckhuys, K.A. 2019. Worldwide decline of the entomofauna: A review of its drivers. Biological Conservation 232:8-27.

Saunders, D.S. 2002. Insect clocks, Elsevier.

Saunders, M.E., Janes, J.K. and O'Hanlon, J.C. 2019. Moving On from the Insect Apocalypse Narrative: Engaging with Evidence-Based Insect Conservation. Bioscience.

Snyder, R.L., Spano, D., Cesaraccio, C. and Duce, P. 1999. Determining degree-day thresholds from field observations. International Journal of Biometeorology 42(4):177-182.

Stålhandske, S., Lehmann, P., Pruisscher, P. and Leimar, O. 2015. Effect of winter cold duration on spring phenology of the orange tip butterfly, Anthocharis cardamines. Ecology and Evolution 5(23):5509-5520.

Storlie, C., Merino-Viteri, A., Phillips, B., VanDerWal, J., Welbergen, J. and Williams, S. 2014. Stepping inside the niche: microclimate data are critical for accurate assessment of species' vulnerability to climate change. Biology letters 10(9):20140576.

Thackeray, S.J., Henrys, P.A., Hemming, D., Bell, J.R., Botham, M.S., Burthe, S., Helaouet, P., Johns, D.G., Jones, I.D., Leech, D.I., Mackay, E.B., Massimino, D., Atkinson, S., Bacon, P.J., Brereton, T.M., Carvalho, L., Clutton-Brock, T.H., Duck, C., Edwards, M., Elliott, J.M., Hall, S.J.G., Harrington, R., Pearce-Higgins, J.W., Hoye, T.T., Kruuk, L.E.B., Pemberton, J.M., Sparks, T.H., Thompson, P.M., White, I., Winfield, I.J. and Wanless, S. 2016. Phenological sensitivity to climate across taxa and trophic levels. Nature 535(7611):241.

Thackeray, S.J., Sparks, T.H., Frederiksen, M., Burthe, S., Bacon, P.J., Bell, J.R., Botham, M.S., Brereton, T.M., Bright, P.W., Carvalho, L., Clutton-Brock, T., Dawson, A., Edwards, M., Elliott, J.M., Harrington, R., Johns, D., Jones, I.D., Jones, J.T., Leech, D.I., Roy, D.B., Scott, W.A., Smith, M., Smithers, R.J., Winfield, I.J. and Wanless, S. 2010. Trophic level asynchrony in rates of phenological change for marine, freshwater and terrestrial environments. Global Change Biology 16(12):3304-3313.

Titley, M.A., Snaddon, J.L. and Turner, E.C. 2017. Scientific research on animal biodiversity is systematically biased towards vertebrates and temperate regions. Plos One 12(12):e0189577.

Visser, M.E. and Both, C. 2005. Shifts in phenology due to global climate change: the need for a yardstick. Proceedings of the Royal Society B: Biological Sciences 272(1581):2561.

Ward, S.E., Schulze, M. and Roy, B. 2018. A long-term perspective on microclimate and spring plant phenology in the Western Cascades. Ecosphere 9(10):e02451.

Wolda, H. 1988. Insect Seasonality: Why? Annual Review of Ecology and Systematics 19(1):1-18.

Woods, H.A., Dillon, M.E. and Pincebourde, S. 2015. The roles of microclimatic diversity and of behavior in mediating the responses of ectotherms to climate change. Journal of Thermal Biology 54:86-97.

Zalom, F.G. and Goodell, P.B. 1983. Degree days: the calculation and use of heat units in pest management, University of California, Division of Agriculture and Natural Resources.

Insect identification

Arnett, R.H. 2000. American Insects: A Handbook of the Insects of America North of Mexico (2nd Edition). CRC Press. Boca Raton, Florida. 1003 pp.

Arnett, R.H., and M.C. Thomas 2001. American Beetles, Vol. 1. CRC Press. Boca Raton, Florida. 443 pp.

Arnett, R.H., M.C. Thomas, P.E. Skelley, and J.H. Frank. 2002. American Beetles, Vol. 2. CRC Press. Boca Raton, Florida. 861 pp.

Covell, C.V. 1984. A Field Guide to the Moths. Houghton Mifflin. Boston, Massachusetts. 496 pp.

McAlpine, J.F., B.V. Peterson, G.E. Shewell, H.J. Teskey, J.R. Vockeroth, and D.M. Wood. 1981. Manual of Nearctic Diptera, Vol. 1-2. Ottawa, Ontario: Biosystematics Research Institute.

Merritt, R.W., K.W. Cummins, and M.B. Berg. 2008. An Introduction to the Aquatic Insects of North America (4th Edition). Kendall/Hunt Publishing Company, Dubuque, Iowa. 862 pp.

Triplehorn, C.A., and N.F. Johnson. 2005. Borror and DeLong's Introduction to the Study of Insects (7th Edition). Thomson Brooks/Cole. Belmont, California. 864 pp.

FIGURES

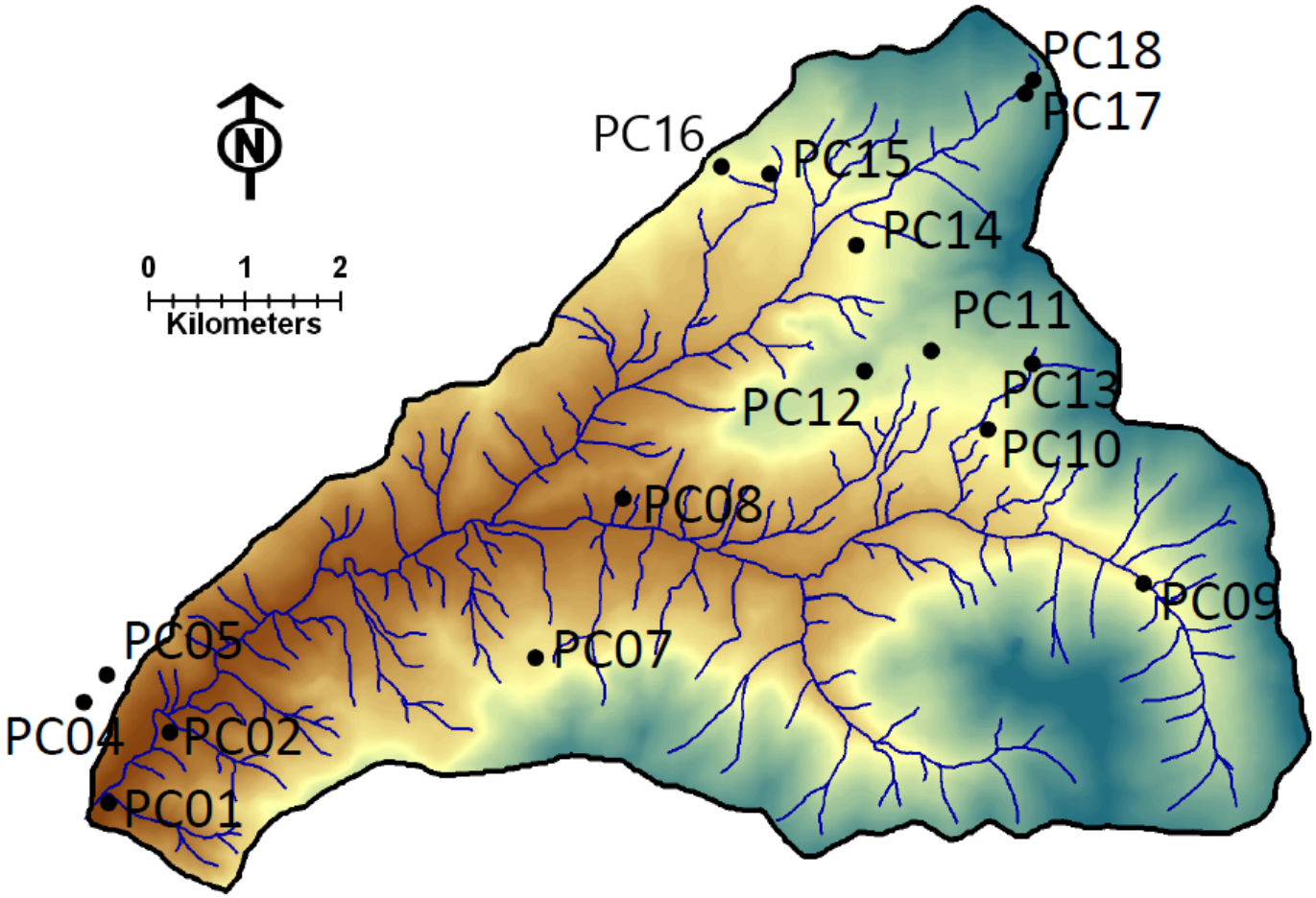

Figure 3.1 Relative location of study sites within the H.J. Andrews Experimental Forest. Brown represents lower elevations and blue represents higher elevations.

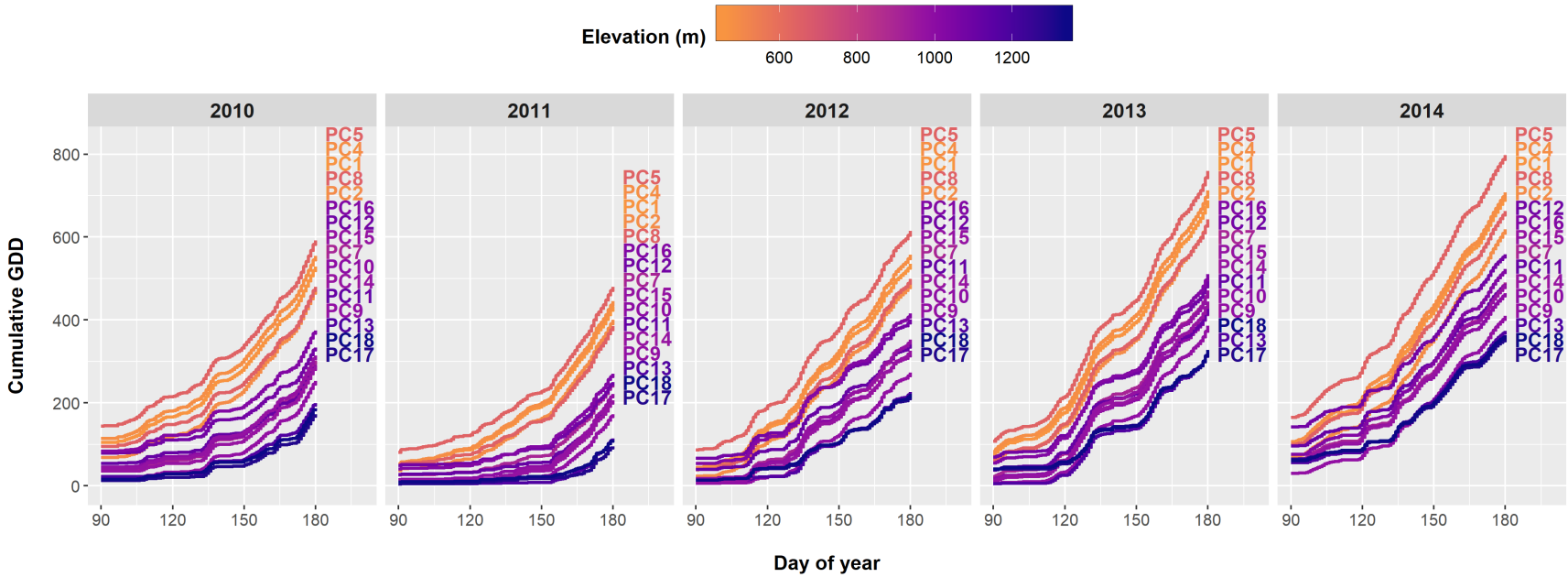

Figure 3.2 Cumulative GDD by day of year from day of year 90 (~April 1) to 180 (~June 30), paneled by sampling year. Curve and site label color indicates elevation. Site labels are ordered by largest to smallest cumulative GDD on day of year 180. Low-elevation sites accumulate significantly more GDD than high-elevation sites by day of year 180, with differences ranging from 390 GDD in 2011 to 447 GDD in 2014. Low- and high-elevation site accumulation rankings are mostly consistent in each year, while the ranking at intermediate elevation sites vary.

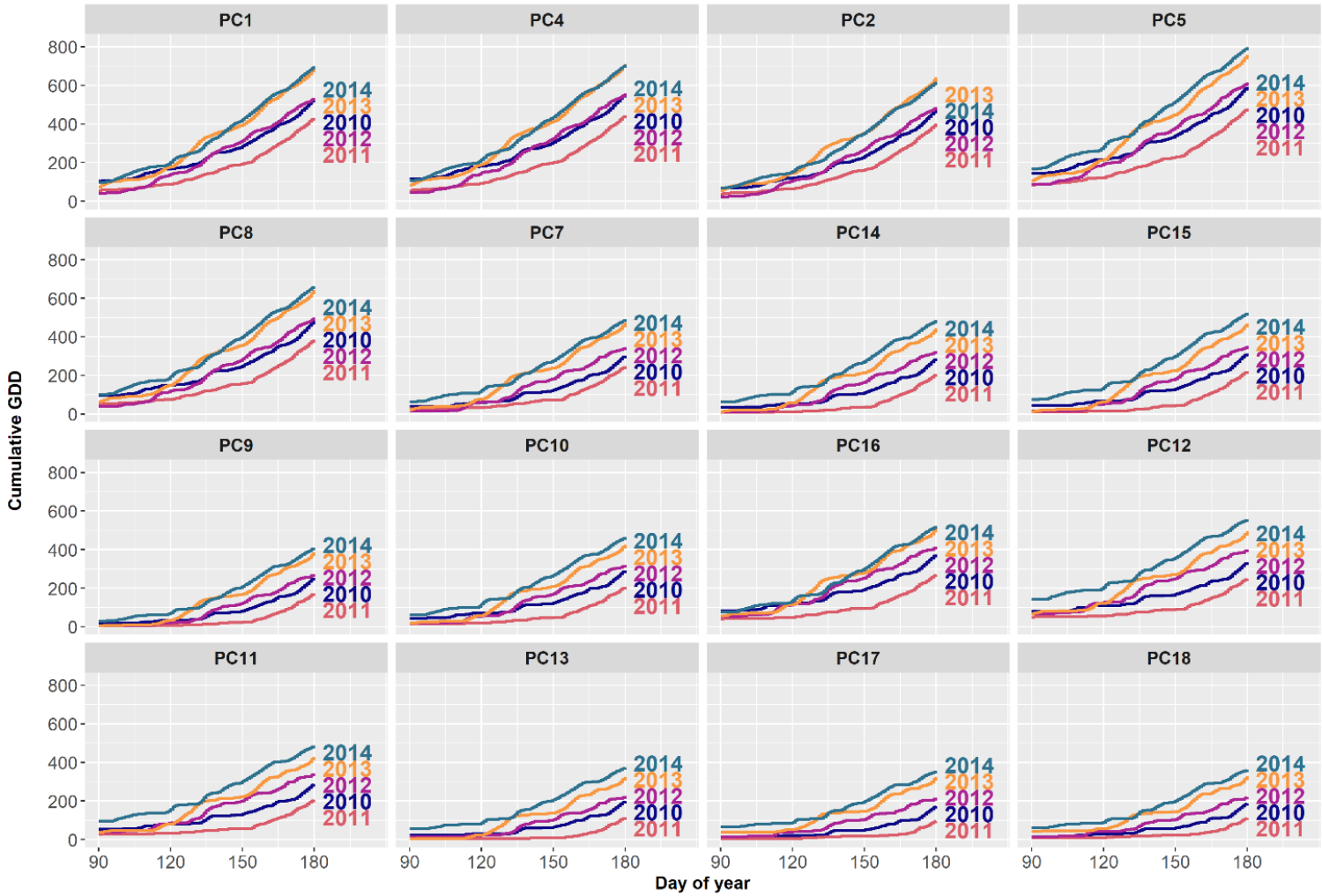

Figure 3.3 Cumulative GDD by day of year, paneled by site. Sites are in order of low to high elevation, from left to right in each row (PC1 is the lowest elevation, PC18 is the highest elevation). Curve and site label color indicates sampling year. Site labels are in order of the largest to smallest spring GDD (cumulative GDD on day of year 180). Within sites, the range of accumulation in winter GDD (cumulative GDD as of day of year 90) varied by 25-93 GDD, and for winter GDD, varied by 237-318 GDD.

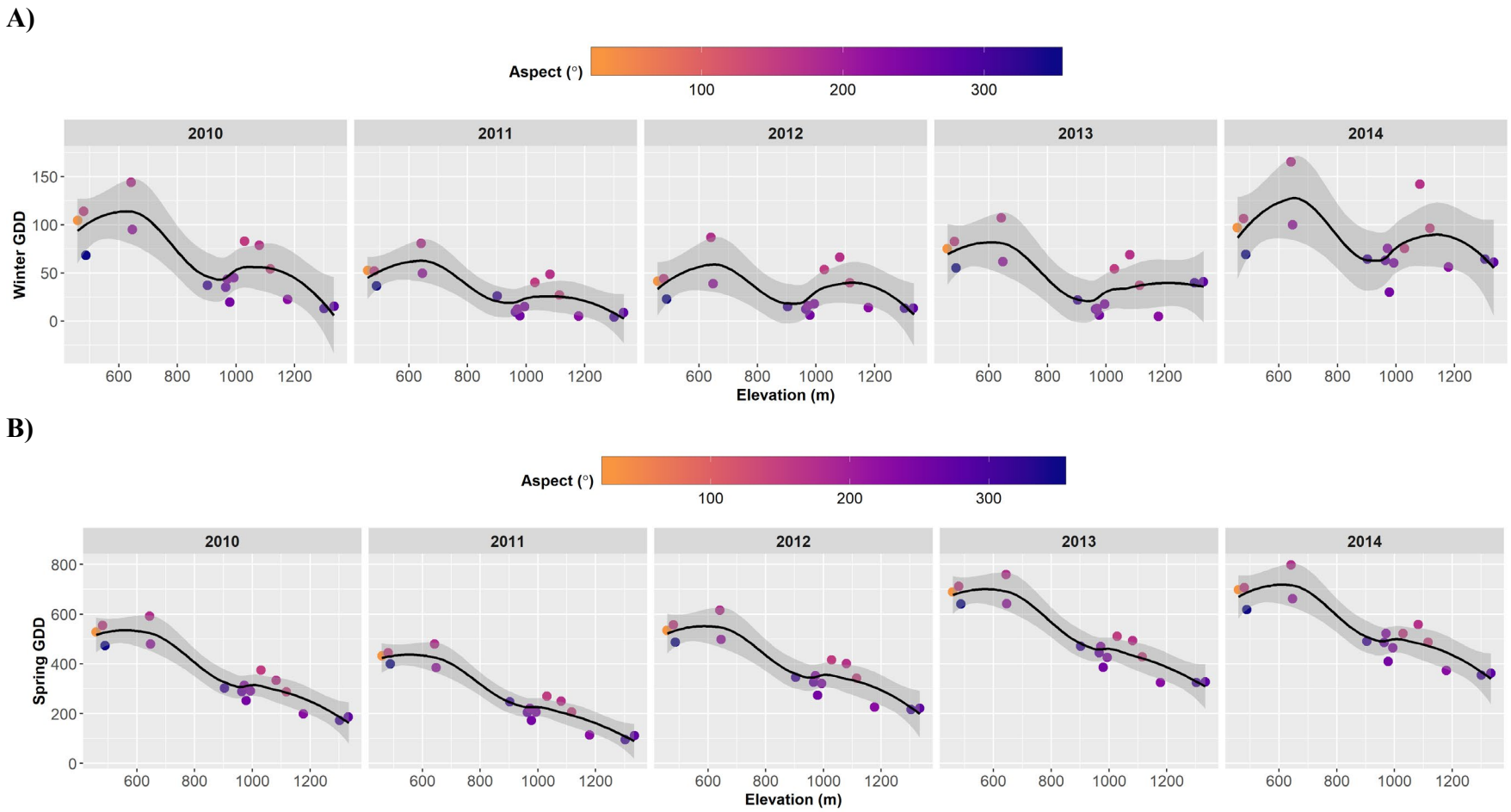

Figure 3.4 Plots show the relationship between: A) winter GDD (cumulative GDD by day of year 90) and elevation (m) and B) spring GDD (cumulative GDD by day of year 180) and elevation (m). Points are colored by aspect (º). Black line is the loess smoothing curve and gray shaded area is the confidence interval. The relationship of elevation with winter GDD was more variable than with spring GDD. Some lower-elevation sites had lower median winter GDD than higher-elevation sites, likely due to topography (such as aspect) and other factors, including cold-air drainage and pooling.

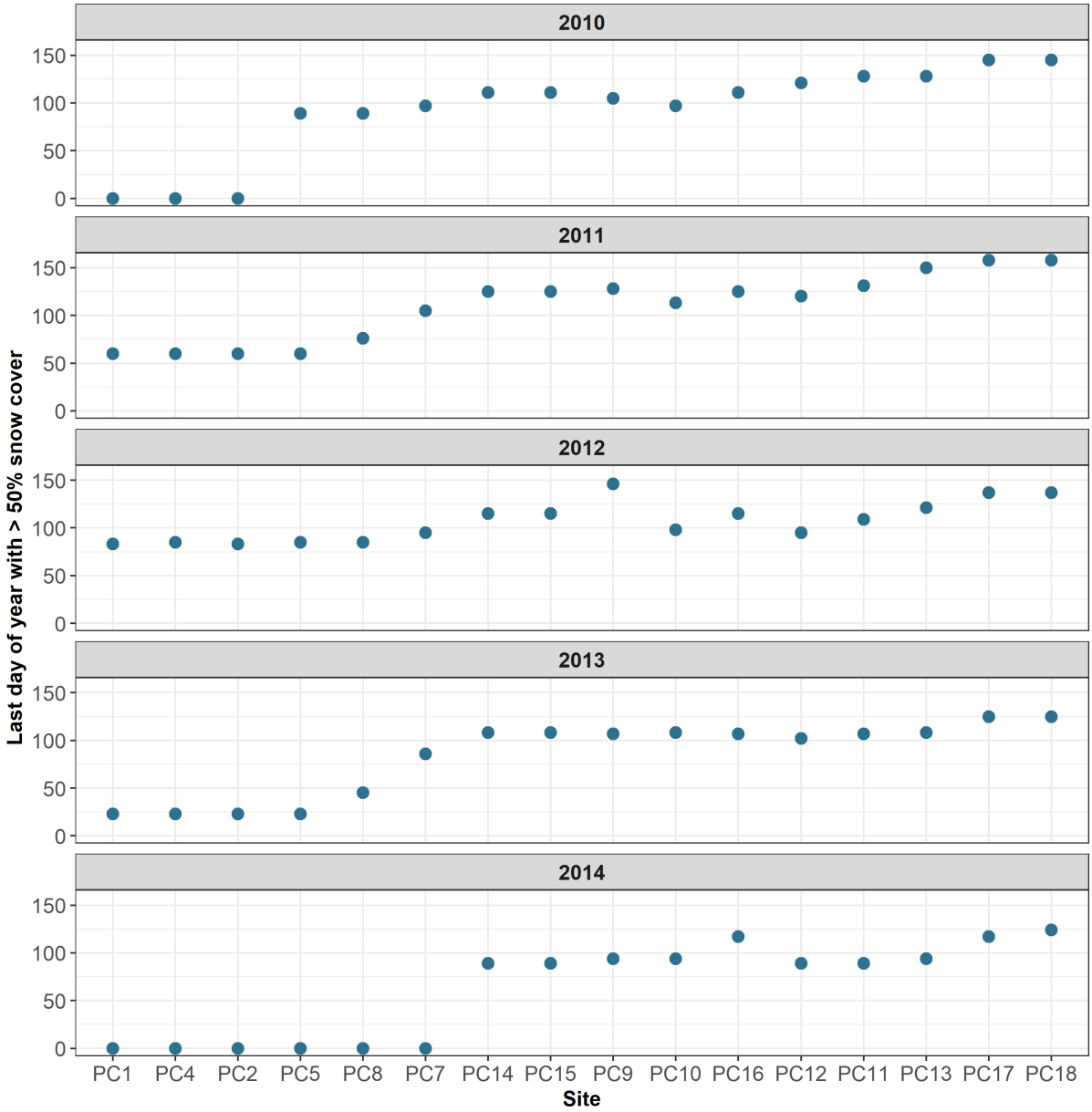

Figure 3.5 Plots shows the last day of year with > 50% snow cover, which we use as an indicator of snow persistence, for each site and sampling year. Day of year 0 indicates that no snow was detected in the sampling year. Sites are ordered from left to right from lowest to highest elevation. Snow persistence was relatively consistent inter-annually at sites > 1100m in elevation, with early snowmelt in 2013 and 2014. Snow persisted at sites < 650m in 2010 and 2012. At sites between 650m-1100m in elevation, persistence was variable inter-annually. PC7 had the most inter-annual variability in snow cover/persistence.

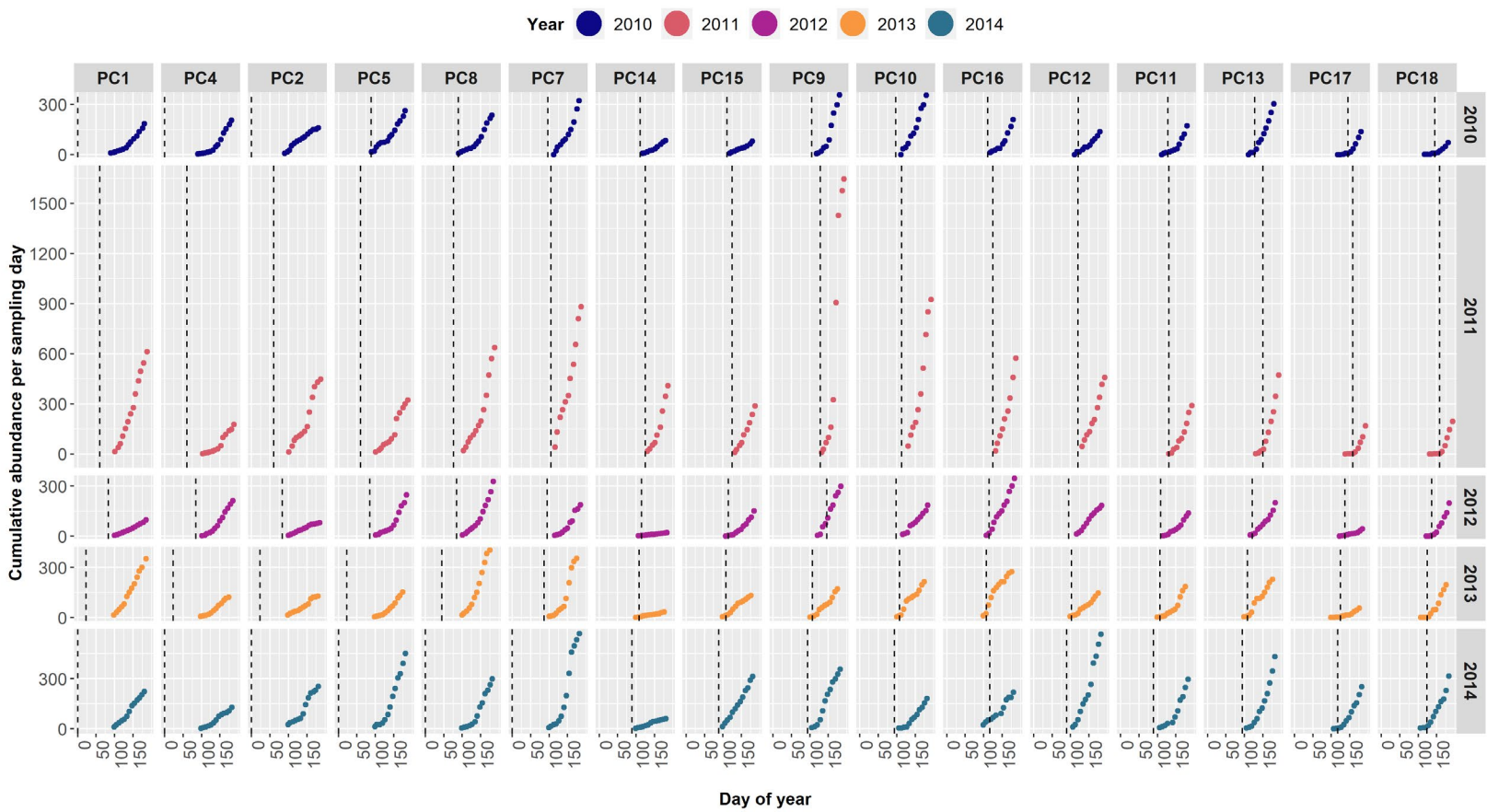

Figure 3.6 Plot shows cumulative abundance per sampling day by day of year, paneled by site and year, with points colored by year. Dotted line indicates the last day of > 50% snow cover at the closest reference site (Table A.8). Sites are listed left to right in order of low to high elevation. Note that y-axis range is different for each year, but the scale sizing is the same. Cumulative abundance per sampling day did not exceed 600 in any year except for 2011.

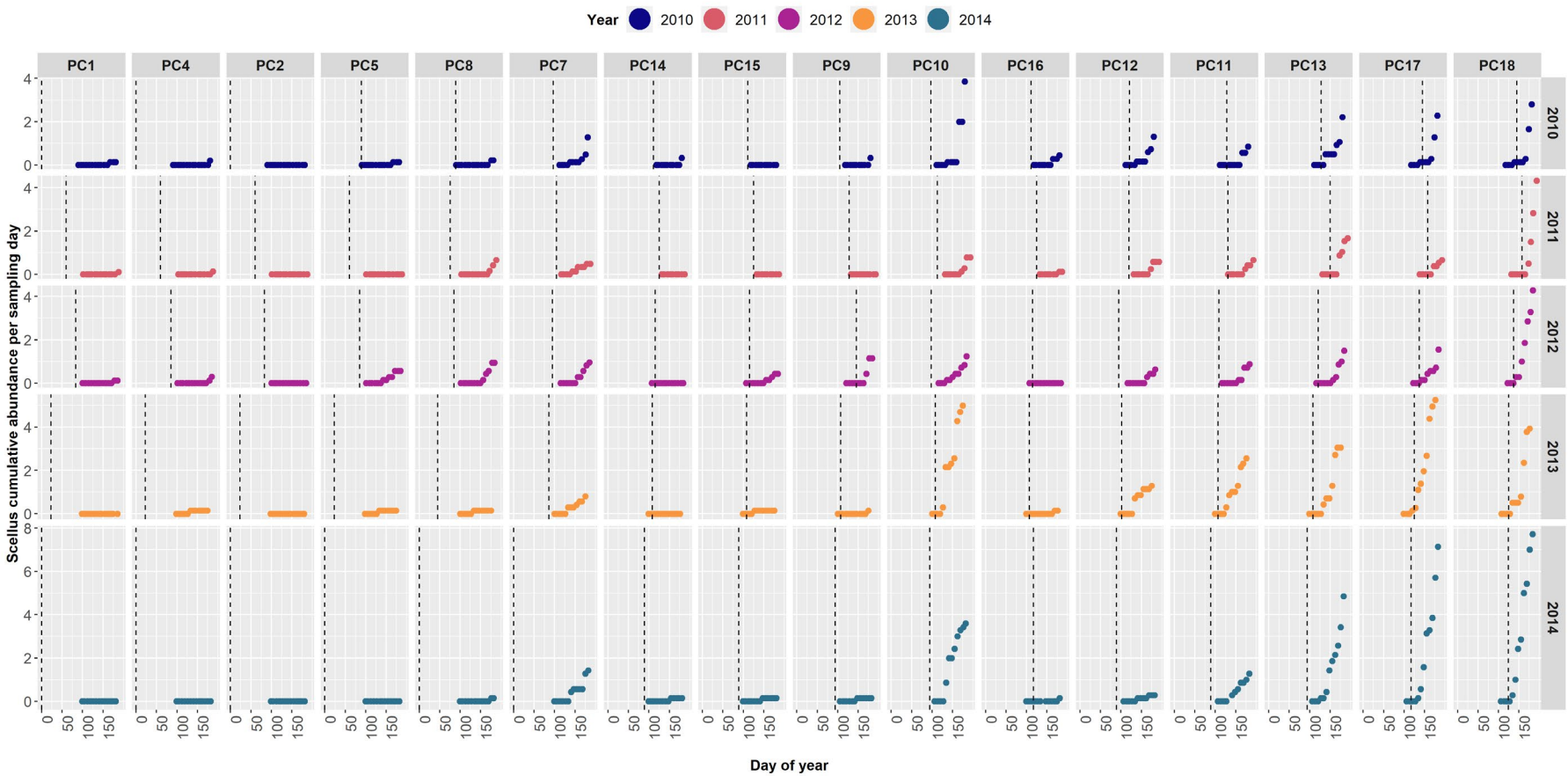

Figure 3.7 Plot shows *Scellus* cumulative abundance per sampling day by day of year, paneled by site and year. Dotted line indicates the last day of > 50% snow cover at the closest reference site (Table A.8). Sites are listed left to right in order of low to high elevation. Note that y-axis range is different for each year, but the scale sizing is the same.

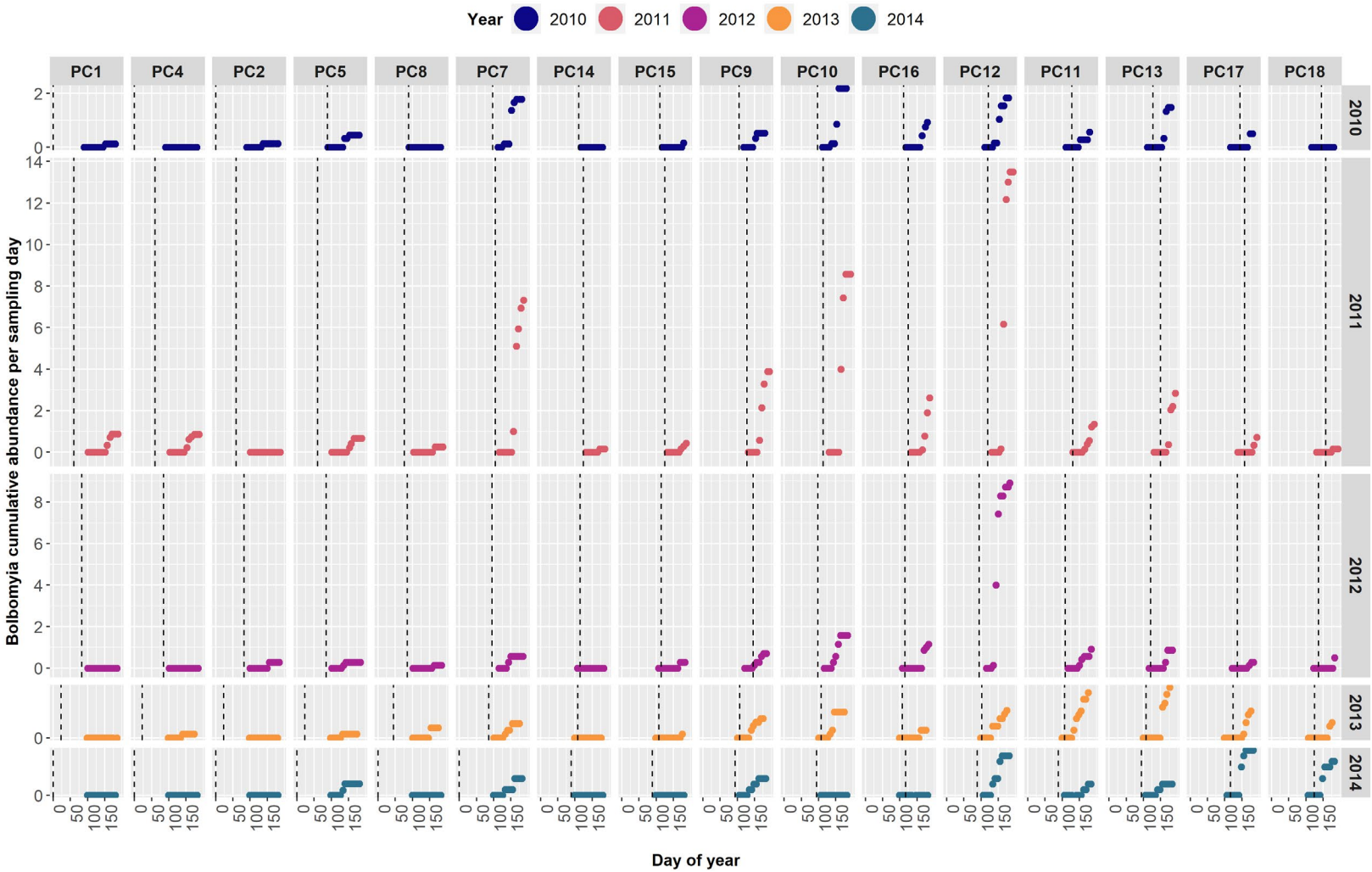

Figure 3.8 Plot shows *Bolbomyia* cumulative abundance per sampling day by day of year, paneled by site and year. Dotted line indicates the last day of > 50% snow cover at the closest reference site (Table A.8). Sites are listed left to right in order of low to high elevation. Note that y-axis range is different for each year, but the scale sizing is the same.

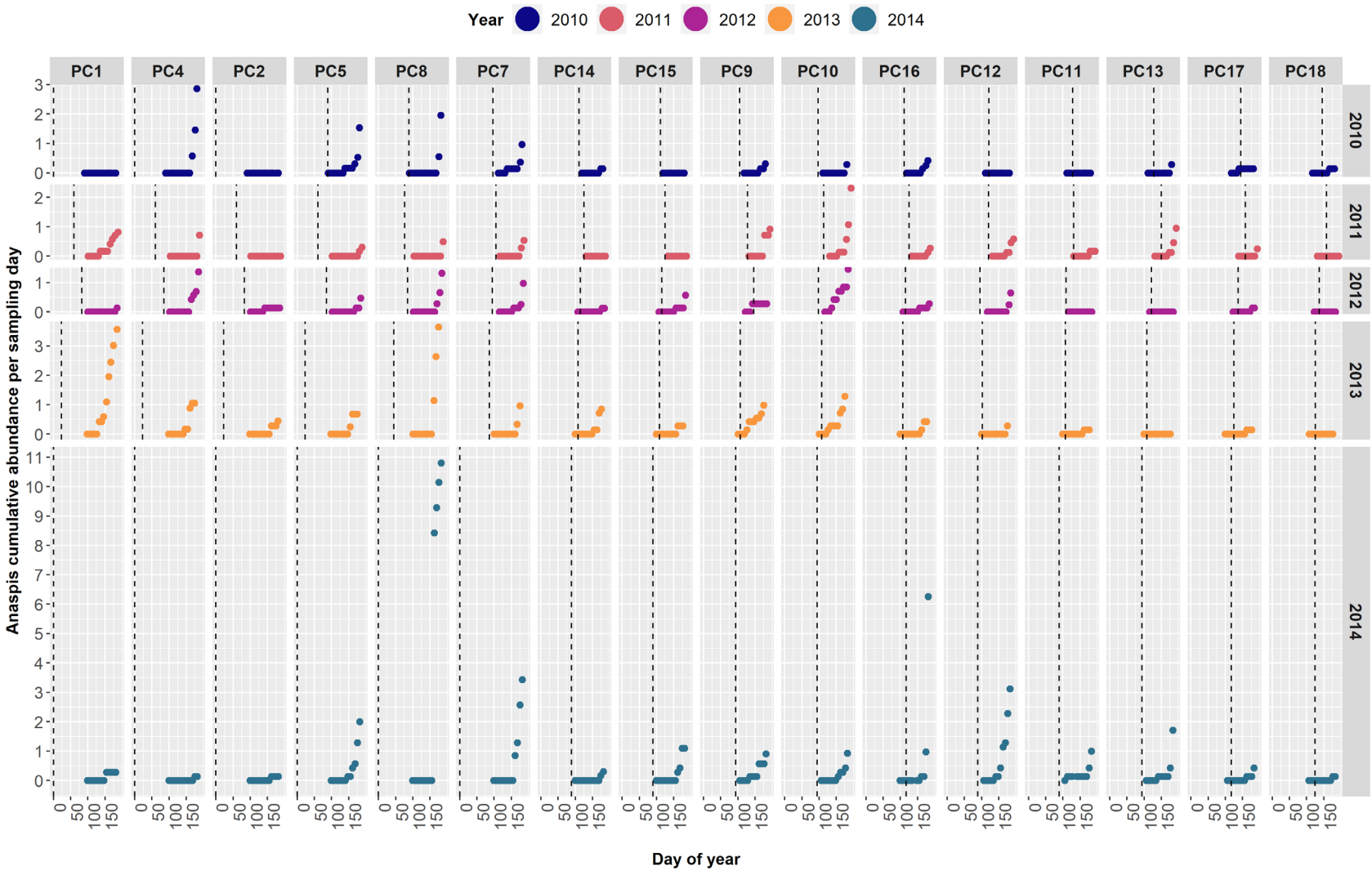

Figure 3.9 Plot shows *Anaspis* cumulative abundance per sampling day by day of year, paneled by site and year. Dotted line indicates the last day of > 50% snow cover at the closest reference site (Table A.8). Sites are listed left to right in order of low to high elevation. Note that y-axis range is different for each year, but the scale sizing is the same.

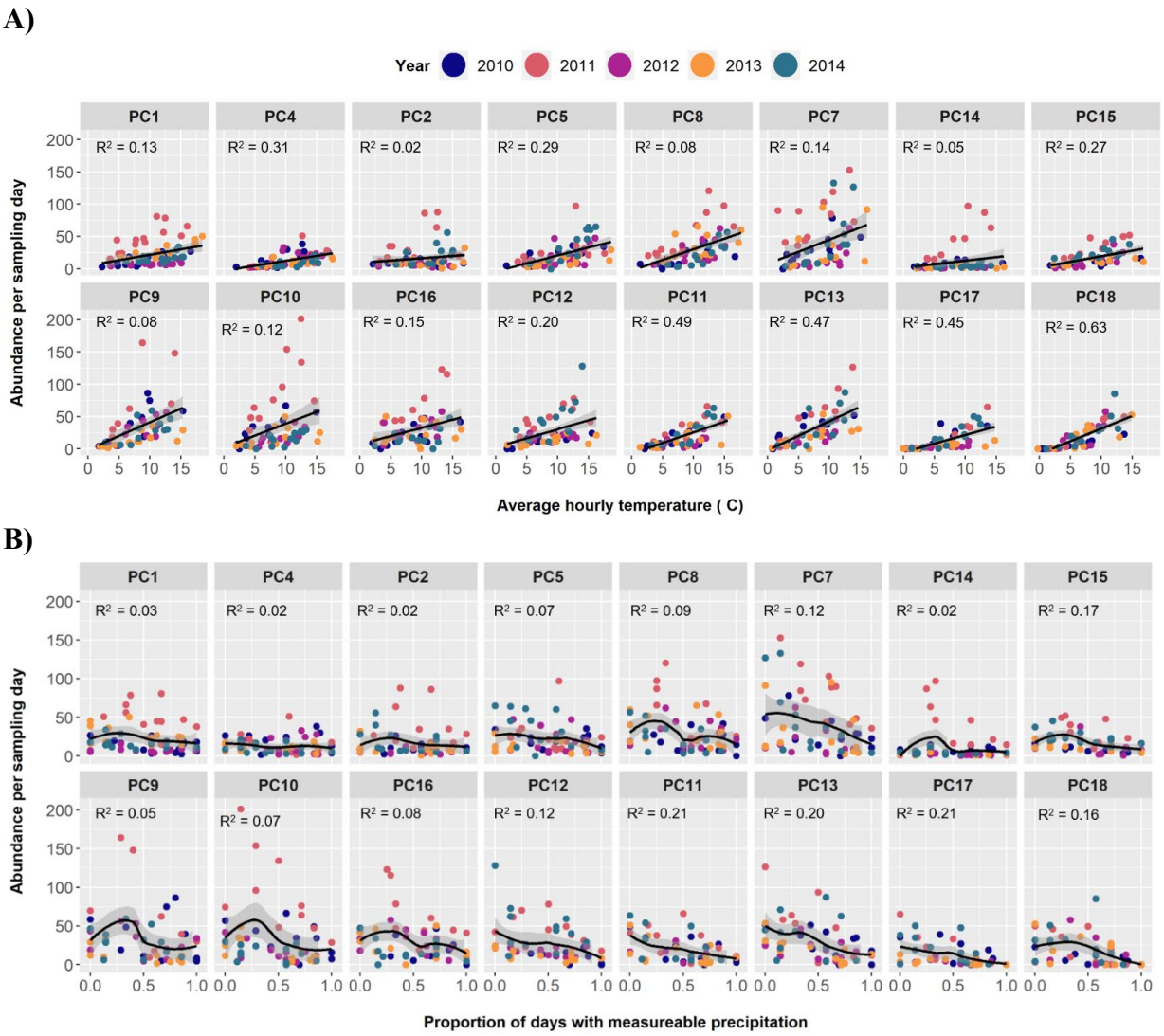

Figure 3.10 Abundance per sampling day by: A) average daily temperature (°C) during the sampling period, and (B) proportion of days with measurable precipitation during the sampling period. Abundance per sampling day had a positive relationship with average hourly temperature and a negative relationship with proportion of days with measureable precipitation (note that temperature values were taken at each site, but precipitation measured at a single climate station). Black line is loess smoothing curve and gray shaded area is confidence interval. Two extreme data points from PC9 in 2011 were removed to improve visualization: 1) abundance 581, average hourly temperature 9.48°C, proportion of days with measurable precipitation .43; 2) abundance 522, average hourly temperature 12.16, proportion of days with measurable precipitation 0.00.

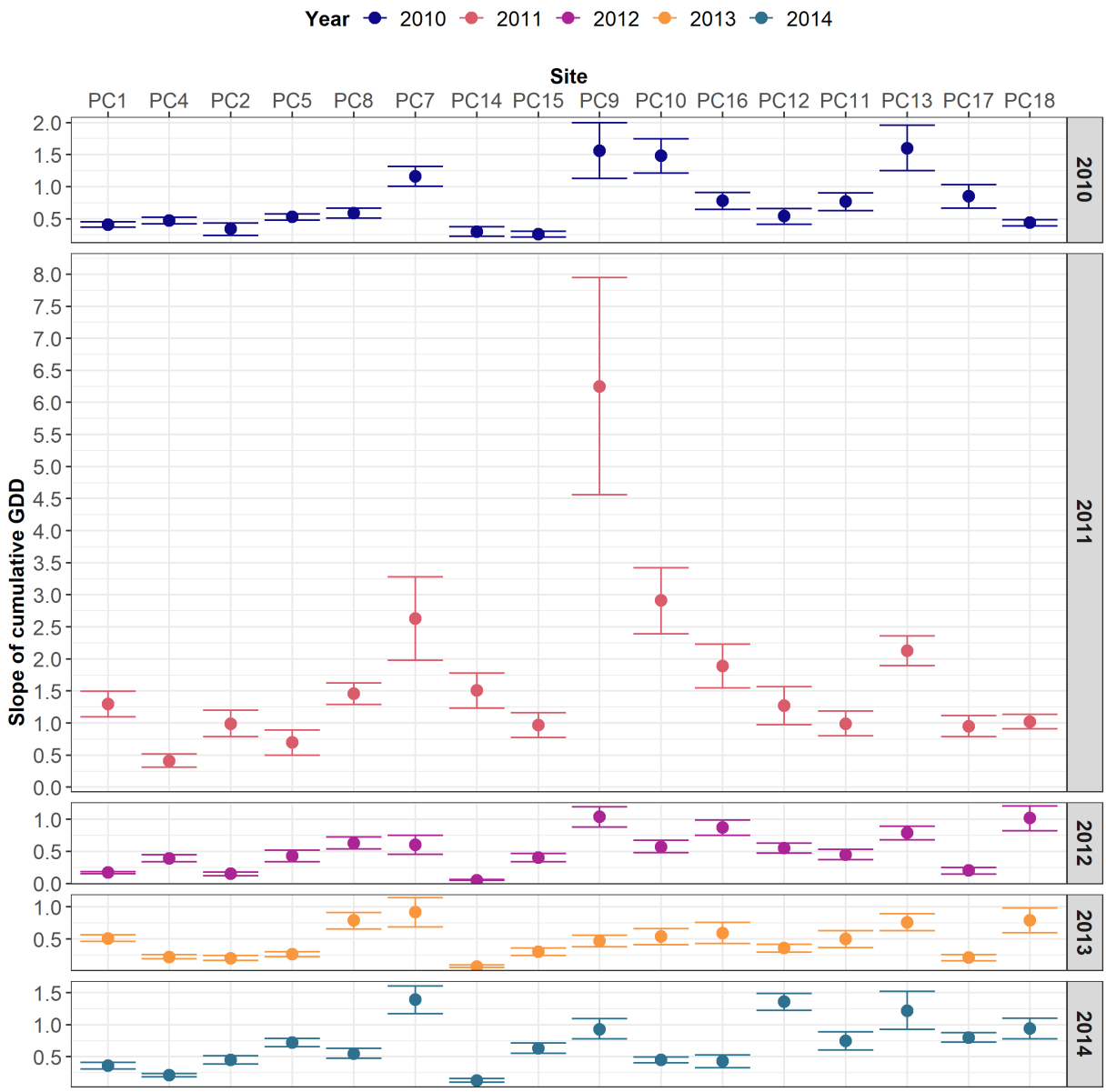

Figure 3.11 Estimates and confidence intervals of the change in cumulative abundance per sampling day per cumulative GDD for each site and sampling year, colored by year. Sites are ordered left to right from low to high elevation. Year 2011 had the largest estimate and confidence interval for most sites. In other years, estimates at sites < 650m elevation were fairly similar within sites among years. Estimates and confidence intervals were larger and more variable at sites > 650m elevation, particularly sites PC7 and PC9.

TABLES

Table 3.1 Characteristics of the selected study sites, which vary in elevation (460m to 1300m), slope (10.8% to 79.2%), aspect (30° to 347°), and forest age.

Site ID	Latitude	Longitude	Elevation (m)	Forest Age	Slope (%)	Aspect (º)
PC1	44.21	-122.26	460	Young	51.35	30
PC2	44.21	-122.25	488	Old	49.58	347
PC4	44.22	-122.26	481	Young	79.22	153
PC5	44.22	-122.26	644	Young	64.74	174
PC7	44.22	-122.20	903	Old	28.19	311
PC8	44.24	-122.19	647	Old	36.16	213
PC9	44.23	-122.12	979	Old	54.41	250
PC10	44.24	-122.14	994	Old	19.35	237
PC11	44.25	-122.15	1116	Young	45.39	147
PC12	44.25	-122.16	1082	Old	35.45	169
PC13	44.25	-122.14	1178	Old	16.8	226
PC14	44.26	-122.16	965	Old	20.41	267
PC15	44.27	-122.17	971	Old	10.8	228
PC16	44.27	-122.18	1030	Young	27.5	153
PC17	44.27	-122.14	1301	Old	43.3	308
PC18	44.27	-122.14	1339	Young	30.1	275

Table 3.2 Total number of samples and total number of days that traps were set by site for each sampling year. The number of samples and the duration of sampling periods varied due to road access and technician availability.

Site ID	Total samples collected					Total sampling days				
	2010	2011	2012	2013	2014	2010	2011	2012	2013	2014
PC1	14	13	13	13	13	97	93	90	94	89
PC2	14	13	13	13	13	97	93	90	88	89
PC4	14	13	13	12	13	97	94	90	80	90
PC5	14	13	13	12	13	98	94	90	80	90
PC7	11	11	11	12	13	93	76	74	81	90
PC8	14	13	13	12	13	98	92	89	81	90
PC9	10	10	10	12	12	68	70	69	83	85
PC10	11	10	11	12	12	92	70	76	83	85
PC11	11	10	11	12	11	92	69	76	84	86
PC12	11	10	11	12	12	92	70	76	83	84
PC13	11	10	11	12	12	92	70	76	84	86
PC14	10	9	12	12	13	68	64	83	83	89
PC15	10	9	12	12	13	68	64	83	82	89
PC16	10	9	12	12	12	68	64	83	82	89
PC17	10	9	10	12	12	70	62	68	84	83
PC18	10	10	10	11	12	68	69	68	77	83

CHAPTER 4: GENERAL CONCLUSION

My research results demonstrate some of the benefits of using long-term data for ecological research. In the second chapter, using air temperature measurements gathered over the course of years (rather than weeks or months) allowed us to better understand the range of variability in measurement differences between instruments, as well as to estimate these differences and their relationship with key drivers in a broad range of environmental conditions. In the third chapter, we saw the value of collecting insect count data over multiple years, as patterns were strikingly different in one year than the other four years in comparison. Also, patterns of abundance were not all consistent within a site over time.

Long-term ecological research data can provide insights to complex ecological phenomena, but it can also introduce complications in data analysis. Maintaining perfectly consistent study methods over several years, especially in field studies, may not be possible or desirable. Advanced statistical methods have developed over time that can address these challenges, but researchers must first recognize the potential issues in their data. Historical climate data is widely available to download online, but researchers cannot assume the methods used to collect this data have been continuous. As discussed in Chapter 2, it is not uncommon for instruments used in climate data collection to be frequently upgraded. However, measurement differences between these instruments can be substantial, and some metrics are particularly sensitive to differences. As discussed in Chapter 3, the insect sampling effort at each site varied due to technician availability and site access, so it was necessary to transform count data in order to make valid abundance comparisons between sites. Without correcting for these types of differences in methods before analysis, researchers are at risk of producing flawed estimates and conclusions about trends.

The results from the analysis in Chapter 2 will be used to supplement H.J. Andrews air temperature metadata, and to educate researchers about best practices when using air temperature time series data collected at H.J. Andrews and similar meteorological stations. The results from the analysis in Chapter 3 will provide a foundation for understanding broader insect population and community dynamics at H.J. Andrews, which will be synthesized with the results from similar vegetation and bird phenology studies that were conducted there during the same time period.

BIBLIOGRAPHY

Arck, M. and Scherer, D. 2001. A physically based method for correcting temperature data measured by naturally ventilated sensors over snow. Journal of Glaciology 47(159):665-670.

Ashcroft, M.B. 2018. Which is more biased: Standardized weather stations or microclimatic sensors? Ecology and Evolution 8(11):5231-5232.

Bale, J.S., Masters, G.J., Hodkinson, I.D., Awmack, C., Bezemer, T.M., Brown, V.K., Butterfield, J., Buse, A., Coulson, J.C. and Farrar, J. 2002. Herbivory in global climate change research: direct effects of rising temperature on insect herbivores. Global Change Biology 8(1):1-16.

Buckley, L.B., Tewksbury, J.J. and Deutsch, C.A. 2013. Can terrestrial ectotherms escape the heat of climate change by moving? Proceedings of the Royal Society B: Biological Sciences 280(1765):20131149.

Cardoso, P., Branco, V.V., Chichorro, F., Fukushima, C.S. and Macías-Hernández, N. 2019. Can we really predict a catastrophic worldwide decline of entomofauna and its drivers? Global Ecology and Conservation 20:e00621.

Cardoso, P., Erwin, T.L., Borges, P.A.V. and New, T.R. 2011. The seven impediments in invertebrate conservation and how to overcome them. Biological Conservation 144(11):2647-2655.

Chen, J., Franklin, J.F. and Spies, T.A. 1993. Contrasting microclimates among clearcut, edge, and interior of old-growth Douglas-fir forest. Agricultural and Forest Meteorology 63(3-4):219-237.

Chen, J., Saunders, S.C., Crow, T.R., Naiman, R.J., Brosofske, K.D., Mroz, G.D., Brookshire, B.L. and Franklin, J.F. 1999. Microclimate in forest ecosystem and landscape ecology: variations in local climate can be used to monitor and compare the effects of different management regimes. Bioscience 49(4):288-297.

Crimmins, M.A. and Crimmins, T.M. 2019. Does an Early Spring Indicate an Early Summer? Relationships Between Intraseasonal Growing Degree Day Thresholds. Journal of Geophysical Research: Biogeosciences 124(8):2628-2641.

Daly, C. 2006. Guidelines for assessing the suitability of spatial climate data sets. International Journal of Climatology: A Journal of the Royal Meteorological Society 26(6):707-721.

Daly, C., Conklin, D.R. and Unsworth, M.H. 2010. Local atmospheric decoupling in complex topography alters climate change impacts. International Journal of Climatology 30(12):1857-1864.

Daly, C. and McKee, W.A. 2019. Meteorological data from benchmark stations at the Andrews Experimental Forest, 1957 to present (MS00103). Forest Science Data Bank. https://doi.org/10.6073/pasta/c96875918bb9c86d330a457bf4295cd9

De Frenne, P., Rodríguez-Sánchez, F., Coomes, D.A., Baeten, L., Verstraeten, G., Vellend, M., Bernhardt-Römermann, M., Brown, C.D., Brunet, J. and Cornelis, J. 2013. Microclimate moderates plant responses to macroclimate warming. Proceedings of the National Academy of Sciences 110(46):18561-18565.

Deutsch, C.A., Tewksbury, J.J., Huey, R.B., Sheldon, K.S., Ghalambor, C.K., Haak, D.C. and Martin, P.R. 2008. Impacts of climate warming on terrestrial ectotherms across latitude. Proceedings of the National Academy of Sciences 105(18):6668-6672.

Dobrowski, S.Z. 2011. A climatic basis for microrefugia: the influence of terrain on climate. Global Change Biology 17(2):1022-1035.

Fisher, M. 2019. The small, the hidden, the less-loved: conserving other species. Oryx 53(2):199-200.

Forrest, J.R.K. 2016. Complex responses of insect phenology to climate change. Current Opinion in Insect Science 17(Supplement C):49-54.

Frey, S.J.K., Hadley, A.S., Johnson, S.L., Schulze, M., Jones, J.A. and Betts, M.G. 2016. Spatial models reveal the microclimatic buffering capacity of old-growth forests. Science advances 2(4).

Gilman, S.E., Urban, M.C., Tewksbury, J., Gilchrist, G.W. and Holt, R.D. 2010. A framework for community interactions under climate change. Trends in Ecology & Evolution 25(6):325-331.

Gwinner, E. 1990. Circannual rhythms in bird migration: control of temporal patterns and interactions with photoperiod. In Bird migration. pp. 257-268, Springer.

Hallmann, C.A., Sorg, M., Jongejans, E., Siepel, H., Hofland, N., Schwan, H., Stenmans, W., Müller, A., Sumser, H. and Hörren, T. 2017. More than 75 percent decline over 27 years in total flying insect biomass in protected areas. Plos One 12(10):e0185809.

Hampton, S.E., Strasser, C.A., Tewksbury, J.J., Gram, W.K., Budden, A.E., Batcheller, A.L., Duke, C.S. and Porter, J.H. 2013. Big data and the future of ecology. Frontiers in Ecology and the Environment 11(3):156-162.

Harrell, F.E. 2018. rms: Regression Modeling Strategies. 5.1-2.

Harrell, F.E., Lee, K.L. and Mark, D.B. 1996. Multivariable prognostic models: issues in developing models, evaluating assumptions and adequacy, and measuring and reducing errors. Statistics in medicine 15(4):361-387.

Harrell, J.F.E., Bickel, P., Diggle, P., Fienberg, S.E., Gather, U., Olkin, I. and Zeger, S. 2015. Regression Modeling Strategies: With Applications to Linear Models, Logistic and Ordinal Regression, and Survival Analysis, Cham: Springer International Publishing, Cham.

Hijmans, R.J. 2019. geosphere: Spherical Trigonometry. 1.5-10. https://CRAN.R-project.org/package=geosphere

Hlavac, M. 2018. stargazer: Well-Formatted Regression and Summary Statistics Tables. 5.2.2. https://CRAN.R-project.org/package=stargazer

Hodgson, J.A., Thomas, C.D., Oliver, T.H., Anderson, B.J., Brereton, T.M. and Crone, E.E. 2011. Predicting insect phenology across space and time. Global Change Biology 17(3):1289-1300.

Hodkinson, I.D. 2005. Terrestrial insects along elevation gradients: species and community responses to altitude. Biological Reviews 80(3):489-513.

Holden, Z.A., Klene, A.E., F. Keefe, R. and G. Moisen, G. 2013. Design and evaluation of an inexpensive radiation shield for monitoring surface air temperatures. Agricultural and Forest Meteorology 180:281-286.

Hubbard, K., Lin, X. and Walter-Shea, E. 2001. The effectiveness of the ASOS, MMTS, Gill, and CRS air temperature radiation shields. Journal of Atmospheric and Oceanic Technology 18(6):851-864.

Hubbard, K.G., Lin, X., Baker, C.B. and Sun, B. 2004. Air temperature comparison between the MMTS and the USCRN temperature systems. Journal of Atmospheric and Oceanic Technology 21(10):1590-1597.

Hubbart, J., Link, T., Campbell, C. and Cobos, D. 2005. Evaluation of a low-cost temperature measurement system for environmental applications. Hydrological Processes 19(7):1517-1523.

Huwald, H., Higgins, C.W., Boldi, M.-O., Bou-Zeid, E., Lehning, M. and Parlange, M.B. 2009. Albedo effect on radiative errors in air temperature measurements. Water Resources Research 45(8):1-13.

Hyndman, R., Athanasopoulos, G., Bergmeir, C., Caceres, G., Chhay, L., O'Hara-Wild, M., Petropoulos, F., Razbash, S., Wang, E. and Yasmeen, F. 2018. forecast: Forecasting functions for time series and linear models. 8.4. http://pkg.robjhyndman.com/forecast

IPPC, I.P.P.C. 2019. Asian longhorned beetle invasive insect model of OSU IPPC model analysis Accessed on December 10, 2019. uspest.org

Jarvis, B. 2018. The Insect Apocalypse Is Here: What does it mean for the rest of life on Earth? The New York Times. Accessed on 12/17/2019. https://www.nytimes.com/2018/11/27/magazine/insect-apocalypse.html

Johnson, S. and Frey, S.J.K. 2009. Air temperature at core phenology sites and additional bird monitoring sites in the Andrews Experimental Forest, 2009-Present. Forest Science Data Bank, Corvallis, Oregon. Retrieved from: http://andlter.forestry.oregonstate.edu/data/abstract.aspx?dbcode=MS045 doi:http://dx.doi.org/10.6073/pasta/f64dc0ba1f0e2015a6b4da92939efe37

Johnson, S. and Li, J. 2016. Aquatic and terrestrial insect activity phenology with trap collections at the Andrews Experimental Forest, 2009-2014. Forest Science Data Bank, Corvallis, OR. Retrieved from: http://andlter.forestry.oregonstate.edu/data/abstract.aspx?dbcode=SA025 doi: http://dx.doi.org/10.6073/pasta/89707e1fc94c1d4fa96f48fc5f273c59

Kearney, M., Shine, R. and Porter, W.P. 2009. The potential for behavioral thermoregulation to buffer “cold-blooded” animals against climate warming. Proceedings of the National Academy of Sciences 106(10):3835-3840.

Kingsolver, J.G., Arthur Woods, H., Buckley, L.B., Potter, K.A., MacLean, H.J. and Higgins, J.K. 2011. Complex life cycles and the responses of insects to climate change. Integrative and Comparative Biology 51(5):719-732.

Lenth, R. 2019. emmeans: Estimated Marginal Means, aka Least-Squares Means. R package. 1.4.2. https://CRAN.R-project.org/package=emmeans

Levno, A. and Schulze, M. 2017. Snow depth and snow water equivalent measurements along a road course and historic snow course in the Andrews Experimental Forest, 1978 to present. Forest Science Data Bank, Corvallis, Oregon. Retrieved from: http://andlter.forestry.oregonstate.edu/data/abstract.aspx?dbcode=MS045 doi:http://dx.doi.org/10.6073/pasta/ff5465b74f592e3114138a79d5cfe290

Lin, X., Hubbard, K., Walter-Shea, E., Brandle, J. and Meyer, G. 2001a. Some perspectives on recent in situ air temperature observations: Modeling the microclimate inside the radiation shields. Journal of Atmospheric and Oceanic Technology 18(9):1470-1484.

Lin, X., Hubbard, K.G. and Meyer, G.E. 2001b. Airflow characteristics of commonly used temperature radiation shields. Journal of Atmospheric and Oceanic Technology 18(3):329-339.

Lin, X., Hubbard, K.G. and Walter-Shea, E.A. 2001c. Radiation loading model for evaluating air temperature errors with a non-aspirated radiation shield. Transactions of the ASAE 44(5):1299-1306.

Lister, B.C. and Garcia, A. 2018. Climate-driven declines in arthropod abundance restructure a rainforest food web. Proceedings of the National Academy of Sciences 115(44):E10397-E10406.

Lundquist, J.D. and Huggett, B. 2008. Evergreen trees as inexpensive radiation shields for temperature sensors. Water Resources Research 44:5.

Maclean, I., Hopkins, J.J., Bennie, J., Lawson, C.R. and Wilson, R.J. 2015. Microclimates buffer the responses of plant communities to climate change. Global Ecology and Biogeography 24(11):1340-1350.

Masson-Delmotte, V., Zhai, P., Pörtner, H., Roberts, D., Skea, J., Shukla, P., Pirani, A., Moufouma-Okia, W., Péan, C. and Pidcock, R. 2018. IPCC, 2018: Summary for Policymakers. Global Warming of 1.5°C. An IPCC Special Report on the impacts of global warming of 1.5°C above pre-industrial levels and related global greenhouse gas emission pathways, in the context of strengthening the global response to the threat of climate change, sustainable development, and efforts to eradicate poverty 1.

Mauder, M., Desjardins, R.L., Gao, Z. and van Haarlem, R. 2008. Errors of Naturally Ventilated Air Temperature Measurements in a Spatial Observation Network. Journal of Atmospheric and Oceanic Technology 25(11):2145-2151.

McAlpine, J., Peterson, B., Shewell, G., Teskey, H., Vockeroth, J. and Wood, D. 1981. Manual of Nearctic Diptera, Volume 1, Research Branch Agriculture Canada.

Menzel, A., Sparks, T.H., Estrella, N., Koch, E., Aasa, A., Ahas, R., Alm-Kubler, K., Bissolli, P., Braslavska, O., Briede, A., Chmielewski, F.M., Crepinsek, Z., Curnel, Y., Dahl, A., Defila, C., Donnelly, A., Filella, Y., Jatcza, K., Mage, F., Mestre, A., Nordli, O., Penuelas, J., Pirinen, P., Remisova, V., Scheifinger, H., Striz, M., Susnik, A., Van Vliet, A.J.H., Wielgolaski, F.E., Zach, S. and Zust, A. 2006. European phenological response to climate change matches the warming pattern. Global Change Biology 12(10):1969-1976.

Michener, W.K. 2015. Ecological data sharing. Ecological Informatics 29:33-44.

Milewska, E.J. and Vincent, L.A. 2016. Preserving continuity of long-term daily maximum and minimum temperature observations with automation of reference climate stations using overlapping data and meteorological conditions. Atmosphere-Ocean 54(1):32-47.

Nakamura, R. and Mahrt, L. 2005. Air temperature measurement errors in naturally ventilated radiation shields. Journal of Atmospheric and Oceanic Technology 22(7):1046-1058.

NOAA. 2018. Solar Calculation Details. Accessed on 6/12/2018. https://www.esrl.noaa.gov/gmd/grad/solcalc/calcdetails.html

Noriega, J.A., Hortal, J., Azcárate, F.M., Berg, M.P., Bonada, N., Briones, M.J.I., Del Toro, I., Goulson, D., Ibanez, S., Landis, D.A., Moretti, M., Potts, S.G., Slade, E.M., Stout, J.C., Ulyshen, M.D., Wackers, F.L., Woodcock, B.A. and Santos, A.M.C. 2018. Research trends in ecosystem services provided by insects. Basic and Applied Ecology 26:8-23.

Ovaskainen, O., Skorokhodova, S., Yakovleva, M., Sukhov, A., Kutenkov, A., Kutenkova, N., Shcherbakov, A., Meyke, E. and Delgado, M.D.M. 2013. Community-level phenological response to climate change. Proceedings of the National Academy of Sciences of the United States of America 110(33):13434.

Oyler, J.W., Dobrowski, S.Z., Ballantyne, A.P., Klene, A.E. and Running, S.W. 2015. Artificial amplification of warming trends across the mountains of the western United States. Geophysical Research Letters 42(1):153-161.

Parmesan, C. 2006. Ecological and evolutionary responses to recent climate change. Annual Review of Ecology, Evolution, and Systematics 37:637-669.

Parmesan, C. and Yohe, G. 2003. A globally coherent fingerprint of climate change impacts across natural systems. Nature 421:37.

Peterson, T.C., Easterling, D.R., Karl, T.R., Groisman, P., Nicholls, N., Plummer, N., Torok, S., Auer, I., Boehm, R. and Gullett, D. 1998. Homogeneity adjustments of in situ atmospheric climate data: a review. International Journal of Climatology 18(13):1493-1517.

Pinheiro, J., Bates, D., DebRoy, S., Sarkar, D., Heisterkamp, S. and Van Willigen, B. 2017. Package 'nlme'. 3.1-141.

Potter, K.A., Arthur Woods, H. and Pincebourde, S. 2013. Microclimatic challenges in global change biology. Global Change Biology 19(10):2932-2939.

Pureswaran, D.S., Roques, A. and Battisti, A. 2018. Forest Insects and Climate Change. Current Forestry Reports.

Quayle, R.G., Easterling, D., Karl, T. and Hughes, P. 1991. Effects of recent thermometer changes in the cooperative station network. Bulletin Of The American Meteorological Society 72(11):1718-1723.

R Core Team. 2016. R: A language and environment for statistical computing. 3.4.3. R Foundation for Statistical Computing. https://www.R-project.org/

Richardson, S.J., Brock, F.V., Semmer, S.R. and Jirak, C. 1999. Minimizing errors associated with multiplate radiation shields. Journal of Atmospheric and Oceanic Technology 16(11):1862-1872.

Rundel, P.W., Graham, E.A., Allen, M.F., Fisher, J.C. and Harmon, T.C. 2009. Environmental sensor networks in ecological research. New Phytologist 182(3):589-607.

Sánchez-Bayo, F. and Wyckhuys, K.A. 2019. Worldwide decline of the entomofauna: A review of its drivers. Biological Conservation 232:8-27.

Saunders, D.S. 2002. Insect clocks, Elsevier.

Saunders, M.E., Janes, J.K. and O'Hanlon, J.C. 2019. Moving On from the Insect Apocalypse Narrative: Engaging with Evidence-Based Insect Conservation. Bioscience.

Sefick, S.J. 2016. Stream Metabolism: A package for calculating single station metabolism from diurnal oxygen curves. 1.1.2.

Smith, J.W. 2002, Mapping the thermal climate of the H.J. Andrews Experimental Forest, Oregon. Retrieved from https://andrewsforest.oregonstate.edu/publications/3117

Snyder, R.L., Spano, D., Cesaraccio, C. and Duce, P. 1999. Determining degree-day thresholds from field observations. International Journal of Biometeorology 42(4):177-182.

Stålhandske, S., Lehmann, P., Pruisscher, P. and Leimar, O. 2015. Effect of winter cold duration on spring phenology of the orange tip butterfly, Anthocharis cardamines. Ecology and Evolution 5(23):5509-5520.

Storlie, C., Merino-Viteri, A., Phillips, B., VanDerWal, J., Welbergen, J. and Williams, S. 2014. Stepping inside the niche: microclimate data are critical for accurate assessment of species' vulnerability to climate change. Biology letters 10(9):20140576.

Terando, A.J., Youngsteadt, E., Meineke, E.K. and Prado, S.G. 2017. Ad hoc instrumentation methods in ecological studies produce highly biased temperature measurements. Ecology and Evolution 7(23):9890-9904.

Thackeray, S.J., Henrys, P.A., Hemming, D., Bell, J.R., Botham, M.S., Burthe, S., Helaouet, P., Johns, D.G., Jones, I.D., Leech, D.I., Mackay, E.B., Massimino, D., Atkinson, S., Bacon, P.J., Brereton, T.M., Carvalho, L., Clutton-Brock, T.H., Duck, C., Edwards, M., Elliott, J.M., Hall, S.J.G., Harrington, R., Pearce-Higgins, J.W., Hoye, T.T., Kruuk, L.E.B.,

Pemberton, J.M., Sparks, T.H., Thompson, P.M., White, I., Winfield, I.J. and Wanless, S. 2016. Phenological sensitivity to climate across taxa and trophic levels. Nature 535(7611):241.

Thackeray, S.J., Sparks, T.H., Frederiksen, M., Burthe, S., Bacon, P.J., Bell, J.R., Botham, M.S., Brereton, T.M., Bright, P.W., Carvalho, L., Clutton-Brock, T., Dawson, A., Edwards, M., Elliott, J.M., Harrington, R., Johns, D., Jones, I.D., Jones, J.T., Leech, D.I., Roy, D.B., Scott, W.A., Smith, M., Smithers, R.J., Winfield, I.J. and Wanless, S. 2010. Trophic level asynchrony in rates of phenological change for marine, freshwater and terrestrial environments. Global Change Biology 16(12):3304-3313.

Thomas, C. and Smoot, A. 2013. An Effective, Economic, Aspirated Radiation Shield for Air Temperature Observations and Its Spatial Gradients. Journal of Atmospheric and Oceanic Technology 30(3):526-537.

Thorne, P.W., Menne, M.J., Williams, C.N., Rennie, J.J., Lawrimore, J.H., Vose, R.S., Peterson, T.C., Durre, I., Davy, R., Esau, I., Klein-Tank, A.M.G. and Merlone, A. 2016. Reassessing changes in diurnal temperature range: A new data set and characterization of data biases. Journal of Geophysical Research: Atmospheres 121(10):5115-5137.

Thorne, P.W., Parker, D.E., Christy, J.R. and Mears, C.A. 2005. Uncertainties in Climate Trends: Lessons from Upper-Air Temperature Records. Bulletin Of The American Meteorological Society 86(10):1437-1442.

Titley, M.A., Snaddon, J.L. and Turner, E.C. 2017. Scientific research on animal biodiversity is systematically biased towards vertebrates and temperate regions. Plos One 12(12):e0189577.

Trewin, B. 2010. Exposure, instrumentation, and observing practice effects on land temperature measurements. Wiley Interdisciplinary Reviews: Climate Change 1(4):490-506.

Visser, M.E. and Both, C. 2005. Shifts in phenology due to global climate change: the need for a yardstick. Proceedings of the Royal Society B: Biological Sciences 272(1581):2561.

Wang, K. 2014. Sampling biases in datasets of historical mean air temperature over land. Scientific Reports 4:4637-4637.

Ward, S.E., Schulze, M. and Roy, B. 2018. A long-term perspective on microclimate and spring plant phenology in the Western Cascades. Ecosphere 9(10):e02451.

Weiss, A. and Hays, C.J. 2005. Calculating daily mean air temperatures by different methods: implications from a non-linear algorithm. Agricultural and Forest Meteorology 128(1):57-65.

Wickham, H. 2016. ggplot2: Elegant Graphics for Data Analysis. 3.0.0.9. Springer-Verlag. https://www.R-project.org/

Wickham, H. 2017. tidyverse: Easily Install and Load the 'Tidyverse'. 1.2.1. https://CRAN.R-project.org/package=tidyverse

Wolda, H. 1988. Insect Seasonality: Why? Annual Review of Ecology and Systematics 19(1):1-18.

Woods, H.A., Dillon, M.E. and Pincebourde, S. 2015. The roles of microclimatic diversity and of behavior in mediating the responses of ectotherms to climate change. Journal of Thermal Biology 54:86-97.

Yamamoto, K., Togami, T., Yamaguchi, N. and Ninomiya, S. 2017. Machine Learning-Based Calibration of Low-Cost Air Temperature Sensors Using Environmental Data. Sensors 17(6):1290.

Zalom, F.G. and Goodell, P.B. 1983. Degree days: the calculation and use of heat units in pest management, University of California, Division of Agriculture and Natural Resources.

Insect identification

Arnett, R.H. 2000. American Insects: A Handbook of the Insects of America North of Mexico (2nd Edition). CRC Press. Boca Raton, Florida. 1003 pp.

Arnett, R.H., and M.C. Thomas 2001. American Beetles, Vol. 1. CRC Press. Boca Raton, Florida. 443 pp.

Arnett, R.H., M.C. Thomas, P.E. Skelley, and J.H. Frank. 2002. American Beetles, Vol. 2. CRC Press. Boca Raton, Florida. 861 pp.

Covell, C.V. 1984. A Field Guide to the Moths. Houghton Mifflin. Boston, Massachusetts. 496 pp.

McAlpine, J.F., B.V. Peterson, G.E. Shewell, H.J. Teskey, J.R. Vockeroth, and D.M. Wood. 1981. Manual of Nearctic Diptera, Vol. 1-2. Ottawa, Ontario: Biosystematics Research Institute.

Merritt, R.W., K.W. Cummins, and M.B. Berg. 2008. An Introduction to the Aquatic Insects of North America (4th Edition). Kendall/Hunt Publishing Company, Dubuque, Iowa. 862 pp.

Triplehorn, C.A., and N.F. Johnson. 2005. Borror and DeLong's Introduction to the Study of Insects (7th Edition). Thomson Brooks/Cole. Belmont, California. 864 pp.

APPENDICES

APPENDICES OF FIGURES

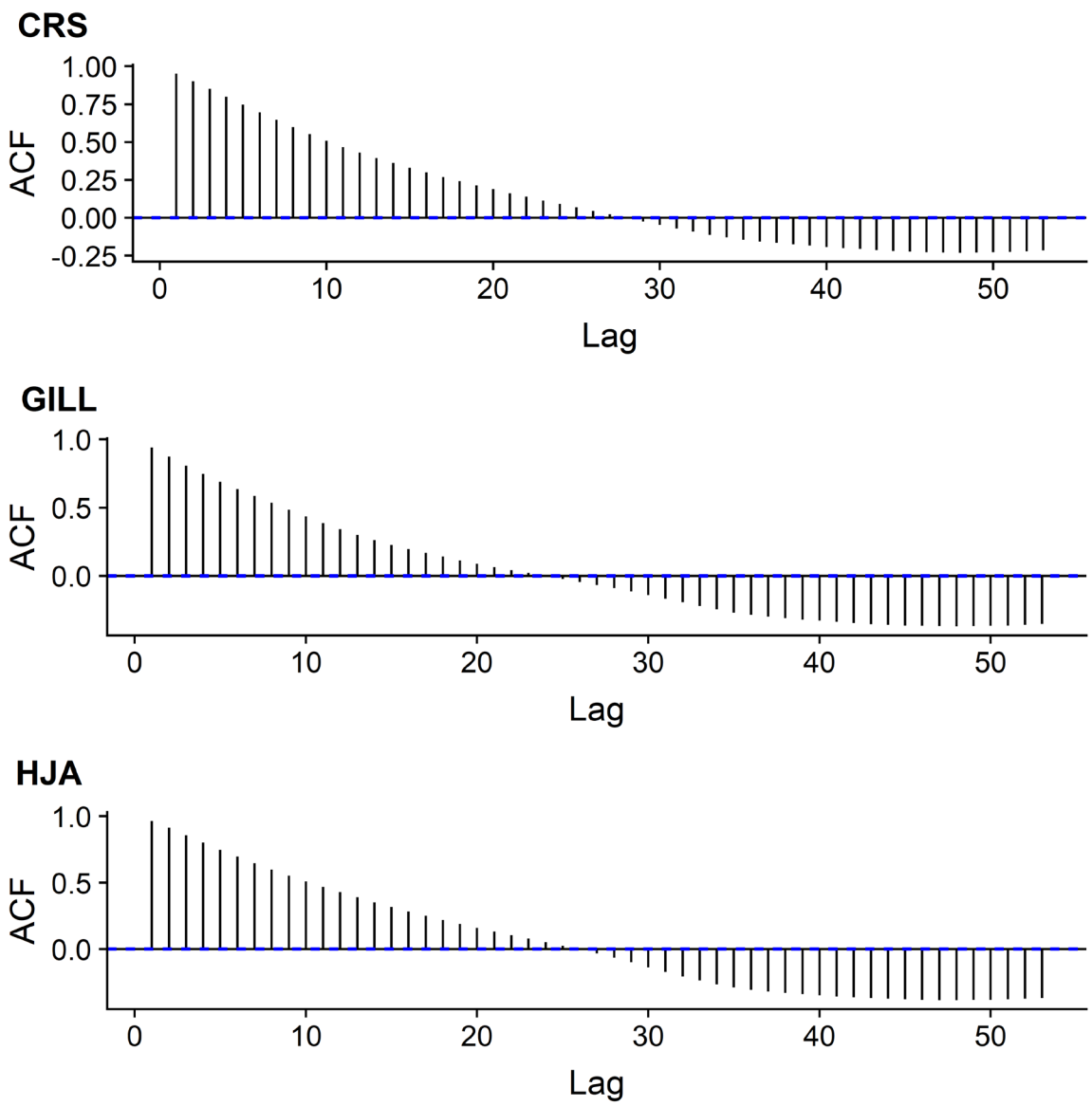

Figure A.1 Autocorrelation function (ACF) plots of the time series of wind-ventilated instrument ΔTs. ΔTs are highly correlated over time.

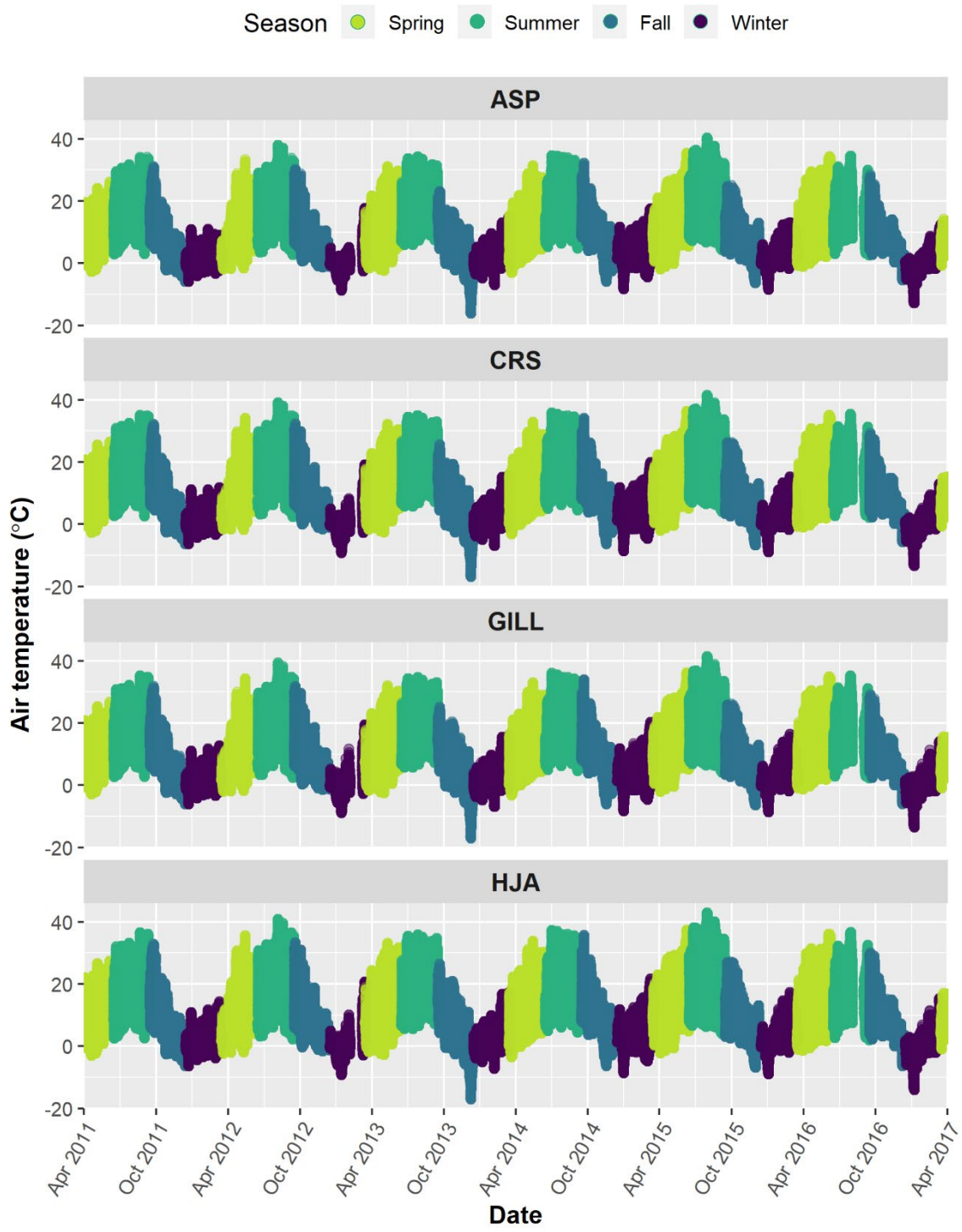

Figure A.2 Time series plots of the 15-minute average temperature recorded by each instrument between July 2010 and July 2016. Colors denote seasons: spring – purple, summer – blue, fall – green, winter - yellow.

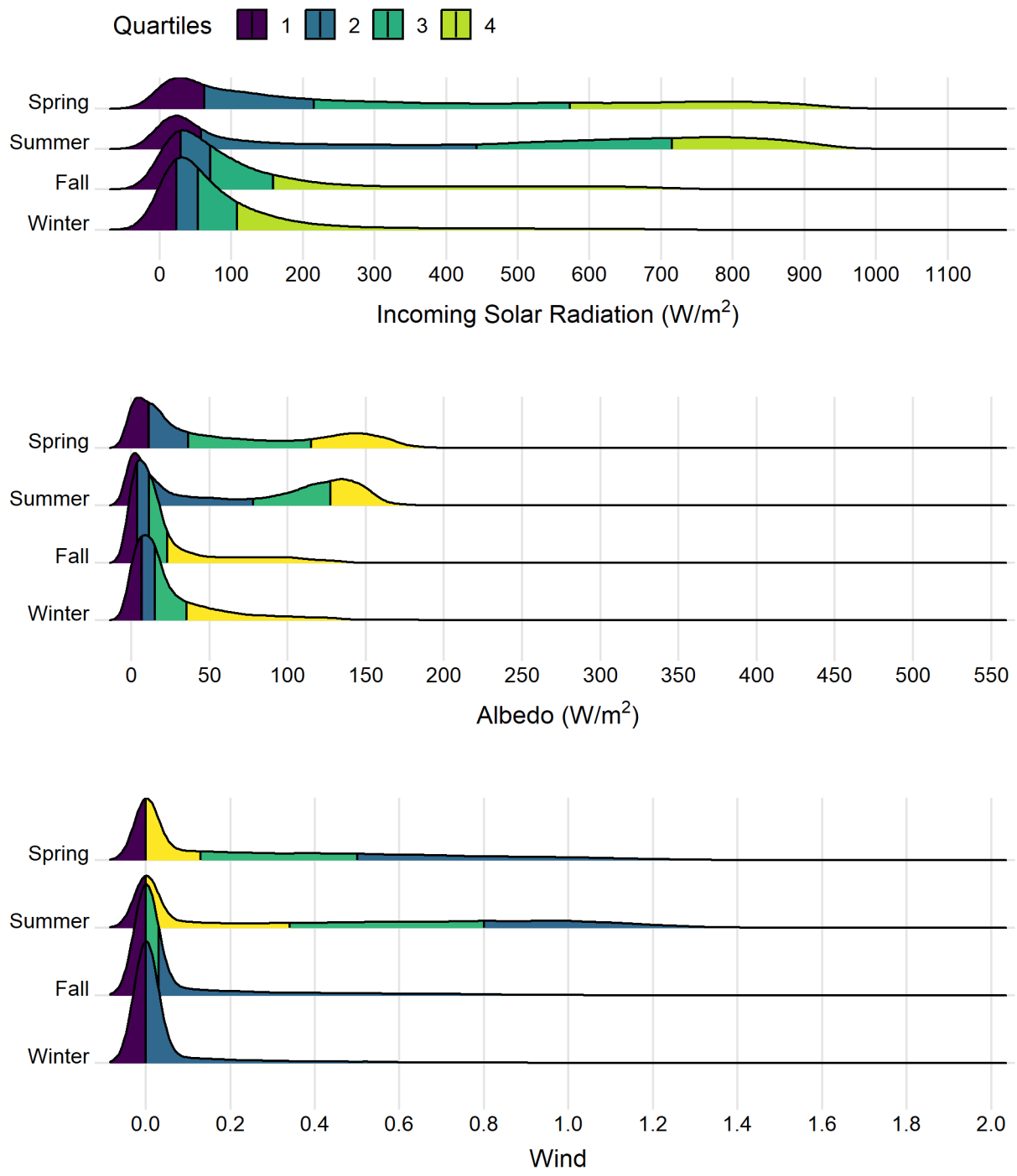

Figure A.3 Ridgeline plots show the distribution of 15-minute average observations between July 2010 and July 2016 for daytime incoming solar radiation and albedo, and day & night wind speeds by season. Colors denote quartiles: first – purple, second – blue, third – green, fourth - yellow.

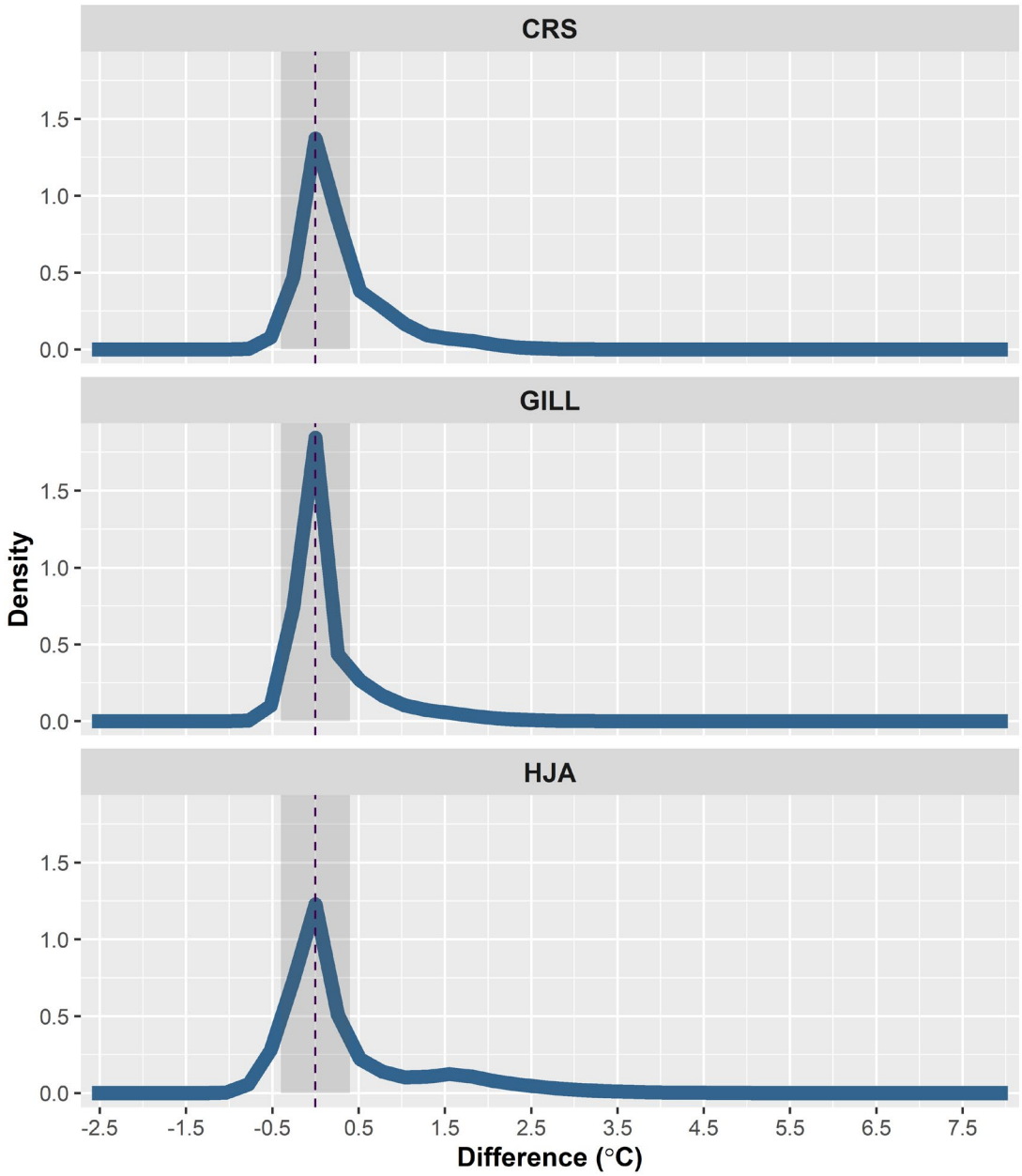

Figure A.4 Density plot of ΔTs for all 15-minute average observations. The ΔTs are calculated as the wind-ventilated instrument temperature measurement minus the fan-aspirated instrument temperature measurement. Vertical dashed line indicates ΔT = 0. The ΔTs outside the shaded region are considered substantial.

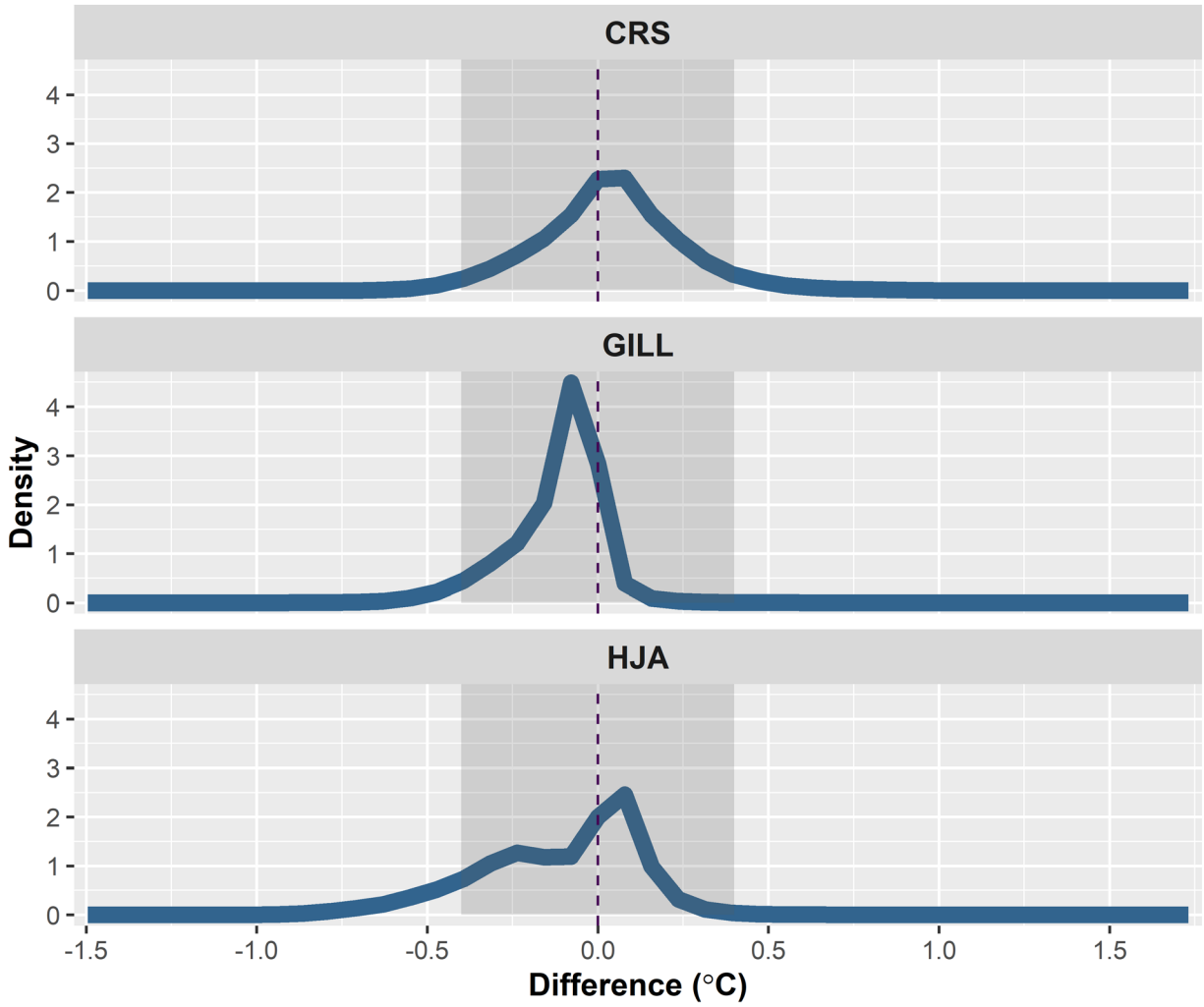

Figure A.5 Density plot of differences in the nighttime 15-minute average observations. The ΔTs are calculated as the wind-ventilated instrument temperature measurement minus the fan-aspirated instrument temperature measurement. Vertical dashed line indicates ΔT = 0. The ΔTs outside the shaded region are considered substantial.

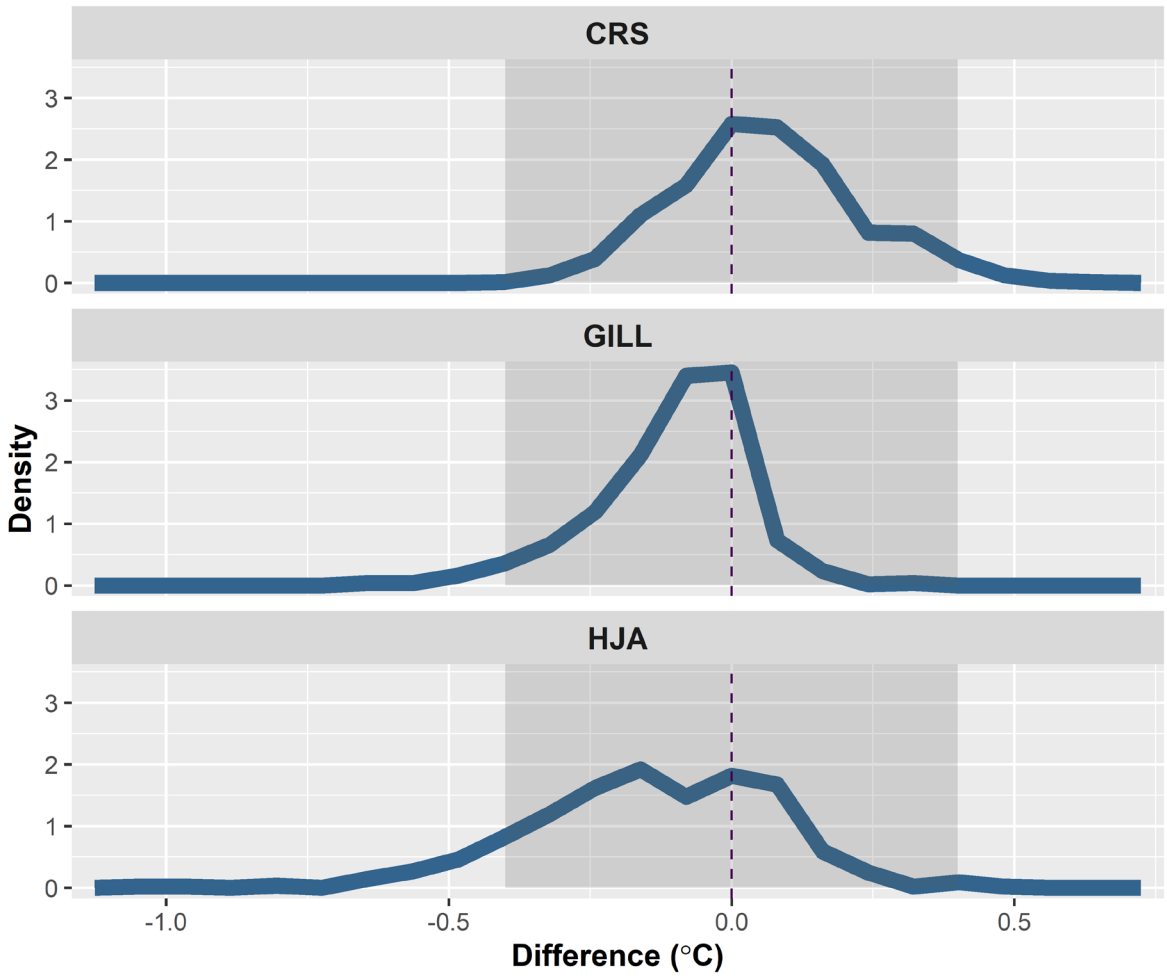

Figure A.6 Density plot of differences in the daily minimum observations. The ΔTs are calculated as the wind-ventilated instrument temperature measurement minus the fan-aspirated instrument temperature measurement. Vertical dashed line indicates ΔT = 0. The ΔTs outside the shaded region are considered substantial.

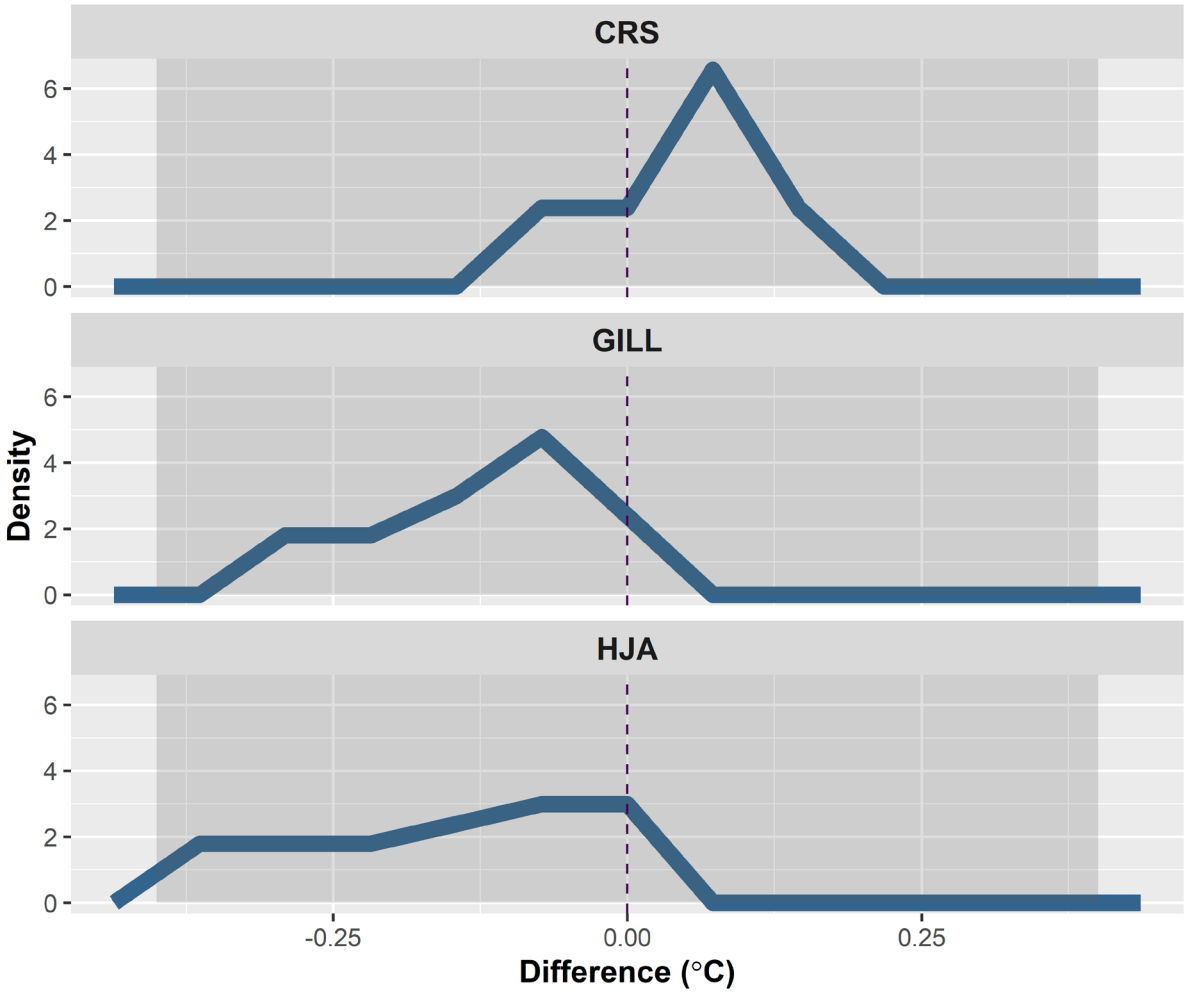

Figure A.7 Density plot of differences in the monthly mean daily minimum observations. The ΔTs are calculated as the wind-ventilated instrument temperature measurement minus the fan-aspirated instrument temperature measurement. Vertical dashed line indicates ΔT = 0. The ΔTs outside the shaded region are considered substantial.

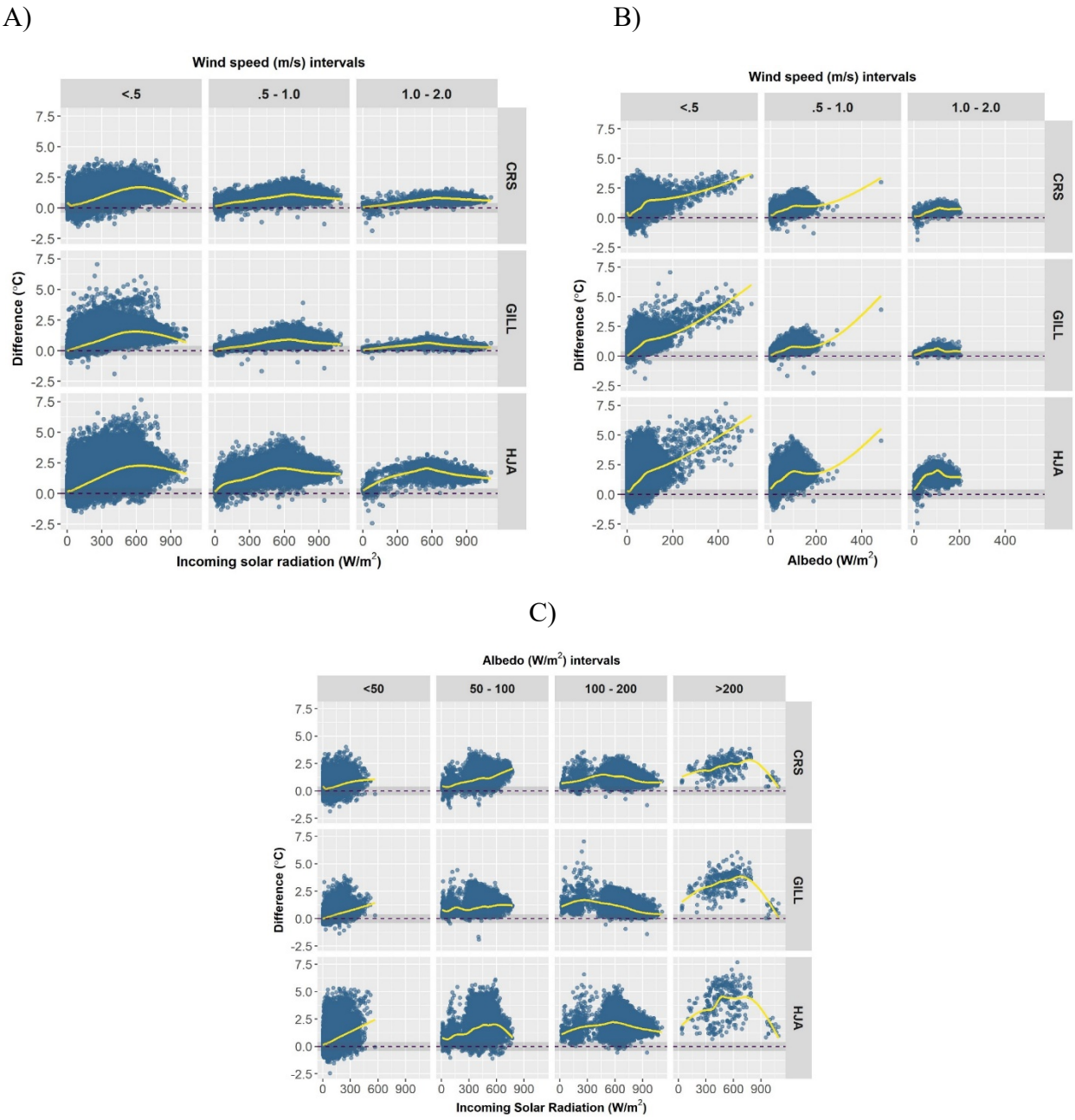

Figure A.8 Conditioning plots for each instrument showing daytime 15-minute average observation differences (°C) against: 1) incoming solar radiation (W/m^2) conditioned on intervals of wind speed (m/s), B) albedo (W/m^2) conditioned on intervals of wind speed (m/s); and C) albedo conditioned on intervals of incoming solar radiation (W/m^2). Differences outside the shaded region are considered substantial ($|\Delta T| > 0.4$°C).The yellow line is the loess smoothing curve. Plots show potential interactions between explanatory variables and a non-linear response.

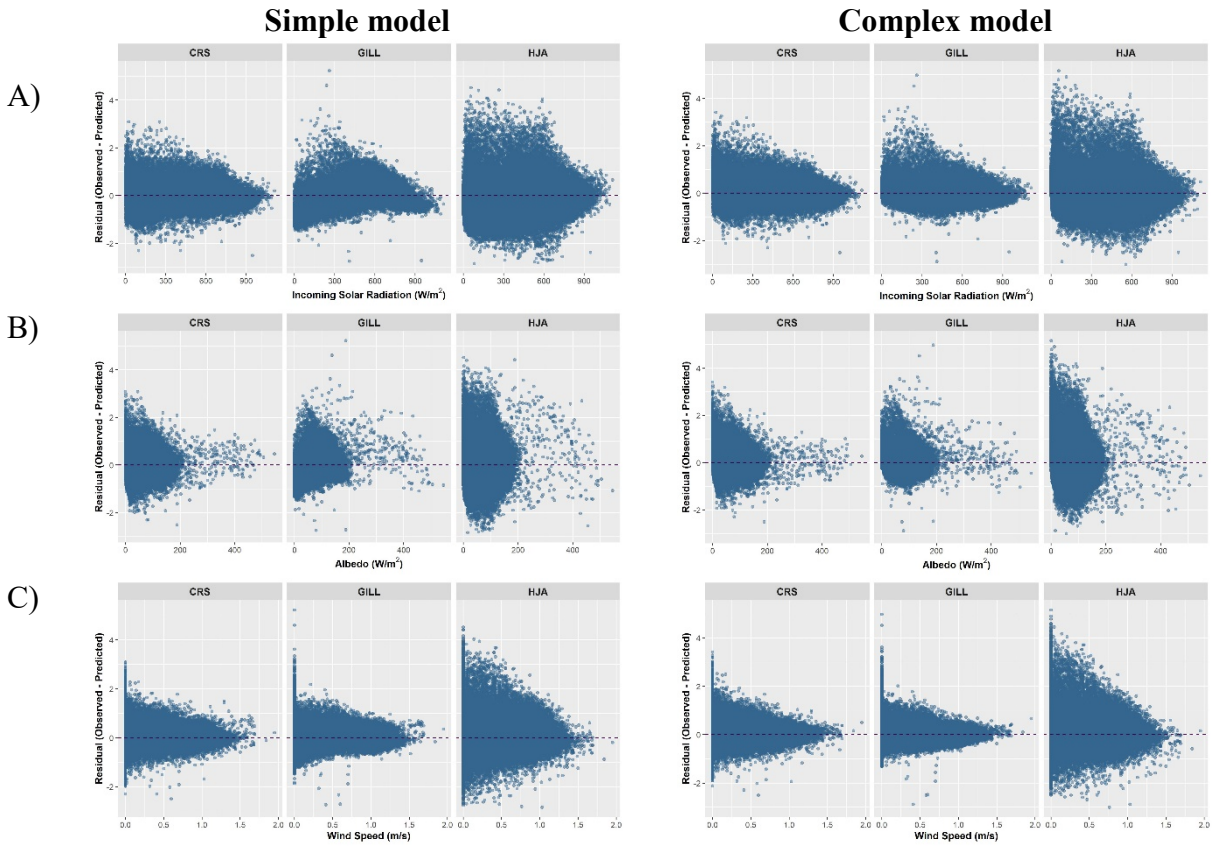

Figure A.9 Plots show the simple and complex model residuals (observed – predicted) against: A) incoming solar radiation (W/m^2), B) albedo (W/m^2), and C) wind speed (m/s) (unbinned daytime 15-minute average observations). Dark dashed line indicates when residual = 0.

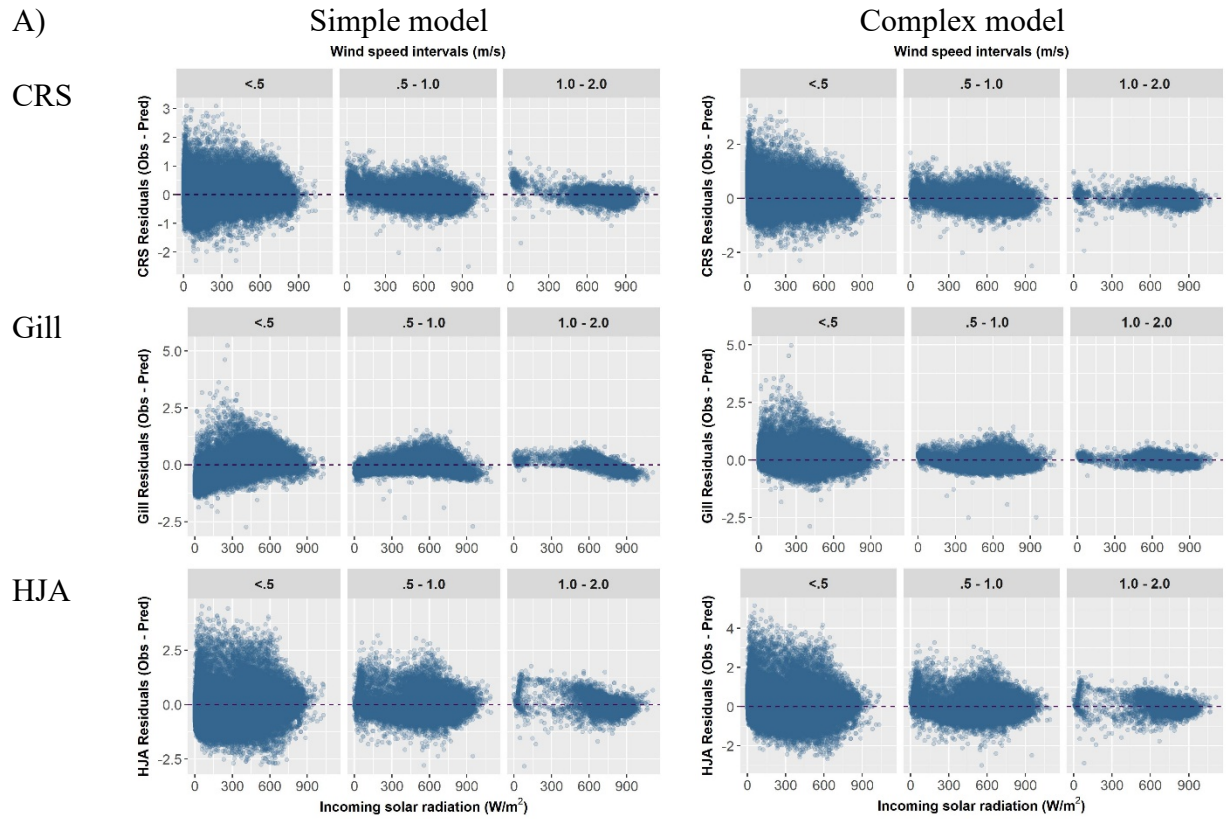

Figure A.10 (Cont'd on next 2 pages) For each plot, the upper panel shows the ranges of an explanatory variable for the subsample of data in the box below it. Plots show the simple and complex model residuals (observed – predicted) against: A) incoming solar radiation (W/m^2), conditioned on intervals of wind speed (m/s), B) albedo (W/m^2), conditioned on intervals of wind speed (m/s); and C) albedo (W/m^2) conditioned on intervals of incoming solar radiation (W/m^2) (unbinned daytime 15-minute average observations). Dark dashed line indicates when residual = 0. Note that y-axis scales are different for each wind-ventilated instrument.

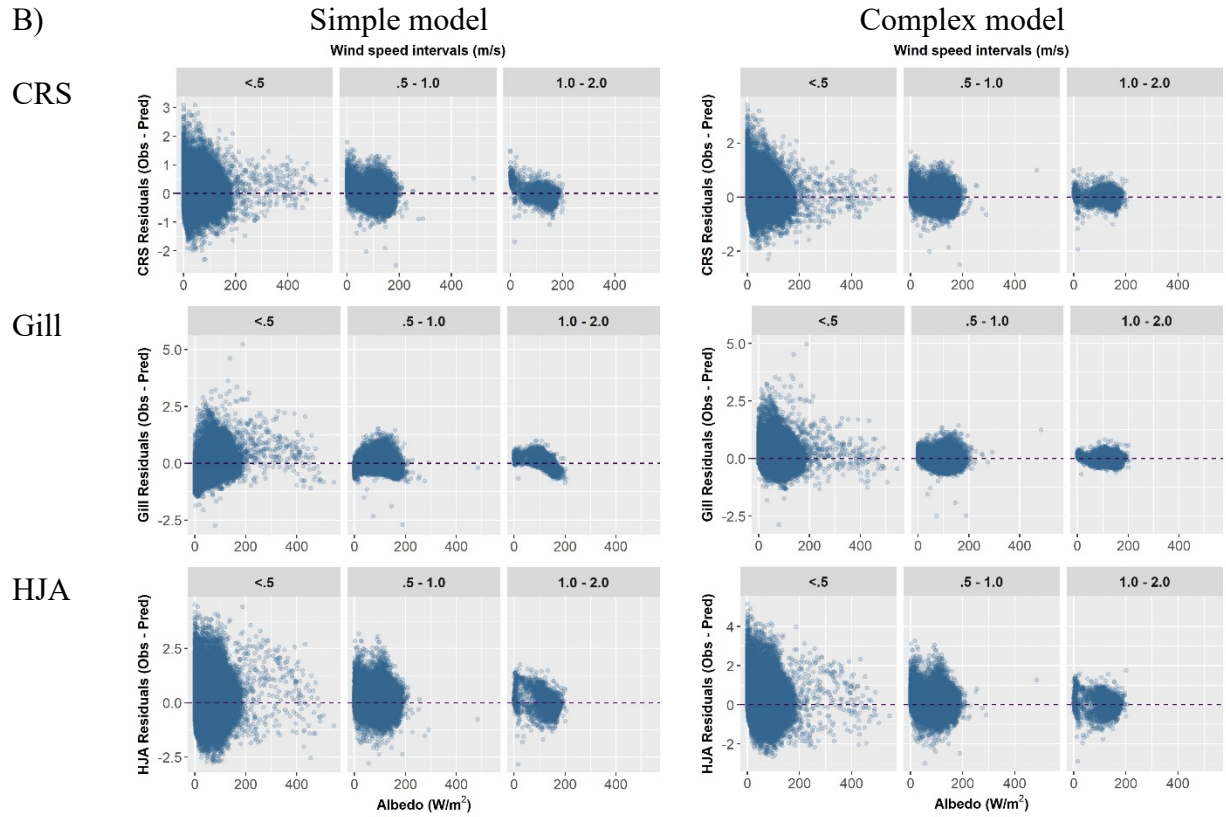

Figure A.10 (Cont'd on next page) For each plot, the upper panel shows the ranges of an explanatory variable for the subsample of data in the box below it. Plots show the simple and complex model residuals (observed – predicted) against: A) incoming solar radiation (W/m^2), conditioned on intervals of wind speed (m/s), B) albedo (W/m^2), conditioned on intervals of wind speed (m/s); and C) albedo (W/m^2) conditioned on intervals of incoming solar radiation (W/m^2) (unbinned daytime 15-minute average observations). Dark dashed line indicates when residual = 0. Note that y-axis scales are different for each wind-ventilated instrument.

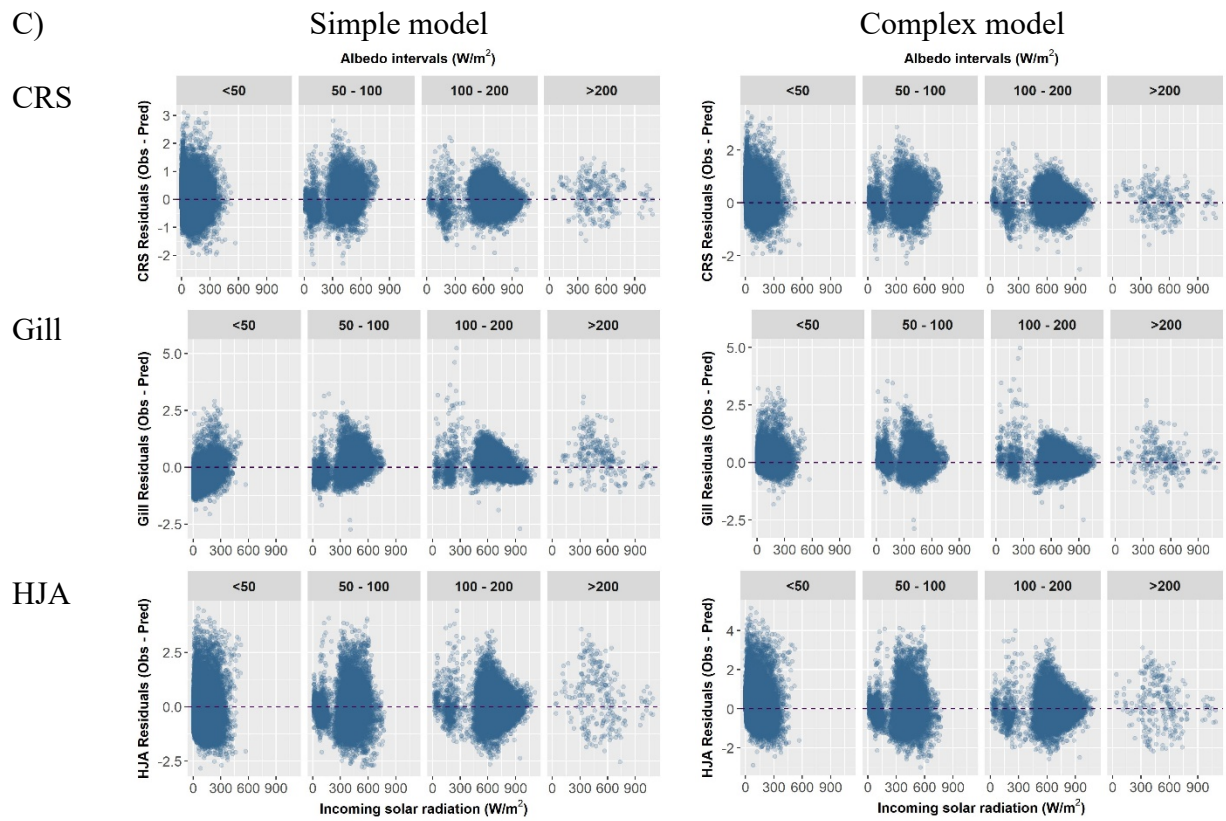

Figure A.10 For each plot, the upper panel shows the ranges of an explanatory variable for the subsample of data in the box below it. Plots show the simple and complex model residuals (observed – predicted) against: **A)** incoming solar radiation (W/m^2), conditioned on intervals of wind speed (m/s), **B)** albedo (W/m^2), conditioned on intervals of wind speed (m/s); and **C)** albedo (W/m^2) conditioned on intervals of incoming solar radiation (W/m^2) (unbinned daytime 15-minute average observations). Dark dashed line indicates when residual = 0. Note that y-axis scales are different for each wind-ventilated instrument.

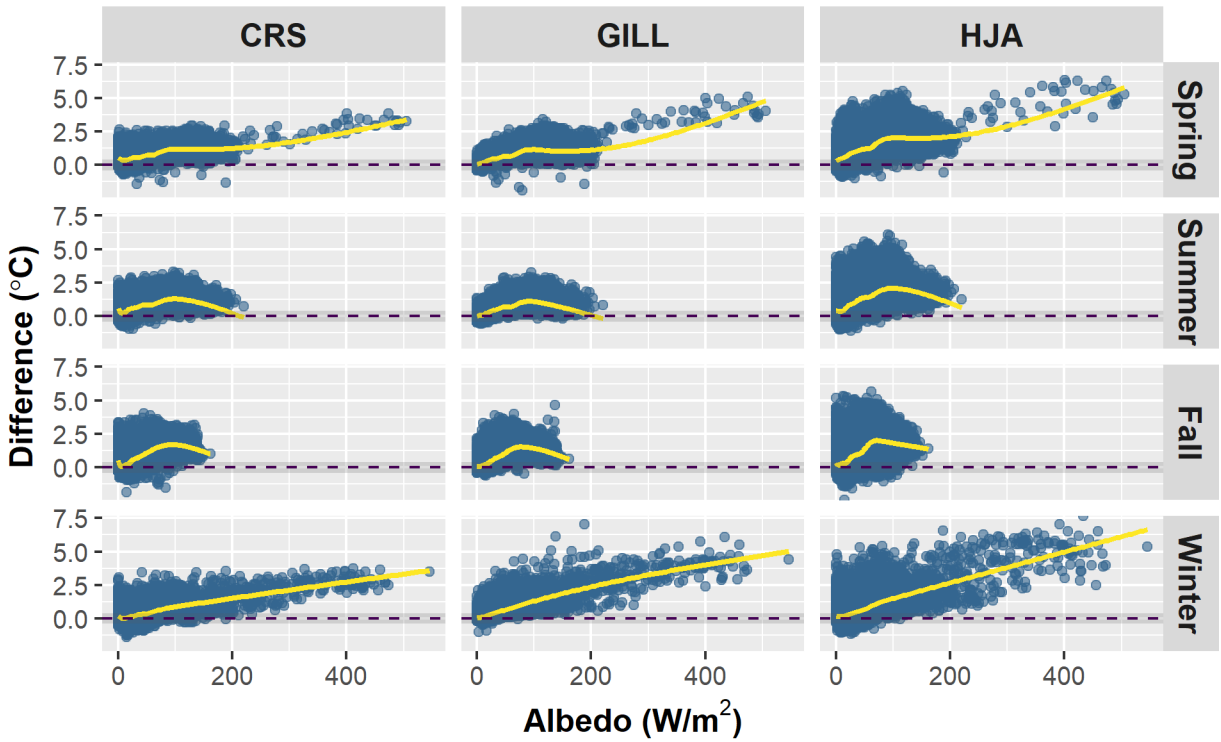

Figure A.11 Plots show ΔT against albedo (W/m^2) by season for each wind-ventilated instrument. While albedo is higher on average in the summer and fall, occurrences of high albedo in the spring and winter, likely due to snow cover, are associated with particularly large differences in each wind-ventilated instrument. Dark dashed line indicates when ΔT = 0. Areas outside of shaded gray region are considered substantial.

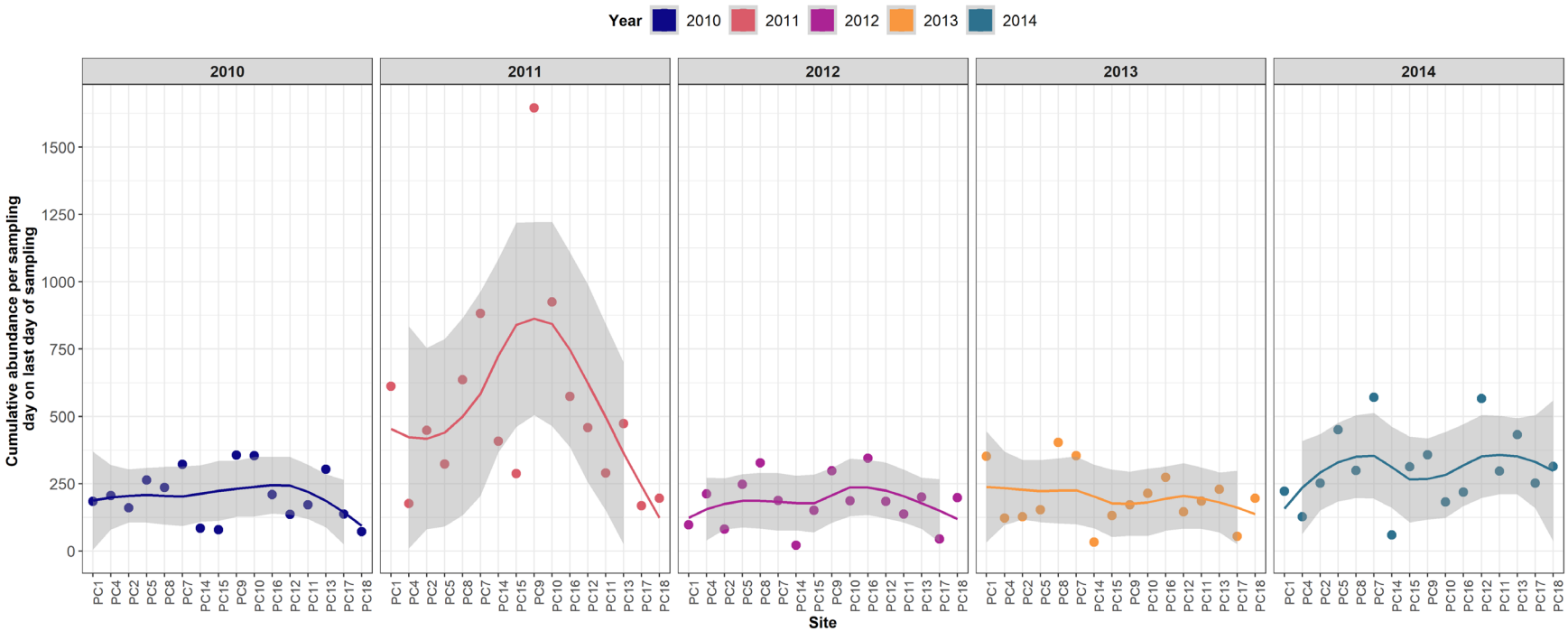

Figure A.12 Plot shows cumulative abundance per sampling day on the last day of sampling by site and year. Color indicates sampling year. Line is loess smoothing curve and gray shaded area is the confidence intervals. Sites are ordered left to right from low to high elevation.

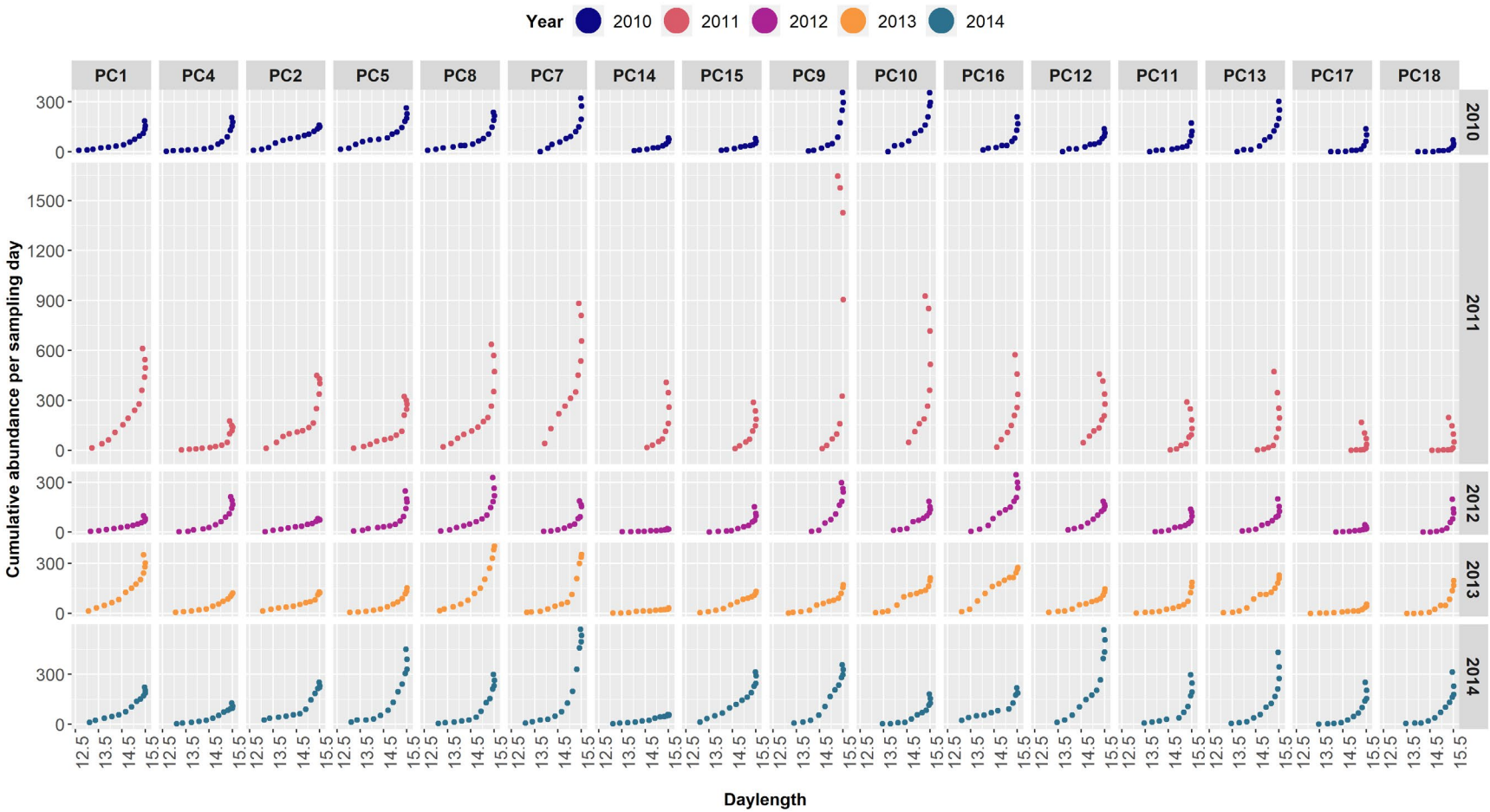

Figure A.13 Plot shows cumulative abundance per sampling day by daylength. Color indicates sampling year. Sites are ordered left to right from low to high elevation.

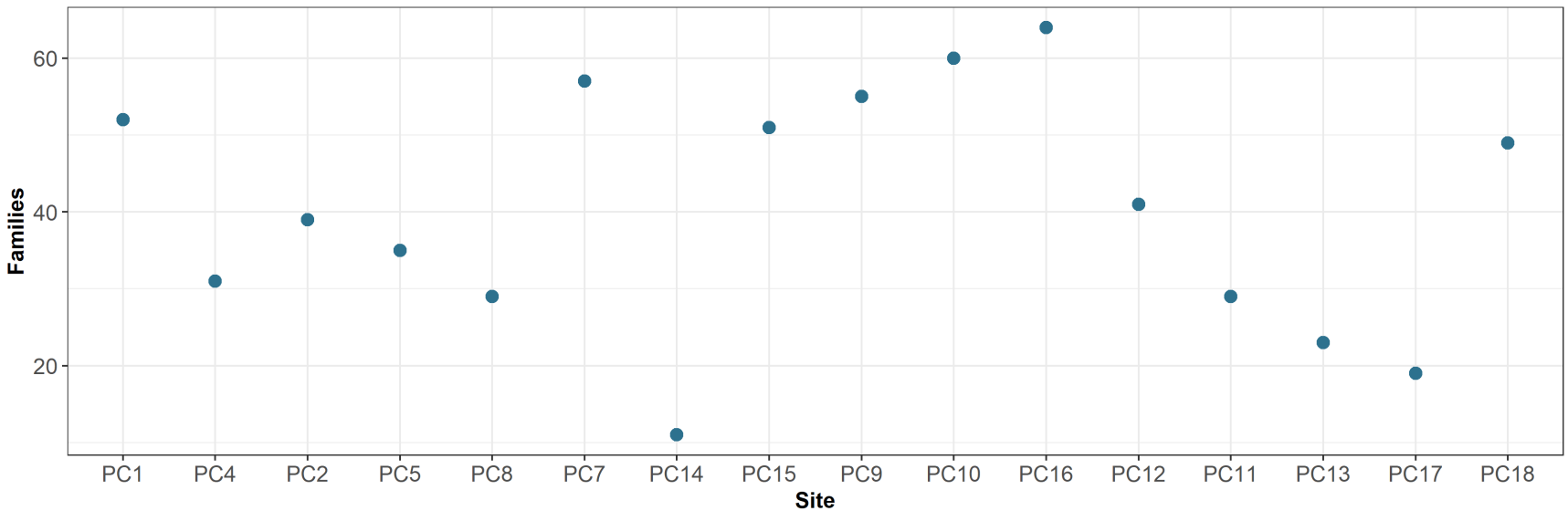

Figure A.14 Plot shows the number of insect families identified at each site in the 2009 sampling year. Sites are ordered left to right from low to high elevation.

APPENDICES OF TABLES

Table A.1 Summary statistics for: (A) 15-minute average - all observations, (B) 15-minute average - daytime observations), (C) 15-minute average - nighttime observations), (D) daily average, (E) daily maximum, and (F) daily minimum, (G) monthly mean daily average, (H) monthly mean daily maximum, and (I) monthly mean daily minimum. *Note that the daily/mean monthly maximum and daily/mean monthly average values for incoming solar radiation, albedo, and wind speed are calculated from instantaneous values, while the daily/mean monthly minimum values are calculated from the daily average values.

(A) 15-minute average (all observations)

Instrument	Units	*n*	Min	Max	Median	Mean	St. Dev.
ASP	°C	204,399	-16.1	40.4	8.2	9.2	7.8
CRS	°C	204,399	-16.8	41.5	8.4	9.4	8.1
Gill	°C	204,399	-17.0	41.5	8.3	9.3	8.0
HJA	°C	204,399	-17.1	43.0	8.4	9.5	8.3
RAD	W/m^2	204,399	0.0	1,112.0	2.1	115.0	227.8
ALB	W/m^2	204,399	0.0	546.0	0.0	21.7	43.3
WIND	m/s	204,399	0.0	2.0	0.0	0.1	0.3

(B) 15-minute average (daytime observations)

Instrument	Units	*n*	Min	Max	Median	Mean	St. Dev.
ASP	°C	87,129	-15.5	40.4	12.0	13.0	8.7
CRS	°C	87,129	-16.1	41.5	12.7	13.6	9.1
Gill	°C	87,129	-16.0	41.5	12.5	13.5	8.9
HJA	°C	87,129	-16.2	43.0	12.9	13.9	9.3
RAD	W/m^2	87,129	0.0	1,112.0	121.0	266.7	285.6
ALB	W/m^2	87,129	0.0	545.8	21.8	50.2	54.7
WIND	m/s	87,129	0.0	2.0	0.0	0.2	0.4

(Cont'd) **Table A.1** Summary statistics for: (A) 15-minute average - all observations, (B) 15-minute average - daytime observations), (C) 15-minute average - nighttime observations), (D) daily average, (E) daily maximum, and (F) daily minimum, (G) monthly mean daily average, (H) monthly mean daily maximum, and (I) monthly mean daily minimum. *Note that the daily/mean monthly maximum and daily/mean monthly average values for incoming solar radiation, albedo, and wind speed are calculated from instantaneous values, while the daily/mean monthly minimum values are calculated from the daily average values.

(C) 15-minute average (nighttime observations)

Instrument	Units	*n*	Min	Max	Median	Mean	St. Dev.
ASP	°C	117,270	-16.1	25.2	6.2	6.3	5.6
CRS	°C	117,270	-16.8	25.2	6.3	6.4	5.6
Gill	°C	117,270	-17.0	24.9	6.1	6.2	5.5
HJA	°C	117,270	-17.1	25.1	6.2	6.2	5.5
RAD	W/m^2	117,270	0.0	160.0	0.0	2.2	8.3
ALB	W/m^2	117,270	0.0	100.0	0.0	0.5	2.0
WIND	m/s	117,270	0.0	2.0	0.0	0.01	0.1

(D) Daily average

Instrument	Units	*n*	Min	Max	Median	Mean	St. Dev.
ASP	°C	700	-9.6	24.1	8.9	9.2	6.8
CRS	°C	702	-9.9	24.6	9.2	9.4	6.9
Gill	°C	702	-9.8	24.4	9.0	9.3	6.8
HJA	°C	702	-10.3	24.9	9.2	9.5	6.9
RAD	W/m^2	702	0.5	284.6	78.1	107.6	91.6
ALB	W/m^2	702	0.1	60.6	16.1	21.0	16.5
WIND	m/s	702	0.0	0.5	0.1	0.1	0.1

(Cont'd) **Table A.1** Summary statistics for: (A) 15-minute average - all observations, (B) 15-minute average - daytime observations), (C) 15-minute average - nighttime observations), (D) daily average, (E) daily maximum, and (F) daily minimum, (G) monthly mean daily average, (H) monthly mean daily maximum, and (I) monthly mean daily minimum. *Note that the daily/mean monthly maximum and daily/mean monthly average values for incoming solar radiation, albedo, and wind speed are calculated from instantaneous values, while the daily/mean monthly minimum values are calculated from the daily average values.

(E) Daily maximum

Instrument	Units	*n*	Min	Max	Median	Mean	St. Dev.
ASP	°C	697	-5.0	41.4	13.7	15.7	10.5
CRS	°C	702	-4.0	41.9	14.2	16.1	10.6
Gill	°C	702	-3.6	42.2	14.7	16.4	10.5
HJA	°C	702	-4.5	43.5	15.2	16.9	10.9
RAD	W/m^2	702	7.0	1,384.0	699.5	616.5	366.8
ALB	W/m^2	702	3.0	478.7	140.1	128.8	74.4
WIND	m/s	702	0.0	10.2	3.1	3.0	1.9

(F) Daily minimum

Instrument	Units	*n*	Min	Max	Median	Mean	St. Dev.
ASP	°C	698	-13.2	18.0	4.6	4.6	4.9
CRS	°C	702	-13.3	18.3	4.6	4.7	4.9
Gill	°C	702	-13.7	17.9	4.5	4.5	4.9
HJA	°C	702	-14.1	17.9	4.5	4.5	4.9
RAD*	W/m^2	702	0.0	1.0	0.0	0.0	0.1
ALB*	W/m^2	702	0.0	0.0	0.0	0.0	0.0
WIND*	m/s	702	0.0	0.0	0.0	0.0	0.0

(Cont'd) **Table A.1** Summary statistics for: (A) 15-minute average - all observations, (B) 15-minute average - daytime observations), (C) 15-minute average - nighttime observations), (D) daily average, (E) daily maximum, and (F) daily minimum, (G) monthly mean daily average, (H) monthly mean daily maximum, and (I) monthly mean daily minimum. *Note that the daily/mean monthly maximum and daily/mean monthly average values for incoming solar radiation, albedo, and wind speed are calculated from instantaneous values, while the daily/mean monthly minimum values are calculated from the daily average values.

(G) Monthly mean daily average

Instrument	Units	*n*	Min	Max	Median	Mean	St. Dev.
ASP	°C	23	-1.5	19.7	9.7	9.1	6.4
CRS	°C	23	-1.5	20.1	9.8	9.4	6.5
Gill	°C	23	-1.5	19.8	9.7	9.2	6.4
HJA	°C	23	-1.6	20.3	9.9	9.4	6.5
RAD	W/m^2	23	12.0	244.0	74.5	107.2	83.2
ALB	W/m^2	23	3.4	45.6	18.1	21.0	14.1
WIND	m/s	23	0.01	0.3	0.1	0.1	0.1

(H) Monthly mean daily maximum

Instrument	Units	*n*	Min	Max	Median	Mean	St. Dev.
ASP	°C	23	0.7	31.6	16.3	15.6	9.7
CRS	°C	23	1.2	31.9	16.8	16.1	9.8
Gill	°C	23	1.9	32.1	17.0	16.3	9.6
HJA	°C	23	1.8	33.2	17.9	16.9	10.1
RAD	W/m^2	23	110.5	1,062.9	610.7	616.1	323.9
ALB	W/m^2	23	42.2	220.2	140.1	129.2	56.6
WIND	m/s	23	0.7	4.8	3.1	3.0	1.2

(Cont'd) **Table A.1** Summary statistics for: **(A)** 15-minute average - all observations, **(B)** 15-minute average - daytime observations), **(C)** 15-minute average - nighttime observations), **(D)** daily average, **(E)** daily maximum, and **(F)** daily minimum, **(G)** monthly mean daily average, **(H)** monthly mean daily maximum, and **(I)** monthly mean daily minimum. *Note that the daily/mean monthly maximum and daily/mean monthly average values for incoming solar radiation, albedo, and wind speed are calculated from instantaneous values, while the daily/mean monthly minimum values are calculated from the daily average values.

(I) Monthly mean daily minimum

Instrument	Units	*n*	Min	Max	Median	Mean	St. Dev.
ASP	°C	23	-3.5	11.3	4.7	4.6	4.2
CRS	°C	23	-3.5	11.3	4.8	4.7	4.2
Gill	°C	23	-3.7	11.0	4.6	4.5	4.2
HJA	°C	23	-3.8	10.9	4.6	4.5	4.2
RAD*	W/m^2	23	0	0	0	0.00	0.01
ALB*	W/m^2	23	0	0	0	0.0	0.0
WIND*	m/s	23	0	0	0	0.0	0.0

Table A.2 Summary of ΔTs (°C) for daily minimum observations. The ΔTs were calculated as the wind-ventilated instrument measurement minus the aspirated instrument measurement. A "substantial ΔT" is defined as |ΔT| > 0.4°C. The percentage in the last column of the table is the percentage of the *n* ΔT values that were considered substantial.

Instrument	*n*	Min	Max	Median	Mean	St Dev	Substantial ΔTs
CRS	698	-0.4	0.6	0.1	0.1	0.2	2.7%
Gill	698	-0.6	0.3	-0.1	-0.1	0.1	3.0%
HJA	698	-1.1	0.4	-0.1	-0.1	0.2	11.3%

Table A.3 Summary of ΔTs (°C) for monthly mean daily minimum observations. The ΔTs were calculated as the wind-ventilated instrument measurement minus the aspirated instrument measurement. A "substantial ΔT" is defined as |ΔT| > 0.4°C. The percentage in the last column of the table is the percentage of the *n* ΔT values that were considered substantial.

Instrument	*n*	Min	Max	Median	Mean	St Dev	Substantial ΔTs
CRS	23	-0.1	0.1	0.1	0.05	0.1	0.0%
Gill	23	-0.3	0.02	-0.1	-0.1	0.1	0.0%
HJA	23	-0.4	0.03	-0.1	-0.2	0.1	0.0%

Table A.4 Summary statistics for the binned daytime 15-minute average values.

Variable	*n*	Min	Max	Median	Mean	St Dev
CRS ΔT (°C)	1051	-0.6	3.6	0.8	0.9	0.7
Gill ΔT (°C)	1051	-0.2	5.1	0.7	1.0	0.9
HJA ΔT (°C)	1051	-0.9	6.1	1.7	1.7	1.0
RAD (W/m^2)	1051	15.1	1090.0	518.3	501.5	286.0
ALB (W/m^2)	1051	0.3	545.8	118.5	125.5	86.3
WIND (m/s)	1051	0.0	2.0	0.5	0.6	0.4

Table A.5 Regression results and optimism-corrected coefficient estimates for each of the best models using the binned daytime 15-minute average data. Simple models do not include interaction terms. Complex models do include interaction terms. ISR = incoming solar radiation (W/m^2), ALB = albedo (W/m^2), WIND = wind speed (m/s).

Model statistics	Variables	Estimate	S.E.
CRS			
Adj R^2 = 0.78 **MSE = 0.09** **$F_{4, 1046}$ = 907**	Intercept	2.10×10^{-1}	3.30×10^{-2}
	ISR	2.74×10^{-3}	1.28×10^{-4}
	ISR^2	-2.15×10^{-6}	1.21×10^{-7}
	ALB	3.72×10^{-3}	1.33×10^{-4}
	WIND	-6.40×10^{-1}	2.39×10^{-2}
Adj R^2 = 0.81 **MSE = 0.08** **$F_{9, 1041}$ = 502**	Intercept	-1.32×10^{-1}	6.44×10^{-2}
	ISR	3.71×10^{-3}	3.24×10^{-4}
	ISR^2	-2.85×10^{-6}	3.62×10^{-7}
	ALB	4.65×10^{-3}	4.60×10^{-4}
	WIND	1.59×10^{-2}	6.54×10^{-2}
	ISR * ALB	-6.80×10^{-7}	1.82×10^{-6}
	ISR^2 * ALB	7.49×10^{-10}	1.91×10^{-9}
	ISR * WIND	-1.44×10^{-3}	2.96×10^{-4}
	ISR^2 * WIND	1.37×10^{-6}	2.74×10^{-7}
	ALB * WIND	-3.80×10^{-3}	4.56×10^{-4}
Gill			
Adj R^2 = 0.82 **MSE = 0.14** **$F_{4, 1046}$ = 1185**	Intercept	8.74×10^{-1}	3.52×10^{-2}
	ISR	-2.24×10^{-5}	5.42×10^{-5}
	ALB	3.35×10^{-3}	4.42×10^{-4}
	ALB^2	8.93×10^{-6}	9.41×10^{-7}
	WIND	-8.49×10^{-1}	2.88×10^{-2}
Adj R^2 = 0.91 **MSE = 0.07** **$F_{9, 1041}$ = 1160**	Intercept	-2.26×10^{-1}	6.02×10^{-2}
	ISR	3.43×10^{-3}	3.03×10^{-4}
	ISR^2	-3.55×10^{-6}	3.38×10^{-7}
	ALB	9.35×10^{-3}	4.30×10^{-4}
	WIND	9.47×10^{-2}	6.12×10^{-2}
	ISR * ALB	-3.82×10^{-6}	1.70×10^{-6}
	ISR^2 * ALB	5.01×10^{-9}	1.79×10^{-9}
	ISR * WIND	-8.92×10^{-4}	2.77×10^{-4}
	ISR^2 * WIND	1.19×10^{-6}	2.56×10^{-7}
	ALB * WIND	-7.98×10^{-3}	4.27×10^{-4}
HJA			
Adj R^2 = 0.66 **MSE = 0.36** **$F_{5, 1045}$ = 408**	Intercept	3.87×10^{-1}	7.23×10^{-2}
	ISR	5.06×10^{-3}	2.52×10^{-4}
	ISR^2	-4.32×10^{-6}	2.36×10^{-7}
	ALB	1.38×10^{-3}	7.13×10^{-4}
	ALB^2	1.32×10^{-5}	1.52×10^{-6}
	WIND	-3.77×10^{-1}	4.68×10^{-2}
Adj R^2 = 0.70 **MSE = 0.31** **$F_{9, 1041}$ = 279**	Intercept	-3.03×10^{-1}	1.27×10^{-1}
	ISR	5.94×10^{-3}	6.40×10^{-4}
	ISR^2	-6.23×10^{-6}	7.16×10^{-7}
	ALB	1.18×10^{-2}	9.09×10^{-4}
	WIND	1.70×10^{-1}	1.29×10^{-1}
	ISR * ALB	-1.47×10^{-5}	3.59×10^{-6}
	ISR^2 * ALB	1.86×10^{-8}	3.78×10^{-9}
	ISR * WIND	2.05×10^{-3}	5.86×10^{-4}
	ISR^2 * WIND	-7.05×10^{-7}	5.42×10^{-7}
	ALB * WIND	-1.28×10^{-2}	9.03×10^{-4}

Table A.6 Table shows the number of hourly air temperature records that were imputed using regression relationships with nearby climate stations, for each site and sampling year. The *n* listed under the sampling year is the total number of hourly air temperature records for the sampling year, which varied based on the sampling period window. There were no imputed values for sampling year 2010.

Study site	**Reference site**	**2011** (*n* = 5807)	**2012** (*n* = 5831)	**2013** (*n* = 5807)	**2014** (*n* = 5807)
PC460_1	RS02			539	5807
PC644_5	RS86			500	5807
PC903_7	RS05			10	
PC979_9	RS12	765	2	850	
PC1116_11	RS26			549	4134
PC1082_12	RS26			28	
PC1178_13	RS26			1	10
PC1030_16	RS05	623		79	
PC1301_17	RS04	2419	884	2318	11
PC1339_18	RS04	1938	1018	2705	10

Table A.7 Regression equations used to fill in any missing or erroneous temperature data.

Site	Equation	Adjusted R^2	df	F-stat	P-value
PC1	PC1 = RS02 x 0.941 + 0.649	0.989	145,215	425924	***
PC2	PC2 = CS2met x 0.933 + 1.074	0.986	149,115	354185	***
PC4	PC4 = RS89 x 0.985 + 0.632	0.994	154,915	979041	***
PC5	PC5 = RS86 x 0.992 + 0.430	0.994	144,049	706341	***
PC7	PC7 = RS05 x 0.987 - 0.075	0.996	155,057	1271158	***
PC8	PC8 = RS10 x 1.000 + 0.115	0.997	154,568	1571495	***
PC9	PC9 = RS12 x 1.001 + 0.381	0.992	153,536	647952	***
PC10	PC10 = RS05 x 1.003 - 0.568	0.986	154,745	376250	***
PC11	PC11 = RS26 x 0.975 - 0.554	0.991	147,045	495211	***
PC12	PC12 = RS26 x 0.979 + 0.107	0.996	154,593	1402571	***
PC13	PC13 = RS26 x 0.952 - 1.235	0.971	154,196	181439	***
PC14	PC14 = RS05 x 1.016 - 0.454	0.989	155,067	485521	***
PC15	PC15 = HI15 x 0.984 + 0.386	0.985	148,635	320198	***
PC16	PC16 = RS26 x 0.996 - 0.026	0.986	154,059	372480	***
PC17	PC17 = RS04 x 0.977 + 0.014	0.992	147,550	595117	***
PC18	PC18 = RS04 x 1.001 - 0.203	0.984	148,787	308451	***

Notes:
-- Non-significant; * P<0.05; ** P<0.01; ***P<0.001; In the site column, PC represents "phenology core"; In the equation column, all abbreviations following = are representative of reference stands (RS) or other climate stations (HI15 and CS2met); df, degrees of freedom.

Table A.8 Count of insects by family and study site from 2009 sampling year.

Family	PC1	PC2	PC4	PC5	PC7	PC8	PC9	PC10	PC11	PC12	PC13	PC14	PC15	PC16	PC17	PC18	Total
Achilidae	2	4	2	3	1	1				1			1	1			16
Acroceridae				2			2										4
Agromyzidae				1												2	3
Aleyrodidae	5		9	4		9	1			1			1			1	31
Anthomyiidae	1				1		1		1		2					1	7
Aphididae	1		1		1	1	2		13	6				1		17	43
Apidae			1														1
Attelibidae			1														1
Baetidae		1															1
Bibionidae							9	1							1		11
Bolbomyiidae		1			7		4	10	1	15	1		1	2	1	3	46
Braconidae	1		1	3	4			1	1	3	1			1	2	2	20
Cantharidae	15		3	3	3	4	2	3		7	2			4		1	47
Cecidomyiidae	134	111	30	17	170	100	54	114	47	51	9	11	63	66	14	12	1003
Cerambycidae					1		1	2									4
Ceratopogonidae	7	1	3	1	3	4	3	8	1	2	1		9	1		10	54
Chalcidoidea_sp.	2	2	5	2	10	3	2	2	5	3	3		2	3		4	48
Chironomidae	156	425	15	9	483	46	779	648	77	116	152	57	323	245	46	97	3674
Chrysomelidae	1								4	1						1	7
Cicadellidae	1	2		1		1	7							3	4	6	25
Cleridae		1		1													2
Clusiidae									1								1

Table A.8 Count of insects by family and study site from 2009 sampling year. (continued)

Family	PC1	PC2	PC4	PC5	PC7	PC8	PC9	PC10	PC11	PC12	PC13	PC14	PC15	PC16	PC17	PC18	Total
Coccinellidae	1													1			2
Coccoidea_sp.			1		1	1	1		2					1			7
Coniopterygidae					1			2	1		2			1			7
Copromorphidae/Tortricidae				1						1				1			3
Culicidae			1										1				2
Curculionidae					1		2			1		1					5
Delphacidae	1																1
Diadocidiidae					1		1	1						2			5
Diapriidae	1	1	4	4		2	3						2			1	18
Diptera_sp															1	1	2
Dolichopodidae	3	1		3	7	1	17	9	6	5	10		2	3	2	15	84
Drosophilidae	2													1	1		4
Dryomyzidae			1			1											2
Elateridae		1	7	5	4	6	1	3			2		1	4	2		36
Empididae	1	9			22	6	40	17	6	29	4	4	3	5	1	3	150
Endomychidae		1															1
Ephydridae																1	1
Eucinetidae							1										1
Formicidae							1	1									2
Geometridae		1					1	5	2	3			1	5			18
Glossosomatidae		1															1
Heleomyzidae									2		2		6				10

Table A.8 Count of insects by family and study site from 2009 sampling year. (continued)

Family	PC1	PC2	PC4	PC5	PC7	PC8	PC9	PC10	PC11	PC12	PC13	PC14	PC15	PC16	PC17	PC18	Total
Hemerobiidae				2													2
Hybotidae	1			2				1									4
Ichneumonidae	2		2	1	4	5	1	5	1		5			3		5	34
Keroplatidae	7		3			1											11
Lampyridae	2	1	1			1											5
Latridiidae	7	2							1				1				11
Lepidoptera_sp.	1		7	3	1	3	1	4		2	1	1	2	6			32
Leuctridae													6				6
Lycidae					1			2		4		1					8
Lygaeoidea_sp								1									1
Melandryidae	2	1					1		1				1	1			7
Microphoridae	1						1	7						1		1	11
Milichiidae	1																1
Miridae														1			1
Muscidae		1									2	1					4
Mycetophilidae	5	2	3	8	14	5	10	14	4	12	2		7	32	5	58	181
Nemouridae		2						5	5				10			3	25
Nitidulidae									2								2
Noctuidae								2								1	3
Pentatomidae							1										1
Phoridae	18	5	4	13	3	9	4	7	4	1	9		6	7	4	20	114
Pipunculidae	1			3		1											5

Table A.8 Count of insects by family and study site from 2009 sampling year. (continued)

Family	PC1	PC2	PC4	PC5	PC7	PC8	PC9	PC10	PC11	PC12	PC13	PC14	PC15	PC16	PC17	PC18	Total
Psocodea_sp.	2			3		2		1									8
Psychodidae	12	6	3	4	6	5	27	22	3	9	3	1	5	10	3	4	123
Psyllidae					1												1
Pyrochroidae	1																1
Rhagionidae	3			2													5
Rhaphidiidae				2													2
Sarcophagidae				1													1
Scathophagidae							1	2							1	2	6
Sciaridae	46	14	13	3	13	8	30	86	23	10	21	3	29	20	5	28	352
Scraptiidae	10	2	7	21	7	13	1	3		1		13	1	3			82
Scydmaenidae													1				1
Simuliidae							1			1	1						3
Sphaeroceridae	3	2	2	1	1			1								2	12
Staphylinidae			1		10	1	20	64	11	2			1	3	1		114
Syrphidae	1	1				4							3	4	1	3	17
Tachinidae			1														1
Tenebrionidae			1														1
Tenthridinidae	1						1	1		1			1		1	3	9
Throscidae	1	1		2			1						1	1			7
Thysanoptera_sp.	9	1	1	1			1	2								8	23
Tipulidae		3		1	1			2	2		6		9				24
Trogossitidae				1					1								2

Table A.8 Count of insects by family and study site from 2009 sampling year. (continued)

Family	PC1	PC2	PC4	PC5	PC7	PC8	PC9	PC10	PC11	PC12	PC13	PC14	PC15	PC16	PC17	PC18	Total
Vespidae			1		1	1										1	4
Xylophagidae		3			1			1	27		1	1		4			38
Grand Total	**472**	**610**	**135**	**134**	**785**	**245**	**1037**	**1060**	**255**	**288**	**242**	**94**	**500**	**447**	**96**	**317**	**Total**